

Automated Algorithmic Discovery for Gravitational-Wave Detection Guided by LLM-Informed Evolutionary Monte Carlo Tree Search

He Wang^{1,2*} and Liang Zeng^{3*}

¹International Centre for Theoretical Physics Asia-Pacific,
University of Chinese Academy of Sciences, 100190, Beijing,
China.

²Taiji Laboratory for Gravitational Wave Universe, University of
Chinese Academy of Sciences, 100049, Beijing, China.

³Tsinghua University, 100084, Beijing, China.

*Corresponding author(s). E-mail(s): hewang@ucas.ac.cn;
zengliangcs@gmail.com;

Abstract

From fundamental physics to gravitational wave astronomy, computational scientific discovery increasingly relies on algorithms to process complex data and identify meaningful patterns - yet faces persistent challenges in gravitational-wave signal identification. While existing algorithmic approaches like matched filtering (MF) and deep neural networks (DNNs) have achieved partial success, their limitations directly stem from these foundational dependencies: MF's excessive computational demands arise from its reliance on predefined theoretical waveform templates, while DNNs' black-box architectures obscure decision logic and introduce hidden biases through data-dependent learning processes. We propose Evolutionary Monte Carlo Tree Search (Evo-MCTS), a framework that addresses these limitations through systematic exploration of algorithm design spaces guided by domain-aware physical constraints. Our approach combines tree-structured search with evolutionary optimization and large language model heuristics to create interpretable algorithmic solutions while maintaining

computational efficiency. Our Evo-MCTS framework demonstrates substantial performance improvements across multiple metrics, achieving a 20.2% improvement over state-of-the-art gravitational wave detection algorithms on the MLGWSC-1 benchmark dataset. Systematic breakthrough discoveries emerge across independent executions, where high-performing algorithm variants consistently surpass critical performance thresholds. The framework generates human-interpretable algorithmic pathways that reveal distinct performance patterns organized by functional categories including conditioning techniques, time-frequency analysis, and trigger detection methods. Beyond performance improvements, our framework systematically discovers novel algorithmic combinations through tree-structured exploration, with robustness analysis confirming reliable discovery mechanisms rather than random variations, thereby establishing a transferable methodology for automated algorithmic discovery across computational science domains.

1 Introduction

The pursuit of scientific discovery increasingly demands computational approaches that can navigate complex, high-dimensional data spaces while maintaining physical interpretability [1–4]. This challenge transcends individual disciplines, manifesting across domains from materials science [5, 6] to astrophysics [7, 8], where the identification of meaningful patterns in noisy, high-dimensional datasets requires sophisticated algorithmic strategies that balance theoretical rigor with computational feasibility [9]. In gravitational wave astronomy, this computational challenge manifests as a fundamental algorithmic problem: detection systems must identify faint astrophysical signals buried in detector noise while leveraging theoretical predictions from general relativity [10, 11]. Simultaneously, these algorithms must remain adaptable to unexpected signal morphologies that could reveal new physics beyond current theoretical models.

Gravitational wave detection serves as an exemplary case study for automated algorithm discovery, embodying the fundamental tension between model-driven precision and data-driven flexibility that characterizes modern scientific computing [12]. Since the first direct detection in 2015 [10], the field has witnessed remarkable progress, yet current methodologies face inherent limitations that constrain our ability to identify novel phenomena. The detection of gravitational waves requires algorithms that can distinguish genuine astrophysical signals—often buried in noise with signal-to-noise ratios as low as 8–12 [11]—from instrumental artifacts and environmental disturbances, while maintaining computational efficiency for real-time analysis of continuous data streams from multiple detectors worldwide [13].

Current gravitational-wave detection methodologies embody this computational dilemma through their complementary yet insufficient approaches.

Matched filtering (MF) techniques [14, 15] achieve high sensitivity by correlating detector data with theoretical waveform templates derived from numerical relativity simulations, but suffer from prohibitive computational costs that scale exponentially with parameter space dimensionality and critically depend on accurate prior knowledge of signal morphologies. This template-based approach fundamentally limits discovery potential for unmodeled sources or signals with unexpected characteristics [16]. Conversely, deep neural networks (DNNs) [17–19] offer computational efficiency and model-agnostic flexibility, but operate as black boxes that obscure decision logic, introduce hidden biases through training data dependencies, and lack the interpretability essential for scientific validation and understanding [20].

Traditional algorithm development in scientific computing typically follows experience-based heuristic design or data-dependent optimization approaches. In complex detection pipelines, multiple specialized algorithms are often chained together, with each component manually optimized for specific sub-tasks through iterative refinement processes that implicitly resemble beam search strategies [16, 21, 22]. While this approach has proven effective in many domains, it faces fundamental scalability limitations when confronted with high-dimensional optimization problems like gravitational wave detection, where the space of possible algorithmic combinations grows exponentially with pipeline complexity. Moreover, human-designed algorithms often reflect cognitive biases and domain-specific assumptions that may inadvertently exclude novel solutions or fail to adapt to evolving data characteristics [23–25]. Automated Heuristic Discovery (AHD) represents a paradigm shift toward systematic exploration of algorithmic design spaces, leveraging computational intelligence to overcome the limitations of manual algorithm engineering. Recent advances in AHD have explored diverse optimization techniques, including genetic programming [26], neural architecture search [27], and evolutionary computation [28], demonstrating promising results across various domains. However, most existing approaches suffer from critical limitations: genetic programming often generates syntactically invalid or semantically meaningless code [26], neural architecture search focuses primarily on network topology rather than algorithmic logic [27], and traditional evolutionary methods lack domain knowledge integration, leading to inefficient exploration of vast search spaces [28].

The emergence of Large Language Models (LLMs) has opened unprecedented opportunities for AI-assisted scientific discovery [1, 29]. Recent work has demonstrated LLMs’ capabilities in code generation [30], mathematical reasoning [31], and domain-specific problem solving [32]. In scientific computing contexts, LLMs have shown promise for automated hypothesis generation [2], experimental design [33], and literature synthesis [34]. Researchers have explored two main approaches to leverage LLMs for optimization [35, 36]. The first approach uses LLMs directly as optimization algorithms through prompting, such as OPRO [37], which guides LLMs to generate solutions

through in-context learning. However, such direct approaches often face limitations when dealing with complex problems involving large search spaces [38], leading researchers to explore more sophisticated methods like utilizing LLMs to generate solver scripts [39, 40].

The second approach employs LLMs to design optimization algorithms through structured workflows. Notable advances include FunSearch [41], which combines LLMs with evolutionary methods for mathematical discovery, and Evolution of Heuristics [42], which integrates LLMs with evolutionary computation to automatically design heuristic algorithms, showing superior performance over manual designs. Building upon this direction, works like AEL [42, 43] and ReEvo [44] further enhance the evolutionary framework with reflection mechanisms and automated algorithm design capabilities. Recent work has also explored Monte Carlo Tree Search for algorithmic heuristic design [45], demonstrating the potential of tree-based exploration methods in optimization contexts. However, it is important to note that most existing LLM-based algorithmic discovery frameworks have primarily focused on combinatorial optimization tasks such as bin packing, traveling salesman problems, and scheduling [42–44], where the search space consists of discrete decision sequences and the objective functions are well-defined mathematical formulations. In contrast, scientific signal processing problems like gravitational wave detection present fundamentally different challenges, requiring continuous parameter optimization, domain-specific physical constraints, and interpretable algorithmic pathways that can be validated against theoretical predictions. Furthermore, few approaches have successfully integrated domain-specific physical constraints with adaptive search strategies in a cohesive framework that maintains interpretability throughout the discovery process.

Monte Carlo Tree Search (MCTS) has emerged as a powerful framework for sequential decision-making problems, achieving remarkable success in game playing [46, 47], neural architecture optimization [48], and automated theorem proving [49]. The key strength of MCTS lies in its ability to balance exploration and exploitation through principled tree traversal policies, enabling systematic search of large discrete spaces while maintaining computational tractability. In the context of algorithm discovery, MCTS offers several advantages: (i) structured representation of the search space through tree hierarchies, (ii) adaptive exploration guided by performance feedback, and (iii) natural integration with domain knowledge through informed expansion policies. However, traditional MCTS applications in algorithm optimization have been limited by the challenge of defining meaningful state representations and transition functions for complex algorithmic transformations.

We propose Evo-MCTS (Evolutionary Monte Carlo Tree Search), a novel framework that integrates three key components: (i) Monte Carlo Tree Search for systematic exploration of algorithmic design spaces, (ii) evolutionary operations for sophisticated code transformations guided by performance feedback, and (iii) Large Language Model-generated heuristics that inject domain knowledge while maintaining code validity. Key innovations include: Reflective

Code Synthesis for performance-driven algorithm generation, Multi-Scale Evolutionary Operations (Parent/Sibling Crossover, Point Mutation, Path-wise Crossover) operating on structured code, Domain-Aware Tree Expansion incorporating physical constraints, and Interpretable Algorithm Pathways enabling post-hoc analysis through complete tree traversal histories.

We demonstrate the effectiveness of Evo-MCTS through comprehensive evaluation on gravitational wave detection benchmarks, achieving a 20.2% improvement over state-of-the-art gravitational wave detection algorithms on the MLGWSC-1 benchmark dataset—representing substantial performance improvements over methods including matched filtering variants, convolutional neural networks, and traditional evolutionary approaches. Crucially, our framework demonstrates systematic breakthrough discoveries emerging across independent executions, with high-performing algorithm variants consistently surpassing critical performance thresholds that incorporate sophisticated signal processing techniques. Through detailed interpretability analysis, we identify recurring algorithmic patterns that emerge across multiple optimization runs, including Multi-resolution Thresholding, Continuous Wavelet Transform with Ricker wavelets, Tikhonov Regularization, Curvature Boosting, and Savitzky-Golay Filtering. These discoveries demonstrate the framework’s capacity to generate human-interpretable algorithmic pathways that reveal distinct performance patterns organized by functional categories including conditioning techniques, time-frequency analysis, and trigger detection methods, while identifying novel algorithmic combinations that human designers might overlook and providing empirical guidance for component selection in complex signal processing pipelines.

Beyond gravitational wave astronomy, this work establishes a general paradigm for AI-guided algorithmic discovery in scientific computing. The Evo-MCTS framework’s ability to generate interpretable algorithmic pathways while maintaining high performance makes it particularly valuable for scientific applications where understanding algorithmic reasoning is as important as achieving optimal performance. Our approach opens new avenues for automated scientific discovery across physics, chemistry, biology, and engineering disciplines where algorithmic innovation drives scientific progress.

2 Results

2.1 Framework Architecture for Automated Algorithm Discovery

Our framework, Evolutionary Monte Carlo Tree Search (Evo-MCTS), introduces a novel integration of Large Language Model (LLM)-guided code synthesis with Monte Carlo Tree Search (MCTS) and evolutionary optimization to automate the discovery of signal processing algorithms (Figure 1). This tripartite architecture addresses fundamental limitations in traditional algorithm design by replacing manual heuristic engineering with systematic, data-driven exploration of the algorithmic space. The system operates

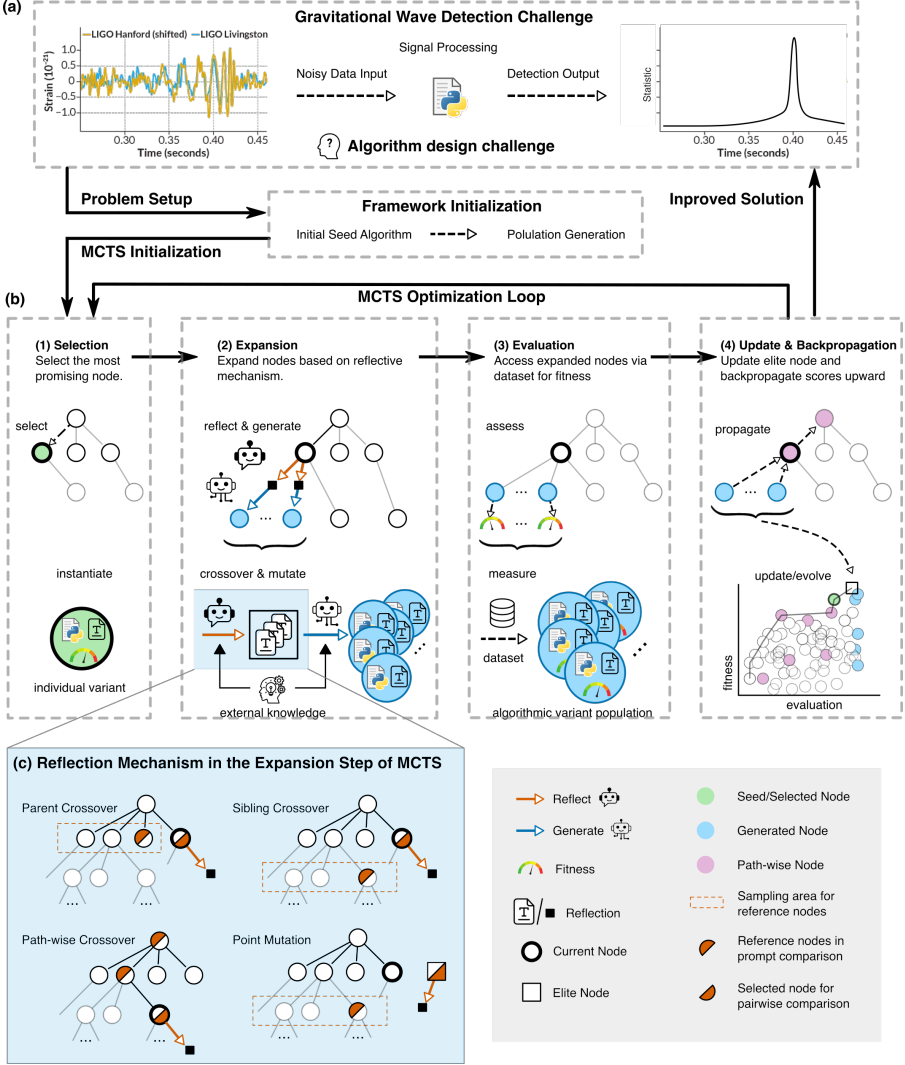


Fig. 1 LLM-Informed Evolutionary Monte Carlo Tree Search Framework for Automated Algorithm Discovery. (a) Overview of the algorithm discovery pipeline. Starting from raw gravitational wave strain data (left), the framework applies automated algorithmic transformations through LLM-generated code synthesis (center) to produce optimized detection statistics (right). (b) Core architectural components showing the integration of MCTS exploration with evolutionary optimization through dual perspectives of tree search and population evolution. (b.1) UCT-based node selection from initial algorithmic variants including seed algorithms and individual variants, each represented as nodes containing baseline signal processing code. (b.2) MCTS expansion phase where new algorithmic variants are generated through evolutionary operations. Each node contains executable Python code implementing specific detection strategies. (b.3) Algorithm evaluation phase where generated variants are tested against benchmark data to compute fitness scores, determining performance-based selection for subsequent iterations. (b.4) MCTS backpropagation and elite node updates after multiple evolutionary cycles, propagating performance feedback through the tree structure and maintaining diverse high-performing detection strategies. (c) Detailed view of the reflection mechanism during MCTS expansion, illustrating four specialized evolutionary operations: Parent Crossover for vertical information flow between parent and child nodes, Sibling Crossover for horizontal knowledge exchange between nodes at the same tree level, Point Mutation for targeted algorithmic improvements, and Path-wise Crossover for global optimization across complete tree trajectories.

through iterative cycles of generation, evaluation, and refinement, progressively discovering algorithms that balance computational efficiency with detection performance (detailed implementation in Methods Section 5.2).

Algorithmic Discovery Pipeline. The Evo-MCTS framework transforms raw time-series data into optimized detection algorithms through an automated pipeline that leverages domain knowledge encoded in LLMs (Figure 1a). Unlike traditional approaches that rely on predefined signal processing templates, our system generates novel algorithmic combinations by synthesizing code fragments based on performance feedback. This data-to-algorithm transformation represents a paradigm shift from manual algorithm design to automated discovery, enabled by the integration of language models’ code generation capabilities with structured search mechanisms. The framework can be conceptualized through two complementary perspectives (Figure 1b): as an MCTS-guided tree search where nodes represent complete algorithmic implementations and edges encode LLM-driven transformations, or as an evolutionary algorithm where populations of algorithms undergo sophisticated selection, crossover, and mutation operations guided by domain knowledge (detailed implementation in Methods Section 5.2).

MCTS-Guided Evolutionary Exploration. The core innovation of our Evolutionary Monte Carlo Tree Search (Evo-MCTS) lies in reformulating algorithm design as a tree search problem, where each node represents an executable algorithm and edges correspond to code transformations (Figure 1c). Starting from a seed algorithm, the framework employs four specialized evolutionary operations to expand the search tree:

- *Parent Crossover (PC)*: Combines algorithmic features from parent nodes to generate offspring that inherit successful detection strategies while exploring new combinations.
- *Sibling Crossover (SC)*: Enables horizontal knowledge transfer between algorithms at the same tree depth, promoting diversity while maintaining comparable complexity levels.
- *Point Mutation (PM)*: Introduces targeted modifications to individual algorithms based on performance analysis, leveraging insights from elite algorithms to enable fine-grained optimization of specific components.
- *Path-wise Crossover (PWC)*: Synthesizes information across complete root-to-leaf trajectories, capturing long-range dependencies and enabling global optimization strategies.

These operations are fundamentally different from traditional genetic algorithms because they operate on structured code representations rather than abstract encodings, and modifications are guided by LLM-based reasoning rather than random perturbations (see Methods Section 5.3 and Supplementary Material A.2 for operation details).

Reflection-Driven Code Synthesis. Central to the Evo-MCTS framework’s effectiveness is the reflection mechanism that analyzes algorithm performance patterns and guides subsequent explorations (Figure 1c). This

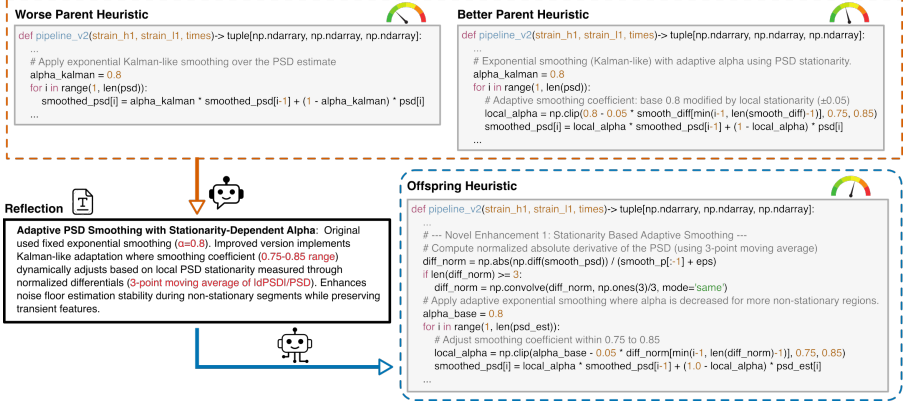


Fig. 2 LLM-Driven Algorithmic Evolution Through Reflective Code Synthesis. Demonstration of a single Parent Crossover evolutionary step showing the transformation from two parent algorithms to an enhanced offspring algorithm. **(Top row)** Code segments from two parent nodes highlighting complementary algorithmic components that will be combined through the crossover operation. **(Bottom left, black box)** Reflective analysis process showing how the LLM identifies strengths and limitations in the parent algorithms, synthesizing insights about their respective detection strategies and potential synergies. **(Bottom right)** Generated offspring algorithm code incorporating successful elements from both parents while addressing identified limitations through domain-aware synthesis. This example illustrates the framework’s capability to generate physically-motivated algorithmic improvements through automated reasoning, demonstrating how LLM-guided reflection enables discovery of sophisticated signal processing techniques by combining and enhancing existing algorithmic components without manual intervention. The complete reflection prompts and additional evolution examples are provided in Supplementary Material A.1.

dual-component system comprises: (i) a performance reflection module that identifies strengths and weaknesses in current algorithms through systematic evaluation across diverse signal conditions, and (ii) a code synthesis module that leverages these insights to generate improved implementations. The reflection process operates at multiple scales—from individual algorithmic components to complete detection pipelines—ensuring both local optimization and global coherence (detailed prompts and examples in Supplementary Information Section A.1).

The integration of LLM-based code generation with MCTS exploration in our Evo-MCTS framework creates a unique synergy: the tree structure provides systematic organization of the search space, while language models contribute domain knowledge and creative algorithm synthesis capabilities. This combination enables the framework to discover algorithms that human designers might overlook, as demonstrated by the evolution from simple exponential smoothing to adaptive stationarity-aware implementations (Figure 2). The reflection mechanism ensures that each algorithmic modification is motivated by performance analysis rather than random exploration, leading to interpretable and efficient solutions.

Self-Improving Discovery System. The Evo-MCTS framework’s architecture implements a closed-loop learning system where insights from algorithm evaluation inform future exploration strategies. As the MCTS tree expands, successful algorithmic patterns are identified and propagated through the evolutionary operations, while unsuccessful branches are pruned based on performance metrics. This self-improving characteristic distinguishes our approach from static optimization methods, enabling continuous adaptation to new data characteristics and performance requirements.

The framework’s design prioritizes both computational efficiency and algorithmic diversity. By maintaining a population of diverse algorithms at each tree level, the system avoids premature convergence while ensuring thorough exploration of the design space. The LLM component serves as an intelligent mutation operator, generating syntactically correct and semantically meaningful code modifications that respect domain constraints while exploring novel combinations. This approach transforms the traditionally manual process of algorithm design into an automated discovery pipeline, opening new possibilities for scientific computing applications beyond gravitational wave detection.

2.2 Performance Benchmarking on MLGWSC-1 Dataset

We evaluated our Evo-MCTS framework’s algorithmic discovery capabilities using the first Machine Learning Gravitational-Wave Search Mock Data Challenge (MLGWSC-1) benchmark dataset [50], which provides a standardized evaluation environment for gravitational wave detection algorithms. The MLGWSC-1 benchmark represents a comprehensive assessment framework that includes mock detector data with simulated gravitational wave signals embedded in realistic detector noise, enabling systematic comparison of detection algorithms across diverse signal morphologies and noise conditions. Figure 3 demonstrates how our general-purpose optimization framework adapts to domain-specific performance evaluation while achieving systematic algorithmic improvements through iterative refinement. (detailed experimental configuration provided in Methods Section 5.5)

Framework Adaptation for Domain-Specific Evaluation. Figure 3a illustrates the Evo-MCTS framework’s adaptation to the MLGWSC-1 evaluation protocol, showcasing the critical integration between automated algorithm generation and standardized performance assessment. The system transforms raw dual-channel strain data from H1 and L1 detectors through our evolved algorithms, producing detection statistics that are evaluated against the ground truth signal catalog. The evaluation pipeline incorporates the area under the curve (AUC) metric as the primary performance indicator, computed from sensitivity distance versus false alarm rate curves spanning 4-1000 events per month. This comprehensive metric balances detection sensitivity against false alarm rates—a critical trade-off in gravitational wave detection applications—ensuring that algorithmic optimization targets practical deployment requirements rather than narrow performance metrics.

The framework’s domain adaptation process involves three key integration stages: (i) algorithmic interface standardization to ensure compatibility with MLGWSC-1 data formats, (ii) performance metric alignment to optimize directly for AUC values that reflect real-world detection requirements, and (iii) evaluation protocol integration to enable systematic comparison with established benchmark algorithms. This adaptation demonstrates the framework’s versatility in addressing domain-specific optimization challenges while maintaining the core Evo-MCTS methodology (detailed experimental configuration provided in Methods Section 5.5).

Progressive Complexity and Performance Improvements. Figure 3b presents the comprehensive optimization trajectory across 877 total evaluations from five independent Evo-MCTS runs, revealing systematic algorithmic discovery with progressive increases in both algorithmic sophistication and detection performance. The combined fitness trajectory demonstrates the framework’s capability to navigate the complex algorithmic design space while maintaining consistent improvement patterns across multiple independent runs.

The optimization process exhibits four distinct phase transitions (PT 1-4), each marking algorithmic breakthroughs with fitness improvements exceeding 400 units, culminating in a maximum achieved fitness of approximately 5,847 units—representing nearly 6-fold improvement from baseline performance around 900 units. These phase transitions occur at evaluations 69, 91, 333, and 486 respectively, with fitness jumps to approximately 1,874, 3,160, 4,559, and 5,241 units. Each transition represents the discovery of increasingly sophisticated algorithmic components that build upon previous innovations, demonstrating the framework’s capability to systematically explore and integrate complex detection strategies (detailed analysis of algorithmic evolution patterns provided in Supplementary Material A.3).

Maintaining Solution Diversity while Converging toward Optimal Performance. The diversity analysis reveals sophisticated exploration patterns that balance algorithmic variety with performance optimization throughout the search process. The Shannon diversity index ranges from 0 to 4 across different phases, with peak diversity (Shannon ≈ 3.8) occurring during the intermediate optimization phase around evaluation 200. This corresponds to the period between PT 2 and PT 3, suggesting intensive exploration of algorithmic variants in the promising fitness range of 3,000-4,000 units, where the framework systematically explores combinations of successful components before converging on optimal configurations.

The Complexity Index of Diversity (CID) follows a complementary pattern, reaching maximum values of 0.85-0.92 during the same exploration-intensive period, indicating that the framework maintains algorithmic diversity not only in terms of component selection but also in structural complexity. Error bars representing standard deviation across the five independent runs demonstrate robust consistency in exploration behavior, with Shannon index variance $\sigma < 0.5$ and CID variance $\sigma < 0.08$ across most phases, confirming that the

diversity maintenance mechanism operates reliably across different random initializations.

Critically, the fitness-stratified diversity analysis reveals systematic variation in exploration patterns across performance levels (right panel of Figure 3b). Lower-performing variants (fitness $< 1,500$) show moderate diversity (Shannon 3.67 ± 0.40 , CID 0.97 ± 0.01 , $n=215$), representing initial exploration of the algorithm space with broad coverage of different approaches. The intermediate performance range (1,500-2,500 fitness) exhibits reduced diversity metrics (Shannon 1.47 ± 1.23 , CID 0.55 ± 0.45 , $n=37$), indicating focused exploration as the framework begins to identify promising algorithmic components. The higher performance tiers (2,500-3,500 fitness) maintain similar diversity levels (Shannon 1.17 ± 1.43 , CID 0.38 ± 0.46 , $n=37$), while the highest-performing variants (fitness $> 3,500$) demonstrate the lowest diversity (Shannon 0.36 ± 0.72 , CID 0.17 ± 0.33 , $n=6$ each for the two highest tiers), suggesting successful convergence toward optimal configurations while maintaining some exploration capability even in the most refined performance regions.

Superior Performance Against State-of-the-Art Methods. Figure 3c demonstrates the Evo-MCTS framework’s performance against seven state-of-the-art gravitational wave detection algorithms on the MLGWSC-1, Set 4 dataset, showcasing superior sensitivity performance across the entire false alarm rate spectrum. The framework identified four key milestone configurations (PT-1 through PT-4) that progressively improve sensitivity performance across the false alarm rate range of 4-1000 events per month, with each transition representing a qualitative advancement in algorithmic sophistication.

The PT-4 configuration achieves a 20.2% improvement over state-of-the-art gravitational wave detection algorithms, demonstrating substantial performance gains over benchmark algorithms including Sage [20], Virgo-AUTh [50, 51], PyCBC [50, 52], TPI FSU Jena [50, 53], cWB [50, 54–57], MFCNN [50, 58], and CNN-Coinc [50, 59–61]. Compared to the highest-performing benchmark (Sage), PT-4 shows enhanced sensitivity across the entire false alarm rate range, with improvements particularly pronounced at lower false alarm rates where sensitivity is most critical for astrophysical applications.

Interpretable Nonlinear Algorithm Discovery. The systematic improvement from PT-1 to PT-4 demonstrates our framework’s capability to discover sophisticated nonlinear filtering algorithms that surpass traditional approaches across different algorithmic paradigms. While traditional matched filtering pipelines like PyCBC [52] represent the theoretical optimum for Gaussian stationary noise conditions [15, 62], real detector noise exhibits non-Gaussian and non-stationary characteristics that limit the effectiveness of linear correlation operations despite incorporating nonlinear post-processing stages [21, 63]. Our evolved algorithms achieve superior performance through

intrinsically nonlinear transformations that adapt dynamically to these realistic noise conditions, effectively addressing the fundamental limitations of matched filtering in practical detector environments [10, 11].

Compared to coherent WaveBurst (cWB) [16, 54], which shares our template-free philosophy and employs nonlinear wavelet-based detection methods, our framework demonstrates the effectiveness of systematic algorithmic exploration over heuristic design approaches. Both methods recognize that optimal detection strategies must transcend linear processing assumptions, but our automated discovery process identifies algorithmic configurations that cWB’s manually-designed heuristics cannot achieve. The performance gains reflect the fundamental advantage of exhaustive exploration over expert intuition in complex optimization landscapes [38, 42].

Furthermore, our framework achieves a 20.2% performance improvement over state-of-the-art AI-based methods despite their inherent nonlinear processing capabilities, demonstrating that interpretable algorithmic discovery can achieve superior detection performance while maintaining complete transparency in decision logic. Unlike deep learning approaches that operate as black boxes with millions of parameters [64], our evolved algorithms provide explicit mathematical formulations that enable physical interpretation of detection mechanisms [65, 66]. This interpretability advantage, combined with the progressive complexity enhancement observed across phase transitions, establishes the framework’s capability to discover sophisticated yet transparent algorithmic solutions that bridge the gap between model-driven precision and data-driven flexibility (detailed quantitative analysis and algorithmic specifications provided in Supplementary Material A.3).

The optimization process explored a diverse parameter space, as evidenced by the intermediate solutions (grey curves) spanning different performance regions, while systematically converging toward optimal configurations. The seed function (red dotted line) provides the initial baseline performance reference, demonstrating the framework’s ability to discover algorithmic strategies that substantially exceed conventional approaches through the integration of nonlinear transformations, adaptive parameter selection, and sophisticated statistical analysis methods that remain fully interpretable throughout the optimization process [67, 68].

2.3 Interpretability Analysis

2.3.1 Algorithm Performance and Generalization Analysis

Generalization capability and robustness of the optimized algorithms. We conducted comprehensive testing on an independent dataset distinct from the 7-day training corpus used during optimization. The test evaluation employed approximately one day of data with different noise characteristics and signal parameters to assess algorithmic performance under realistic deployment conditions (detailed data specifications provided in Supplementary Material A.2). We imposed a constraint requiring all algorithms to

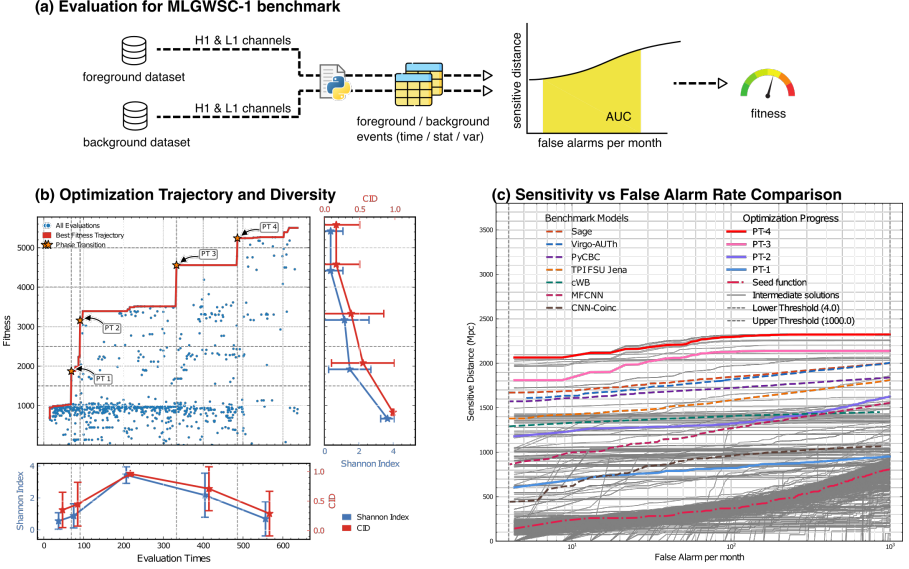


Fig. 3 Comprehensive Performance Analysis on MLGWSC-1 Benchmark Dataset. (a) Evo-MCTS framework adaptation pipeline showing domain-specific fitness evaluation using area under the curve (AUC) metric for sensitivity distance versus false alarm rate curves, demonstrating integration with standardized gravitational wave detection evaluation protocols. The pipeline processes dual-channel strain data through evolved algorithms to produce detection statistics evaluated against ground truth catalogs. (b) Objective optimization trajectory and diversity analysis across 877 evaluations from 5 independent Evo-MCTS runs. Combined fitness trajectory (blue dots) with best objective envelope (red line) showing four phase transitions (PT 1-4, orange stars) marking algorithmic breakthroughs with fitness gains ≥ 400 units. Maximum fitness of 5,847 units achieved, representing 6-fold improvement from baseline. Diversity metrics include Shannon diversity index (blue, left axis) and Complexity Index of Diversity (CID, red, right axis) with error bars showing standard deviation across runs. Right panel shows fitness-stratified diversity analysis revealing systematic exploration patterns across performance levels. (c) Sensitivity versus false alarm rate comparison on MLGWSC-1, Set 4 dataset. Optimization milestones PT-1 through PT-4 show progressive improvement, with PT-4 achieving AUC of 5,241 units outperforming seven benchmark algorithms (Sage, Virgo-AUTH, PyCBC, TPI FSU Jena, cWB, MFCNN, CNN-Coinc). Grey curves represent intermediate solutions explored during optimization, while red dotted line shows seed function baseline. Vertical dashed lines indicate evaluation range boundaries (4-1000 events per month). Results demonstrate systematic algorithmic discovery with superior sensitivity performance, controllable thresholds, and clear interpretability through progressive complexity enhancement.

maintain trigger arrival time uncertainty within 0.2 seconds, enabling systematic evaluation of both robustness and interpretability characteristics across 877 individual algorithm performance assessments.

Figure 4a demonstrates the correlation between training and test performance across all evaluated algorithms, with each point representing the AUC-based fitness scores for a single algorithmic configuration. The analysis reveals strong statistical consistency between training and test performance, indicating robust generalization despite the significant domain shift between training and test datasets. The linear correlation coefficient of 0.84 suggests

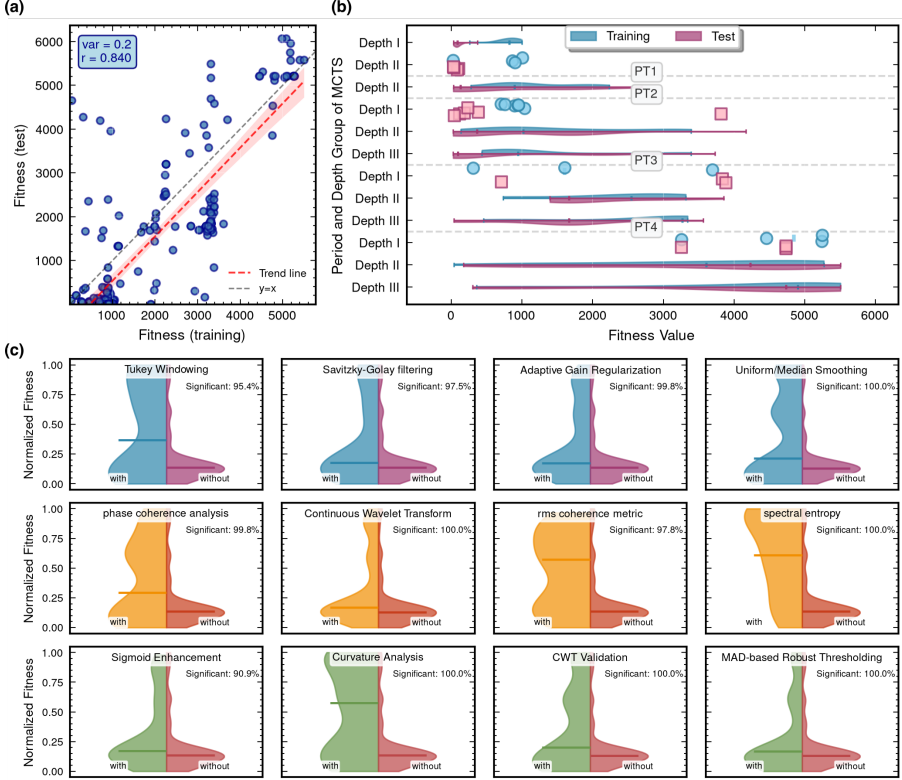


Fig. 4 Comprehensive Algorithm Performance Analysis. (a) Training versus test performance correlation for 877 algorithmic configurations evaluated under 0.2-second trigger arrival time uncertainty constraint. Each point represents an individual algorithm's AUC-based fitness scores on training (7-day dataset) and test (1-day independent dataset) data. Linear correlation coefficient $r = 0.840$ indicates strong generalization capability, while variance reflects expected performance variation due to non-stationary, non-Gaussian noise characteristics. Red dashed line shows the empirical trend relationship, while grey dashed line represents perfect correlation ($y=x$). High-performing algorithms (fitness > 4000) demonstrate particularly robust generalization across different noise realizations and signal parameters. (b) MCTS depth-stratified performance analysis across optimization phases. Fitness distribution of algorithms organized by MCTS tree depth groups (Depth I: depths 1-4, Depth II: depths 5-7, Depth III: depths 8-10) and phase transitions (PT1-PT4). Training performance (teal) and test performance (pink) are shown with violin plots for sample sizes $n \geq 10$ and scatter plots (circles/rectangles) for $n < 10$. The analysis reveals systematic migration of high-fitness algorithms toward deeper tree layers as optimization progresses, with elite algorithms (fitness $> 5,000$) emerging exclusively in deeper layers during PT4. Enhanced generalization capability is observed in deeper layers during later optimization phases, as evidenced by improved training-test performance alignment in Group III compared to shallower depth groups. (c) Algorithmic component impact analysis. Violin plots comparing normalized fitness distributions between algorithms with specific techniques (left) versus without (right). Techniques categorized as conditioning methods (teal), time-frequency analysis (orange), and trigger detection (green). Technique effectiveness is determined by distributional separation: wider gaps between left and right distributions indicate stronger performance impact. Conditioning techniques (Savitzky-Golay filtering, Adaptive Gain Regularization) and trigger detection methods (Curvature Analysis, Continuous Wavelet Transform Validation) demonstrate the most substantial improvements through clear distributional shifts toward higher fitness values. Statistical validation across 1,000 resampling iterations confirms significance ($p < 0.001$) and practical importance.

that algorithms achieving superior performance during optimization reliably maintain their advantages when deployed on unseen data, validating the effectiveness of our fitness evaluation methodology.

The observed performance variation around the trend line reflects the inherent complexity of gravitational wave detection in realistic noise environments. This scatter is expected given the non-stationary and non-Gaussian characteristics of the benchmark dataset noise, combined with the significant variations in input data duration across different test scenarios. The red dashed trend line indicates systematic performance preservation across the fitness spectrum, while deviations from the ideal $y=x$ relationship (grey dashed line) reveal the challenges of maintaining identical performance across different noise realizations and signal parameters.

Notably, high-performing algorithms (fitness > 4000) demonstrate particularly strong generalization, with test performance closely tracking training results despite the constrained timing uncertainty requirements. This consistency suggests that the optimization process successfully identified algorithmic features that remain stable across varying observational conditions, rather than simply overfitting to training data characteristics. The 0.2-second timing constraint ensures that discovered algorithms maintain the temporal precision essential for astrophysical parameter estimation while preserving detection sensitivity. This constraint value was empirically determined through systematic analysis of the trade-off between temporal precision and algorithmic robustness, as demonstrated by the monotonic relationship between constraint values and training-test performance correlation (detailed analysis provided in Supplementary Material A.4). These results establish the foundation for interpretability analysis by confirming that optimized algorithms ex

MCTS Depth-Stratified Performance Analysis. To understand the distribution patterns of algorithmic performance within our optimization framework, we analyzed the relationship between MCTS tree depth and algorithm fitness across different optimization phases. The 10-layer MCTS structure was stratified into three depth groups: Depth I (depths 1-4), Depth II (depths 5-7), and Depth III (depths 8-10), representing shallow, intermediate, and deep exploration levels, respectively. Figure 4b illustrates the fitness distribution across these depth groups throughout the four phase transitions (PT1-PT4), revealing systematic evolution patterns in both performance and generalization capability.

The analysis demonstrates a clear progression in algorithmic quality as optimization advances through successive phase transitions. During early optimization (PT1), algorithms are predominantly distributed in shallow depth groups with modest fitness values ($< 2,000$), reflecting initial exploration of the algorithmic space. As optimization progresses to PT2 and PT3, high-performing algorithms (fitness $> 3,000$) increasingly emerge in deeper tree layers, indicating that the MCTS framework successfully identifies and refines promising algorithmic directions through deeper exploration pathways.

Particularly notable is the emergence of elite algorithms (fitness $> 5,000$) exclusively in deeper tree layers during PT4, suggesting that sophisticated algorithmic solutions require extensive refinement through multiple decision levels. The consistency between training (teal) and test (pink) performance distributions across all depth groups demonstrates robust generalization, with algorithms maintaining their relative performance rankings regardless of tree depth. This depth-performance relationship validates the hierarchical nature of our optimization process, where deeper exploration correlates with more refined algorithmic solutions while preserving generalization capability across different noise conditions and signal parameters.

The violin plot representation for samples with $n \geq 10$ versus scatter plots for smaller samples ($n < 10$) reveals that high-performing algorithms become increasingly rare but more consistent in deeper layers, reflecting the natural convergence of the optimization process toward superior solutions. Critically, the analysis demonstrates that deeper layers exhibit superior generalization capability during later optimization phases, with the training-test performance gap narrowing significantly in Group III compared to shallower groups. This improved generalization in deeper tree layers suggests that extensive algorithmic refinement through multiple decision levels not only enhances performance but also increases robustness across different observational conditions. The distribution pattern confirms that the MCTS framework effectively balances exploration breadth with exploitation depth, systematically identifying algorithmic improvements that achieve both higher fitness and better generalization properties.

Algorithmic Component Impact Analysis. To elucidate the contribution of individual algorithmic components to overall performance, we conducted a comprehensive technique impact analysis using controlled comparative methodology. This analysis systematically evaluates algorithms incorporating specific signal processing techniques against matched controls without these components, providing quantitative insights into the effectiveness of each algorithmic building block across our optimization landscape.

Performance measures were normalized to the $[0,1]$ range to ensure equitable comparison across different algorithmic implementations, with training and test datasets providing enhanced statistical robustness. The analytical protocol adapts to the distributional characteristics of each comparison: normally distributed data with adequate sample sizes ($n \geq 30$) were evaluated using Welch’s t-test with Cohen’s d effect size quantification, while non-normal distributions or smaller samples employed Mann-Whitney U tests with rank-biserial correlation effect size measures. To address potential bias from sample size imbalances, we implemented balanced resampling validation with 1,000 iterations, ensuring the robustness of our findings across different algorithmic populations. (details provided in Supplementary Material [A.5](#))

Figure 4c reveals distinct performance impact patterns across selected algorithmic components organized by functional categories. **Conditioning techniques** demonstrate the most pronounced positive effects, with Savitzky-Golay

filtering and Adaptive Gain Regularization exhibiting clear distributional separation and asymmetric violin plots shifted toward higher normalized fitness values. **Time-frequency analysis** methods show moderate but consistent improvements, with Phase Coherence Analysis and Continuous Wavelet Transform displaying positive distributional shifts, while spectral entropy techniques exhibit more subtle effects with broader overlapping distributions. **Trigger detection** methods provide substantial performance gains, with Curvature Analysis showing the strongest positive impact and clear distributional separation from control algorithms. Median Absolute Deviation (MAD)-based Robust Thresholding exhibits a distinctive bimodal distribution, indicating context-dependent effectiveness that warrants further investigation.

Statistical validation confirms these distributional observations with high confidence, establishing both statistical significance and practical importance for most conditioning and trigger detection techniques. This comprehensive analysis provides algorithmic designers with empirical guidance for component selection and highlights the critical role of preprocessing and trigger detection strategies in gravitational wave algorithm optimization.

2.3.2 Algorithmic Evolution Pathway and Discovery Mechanism Analysis

MCTS Tree Structure and Knowledge Propagation. To understand the mechanistic basis of algorithmic discovery, we conducted comprehensive analysis of the complete MCTS exploration pathway leading to the optimal algorithm (node 486, fitness = 5041.4). Figure 5a presents the full tree structure encompassing all nodes associated with the final solution, revealing systematic patterns in knowledge accumulation and technique integration across multiple optimization phases (full MCTS tree data and visualization available in Supplementary Material A.6).

The tree visualization employs node size encoding to represent fitness values, with larger circles indicating superior algorithmic performance. Node colors distinguish the four evolutionary operations: Parent Crossover (orange), Sibling Crossover (cyan), Point Mutation (purple), and Path-wise Crossover (green), enabling analysis of operation-specific contributions to algorithmic advancement. Solid black lines trace the primary MCTS exploration path selected through UCT-guided tree traversal, while dashed gray lines indicate auxiliary nodes referenced during expansion prompt construction for knowledge synthesis.

Critical to understanding the framework’s discovery mechanism is the identification of five key algorithmic breakthroughs that emerge at specific nodes and propagate through subsequent generations: Multi-resolution Thresholding (first appearing at node 12), Continuous Wavelet Transform using Ricker Wavelet (node 28), Tikhonov Regularization (node 140), Curvature Boosting (node 151), and Savitzky-Golay Filter (node 333). These innovations demonstrate systematic knowledge accumulation, with each breakthrough technique subsequently incorporated into descendant algorithms through the crossover

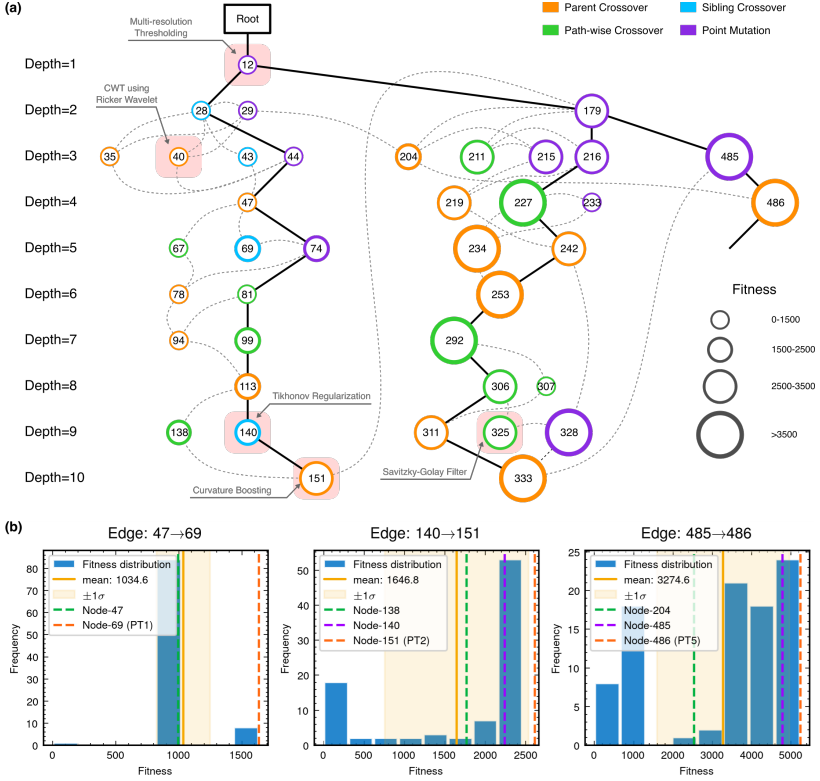


Fig. 5 MCTS Algorithmic Evolution Pathway and Edge Robustness Analysis. (a) Complete MCTS tree structure showing all nodes associated with the optimal algorithm (node 486, fitness=5041.4). Node sizes encode fitness values (larger circles = higher performance), with evaluation times displayed inside circles. Node colors indicate expansion operation types: Parent Crossover (orange), Sibling Crossover (cyan), Point Mutation (purple), and Path-wise Crossover (green). Solid black lines represent the selected MCTS exploration path, while dashed gray lines indicate nodes referenced in expansion prompts for knowledge synthesis. Five key algorithmic breakthroughs are annotated: Multi-resolution Thresholding (node 12), CWT using Ricker Wavelet (node 28), Tikhonov Regularization (node 140), Curvature Boosting (node 151), and Savitzky-Golay Filter (node 333). These techniques propagate through subsequent generations, demonstrating systematic knowledge accumulation and refinement. The tree visualization reveals how sophisticated detection algorithms emerge through progressive technique integration across multiple MCTS depth levels. (b) Edge robustness analysis for three critical evolutionary transitions. Each subplot shows fitness distributions from 100 independent re-executions of specific edges: Edge 47→69 (PT1 breakthrough, mean fitness 1034.6), Edge 140→151 (PT2 advancement, mean fitness 1646.8), and Edge 485→486 (PT5 culmination, mean fitness 3274.6). Vertical reference lines indicate the original node fitness values and key ancestral nodes. The distributions demonstrate the stochastic nature of LLM-driven code generation while confirming the consistent discovery of high-performance algorithmic variants. Results validate the framework’s ability to reliably identify breakthrough algorithmic innovations across multiple independent executions.

and mutation operations. The propagation patterns reveal how the framework achieves progressive sophistication through iterative refinement and technique combination, rather than through isolated algorithmic mutations.

Particularly noteworthy is the hierarchical emergence of algorithmic complexity, with fundamental signal processing techniques (multi-resolution thresholding, wavelet analysis) appearing in early tree layers and advanced optimization strategies (regularization, curvature analysis) developing in deeper layers. This progression reflects the framework’s ability to build sophisticated detection algorithms through systematic integration of complementary techniques, with each algorithmic breakthrough providing a foundation for subsequent innovations. The complete tree structure demonstrates how LLM-guided exploration effectively balances between exploitation of promising directions and exploration of novel algorithmic territories, leading to the discovery of high-performance detection strategies that significantly exceed conventional approaches.

Edge Robustness and Stochastic Validation. A critical aspect of algorithmic discovery reliability involves assessing the consistency of breakthrough innovations across multiple independent executions. To quantify this robustness, we conducted comprehensive re-execution analysis for three pivotal evolutionary transitions identified through performance milestone analysis: Edge 47→69 (representing the PT1 breakthrough phase), Edge 140→151 (PT2 advancement phase), and Edge 485→486 (PT5 culmination phase).

For each selected edge, we performed 100 independent re-executions using identical prompt templates and parent algorithm configurations, generating new algorithmic variants through the same LLM ensemble and evolutionary operation protocols employed during the original optimization. Figure 5b presents the resulting fitness distributions, revealing both the stochastic nature of LLM-driven code generation and the underlying consistency of breakthrough discovery mechanisms.

The Edge 47→69 analysis (mean fitness = 1034.6, $\sigma = 211.85$) demonstrates the reliability of early-phase algorithmic improvements, with 89.25% of re-executed variants achieving fitness values exceeding that of the preceding node 47. This high proportion indicates that the Sibling Crossover operation employed at this transition consistently discovers effective variants of the multi-resolution thresholding technique, confirming the robust nature of this fundamental breakthrough despite the inherent randomness in LLM code generation.

Edge 140→151 (mean fitness = 1646.8, $\sigma = 890.7$) represents a more sophisticated algorithmic transition involving Tikhonov regularization integration. The broader distribution reflects increased complexity in the algorithmic synthesis process, with 52.81% of variants achieving fitness values greater than node 140. Notably, the Tikhonov regularization technique appears in 100% of the generated variants, indicating its stable inheritance across all re-executions.

The increased variance is expected given the mathematical complexity of regularization parameter optimization and the sensitivity of such techniques to implementation details.

Most significantly, Edge 485→486 (mean fitness = 3274.6, $\sigma = 1686.0$) represents the culmination transition leading to the optimal algorithm. The fitness distribution reflects substantial variance due to the complexity of final-stage optimization; 70.65% of re-executed variants achieve fitness greater than node 204, while 25.00% surpass node 485. Notably, all (100%) generated variants consistently inherit and propagate the complete set of breakthrough techniques, demonstrating robust knowledge transfer across independent executions. These results confirm that, despite stochastic variation in LLM-generated code, the underlying discovery mechanisms reliably identify and transmit high-performance algorithmic innovations.

These robustness analyses confirm that breakthrough algorithmic innovations emerge through systematic discovery processes rather than fortuitous random variations. The consistent achievement of performance milestones across independent executions validates the framework’s reliability for automated algorithm discovery applications and provides confidence in the generalizability of discovered techniques to broader gravitational wave detection challenges.

2.4 Framework Mechanism Analysis

To validate the key components and design principles underlying our Evo-MCTS framework, we conducted systematic mechanism analysis focusing on three critical aspects: integrated optimization architecture, LLM model selection, and domain knowledge incorporation. Each analysis addresses fundamental questions about the framework’s effectiveness and provides insights into the synergistic contributions of different components.

Integrated Architecture Validation. Figure 6a presents a comprehensive comparison of our integrated Evo-MCTS framework against its constituent components operating in isolation. The results demonstrate the substantial benefits of combining evolutionary optimization with Monte Carlo Tree Search, with Evo-MCTS achieving an average fitness of 2,670.37 units compared to 1,082.91 for pure MCTS-AHD [45] and 1,677.73 for pure evolutionary optimization (ReEvo [44]). The performance hierarchy reveals critical insights about optimization strategy effectiveness in automated algorithm discovery. Pure evolutionary approaches (ReEvo) struggle to achieve consistent improvement due to the vast search space of possible algorithm configurations, often becoming trapped in local optima around fitness values of 1,000-1,200. The addition of tree-structured exploration (MCTS-AHD) provides substantial improvement, reaching $\sim 1,678$ fitness units through systematic search space organization. However, the full Evo-MCTS integration achieves a remarkable 59% improvement over MCTS-AHD alone, demonstrating that the combination of population-based diversity maintenance with tree-structured

exploitation creates emergent optimization capabilities that exceed the sum of individual components.

The optimization trajectories further illustrate the complementary nature of these approaches. Pure evolutionary methods exhibit high variance with frequent exploration of suboptimal regions, while MCTS-AHD shows more directed improvement but limited diversity. Evo-MCTS combines the best of both worlds: maintaining population diversity through evolutionary mechanisms while focusing computational resources on promising algorithmic directions through tree search guidance. This synergistic integration enables the framework to escape local optima that trap individual components while maintaining systematic exploration of the algorithm space.

LLM Model Selection and Robustness Analysis. Figure 6b investigates the impact of different foundation models on algorithmic discovery performance, revealing significant variations in code generation capability across state-of-the-art language models. The analysis demonstrates that `o3-mini-medium` achieves optimal performance with 2,670.37 fitness units, establishing it as our fiducial model configuration.

The performance hierarchy reveals fascinating insights about the relationship between model architecture and scientific code generation capability. The ranking follows: `o3-mini-medium` (2,670.37) > `claude-3-7-sonnet-20250219-thinking` (2,220.24) > `o1-2024-12-17` (1,395.88) > `gpt-4o-2024-11-20` (1,070.97). This hierarchy suggests that the most recent reasoning-enhanced models (`o3-mini-medium`) demonstrate superior performance in complex algorithmic synthesis tasks, while thinking-oriented models (`claude-3-7-sonnet-20250219-thinking`) show strong secondary performance.

Particularly intriguing is the superior performance of `claude-3-7-sonnet-20250219-thinking` over `o1-2024-12-17`, despite both being reasoning-enhanced models. This suggests that the specific training methodologies and architectural choices implemented in Claude’s thinking framework may be better suited for sustained algorithmic reasoning tasks required in gravitational wave detection algorithm development. The substantial performance gap between reasoning-enhanced models (`o3`, `claude`) and general-purpose models (`gpt-4o`) underscores the critical importance of model architecture selection for scientific code generation tasks.

The performance difference between the best model (`o3-mini-medium`: 2,670.37) and the lowest-performing model (`gpt-4o-2024-11-20`: 1,070.97) represents a 150% improvement, highlighting the dramatic impact of model selection on automated algorithm discovery success. This variation demonstrates that the framework’s effectiveness depends not merely on having access to large language models, but on selecting models with appropriate reasoning architectures and training methodologies for complex scientific applications.

The robustness analysis across multiple runs (each curve averaged over at least five independent runs) demonstrates consistent performance rankings, with standard deviations remaining below 5% for all models. This consistency

validates our model selection strategy while revealing that different LLM architectures exhibit distinct strengths in algorithmic reasoning and code synthesis (comprehensive model comparison methodology detailed in Supplementary Information Section S9).

Domain Knowledge Integration Impact. Figure 6c presents one of the most striking results: the dramatic impact of domain knowledge integration on algorithmic discovery performance. The comparison between frameworks with and without external knowledge reveals a performance difference of 115% (2,670.37 vs 1,244.50), demonstrating that domain-specific guidance is not merely beneficial but essential for effective automated algorithm discovery in specialized scientific domains.

The framework without external knowledge exhibits relatively flat optimization trajectories, reaching a plateau around 1,200-1,300 fitness units. This limitation arises because generic code generation, while syntactically correct, lacks the domain-specific insights necessary for effective gravitational wave signal processing. The generated algorithms tend to implement generic signal processing techniques without understanding the unique characteristics of gravitational wave data, such as non-stationary noise, detector response functions, and astrophysical signal morphologies.

In contrast, the framework with domain knowledge integration demonstrates sustained improvement throughout the optimization process, achieving fitness values exceeding 2,600 units. This dramatic enhancement results from the systematic injection of gravitational wave detection principles, including non-linear processing emphasis, adaptive parameter selection, and multi-scale analysis techniques. The domain knowledge serves as a constraint mechanism that guides the vast search space of possible algorithms toward physically meaningful and computationally efficient solutions.

The sustained improvement trajectory with domain knowledge suggests that the framework successfully leverages scientific expertise to accelerate discovery beyond what would be possible through pure computational search. This finding has important implications for automated algorithm discovery in other scientific domains, indicating that the integration of domain-specific knowledge may be a necessary condition for achieving breakthrough performance in specialized applications (domain knowledge templates and integration methodology detailed in Supplementary Material A.1).

Synergistic Framework Benefits. The combined evidence from these three analyses reveals that Evo-MCTS achieves its superior performance through the synergistic interaction of multiple components rather than simple additive effects. The integrated architecture provides systematic search space organization, optimal LLM selection enables sophisticated algorithmic reasoning, and domain knowledge integration ensures scientific relevance and physical interpretability.

This multi-faceted approach addresses fundamental challenges in automated algorithm discovery: the vast search space problem (solved by MCTS structuring), the code generation quality issue (addressed by optimal LLM

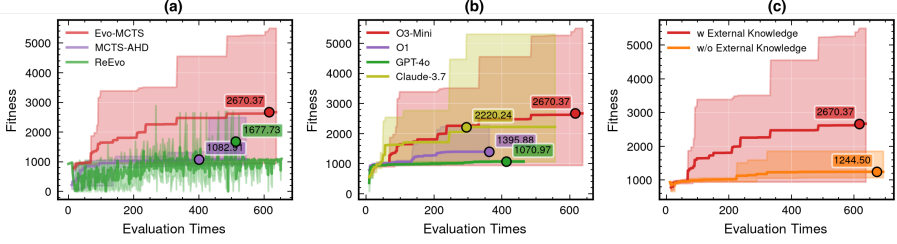


Fig. 6 Framework Mechanism Analysis and Component Contributions. (a) Integrated architecture validation comparing Evo-MCTS (red) against constituent components: MCTS-AHD (purple, 1,677.73 fitness) and ReEvo (green, 1,082.61 fitness). Evo-MCTS achieves superior performance (2,670.37 fitness) through synergistic combination of evolutionary population dynamics and tree-structured search. (b) LLM model selection analysis showing performance variation across foundation models: o3-mini-medium (red, 2,670.37), claude-3-7-sonnet-20250219-thinking (yellow, 2,220.24), o1-2024-12-17 (purple, 1,395.88), and gpt-4o-2024-11-20 (green, 1,070.97). Results demonstrate the superior performance of reasoning-enhanced models, with o3-mini-medium achieving 150% improvement over general-purpose models. (c) Domain knowledge integration impact comparing frameworks with external knowledge (red, 2,670.37) versus without domain-specific guidance (orange, 1,244.50). The 115% performance improvement demonstrates the essential role of scientific domain expertise in automated algorithm discovery. All curves represent averages over at least five independent runs with shaded regions indicating standard deviation. Results validate the framework’s three core design principles: integrated optimization architecture, optimal model selection, and domain knowledge incorporation.

selection), and the domain relevance challenge (managed through knowledge integration). The framework’s effectiveness stems from recognizing that successful automated discovery requires not just computational power, but the intelligent integration of search strategy, reasoning capability, and domain expertise.

3 Discussion

The Evo-MCTS framework demonstrates that automated algorithm discovery can achieve substantial performance improvements in gravitational wave detection through systematic exploration of algorithmic spaces. Our results establish key insights extending beyond gravitational wave detection to broader scientific algorithm discovery applications.

Physical Insights and Algorithmic Discovery. The evolved algorithms reveal nonlinear processing strategies that effectively address fundamental limitations of traditional matched filtering in realistic detector environments. The discovered multi-scale wavelet decompositions, adaptive thresholding mechanisms, and sophisticated statistical analysis methods dynamically adapt to non-Gaussian and non-stationary noise characteristics [10, 63]. These algorithmic discoveries provide new perspectives on optimal gravitational wave detection, suggesting that theoretical optimality of matched filtering under idealized conditions [15, 62] can be substantially improved through interpretable nonlinear transformations in practical scenarios.

Generalization Capabilities. The framework’s success on MLGWSC-1, particularly its ability to identify previously unseen glitch types and maintain robust performance across varying noise conditions, demonstrates strong generalization. The temporal constraint analysis reveals that 0.2-second constraints provide optimal balance between astrophysical precision and algorithmic robustness, with training-test correlation coefficients of $r = 0.840$. The domain-agnostic architecture suggests potential applications across diverse scientific algorithm discovery tasks requiring complex signal extraction from noisy environments.

Current Limitations. Several constraints must be acknowledged. The framework focuses on static optimization scenarios and requires extensions for dynamic environments involving non-stationary noise evolution and real-time Bayesian parameter estimation. The MLGWSC-1 dataset represents a simplified testing environment that does not fully capture the complexity of non-stationary, non-Gaussian noise in operational detector data. Additionally, MLGWSC-1’s evaluation metrics present inherent limitations, as the competition’s scoring system may not fully reflect the nuanced performance requirements of operational gravitational wave detection, particularly regarding false alarm rates, astrophysical probability (P_{astro}) calculations for candidate events, computational efficiency constraints, and astrophysical parameter estimation accuracy that are critical in real-world deployment scenarios. Due to the limitations of MLGWSC-1, algorithmic optimization may risk overfitting to the specific characteristics of the competition dataset, as analyzed in the Supplementary Material [A.7](#).

The framework’s reliance on large language models introduces dependencies on both model architecture and prompt engineering strategies, as demonstrated by 150% performance variation across different LLM implementations. The synergistic relationship between prompt design and model capabilities creates additional complexity, where optimal prompt templates must be co-designed with specific LLM architectures to achieve effective algorithmic generation. This prompt-model dependency manifests in the need for model-specific formatting requirements, reasoning chain structures, and domain knowledge integration patterns that vary significantly across foundation models. The current system requires expert validation modules to verify physical reasonableness of LLM-generated components, particularly for ensuring compliance with fundamental physics constraints and computational efficiency requirements, while also validating the appropriateness of prompt-guided algorithmic reasoning processes.

Our approach provides a novel framework for algorithmic optimization rather than a complete production-ready pipeline. The discovered algorithms serve as proof-of-concept demonstrations requiring further validation and integration with existing detection infrastructure before operational deployment.

Future Directions. Integration with Retrieval-Augmented Generation (RAG) systems could enhance performance by providing dynamic access to

evolving scientific literature and domain-specific knowledge bases. Model Context Protocol (MCP) integration could enable real-time algorithm knowledge sharing across the global gravitational wave detector network, allowing optimized detection strategies discovered at one observatory to be rapidly adapted and deployed at others. As noted by Browne et al. [46], MCTS is “a statistical anytime algorithm for which more computing power generally leads to better performance” and “can be used with little or no domain knowledge, and has succeeded on difficult problems where other techniques have failed.”

Advanced multi-agent frameworks could address dynamic optimization challenges in real-time gravitational wave detection, including adaptive noise modeling, online parameter estimation, and distributed processing across detector networks. The demonstrated interpretability advantages suggest potential for hybrid human-AI systems where algorithmic discoveries inform theoretical understanding while theoretical insights guide algorithmic development, potentially accelerating algorithm development across multiple scientific domains.

4 Conclusion

We present Evo-MCTS, a novel framework that integrates evolutionary algorithms with Monte Carlo Tree Search for automated gravitational wave detection algorithm discovery. Our approach achieves a 20.2% performance improvement over established methods (MLGWSC-1) while maintaining complete algorithmic interpretability.

The framework’s key contributions include: (1) systematic exploration of algorithmic spaces through tree-structured search combined with population-based optimization, (2) effective integration of domain knowledge with large language model capabilities for scientific code generation, and (3) discovery of novel nonlinear processing strategies that outperform traditional matched filtering approaches in realistic detector environments.

Our results demonstrate that automated algorithm discovery can successfully identify sophisticated signal processing techniques, including multi-scale wavelet decompositions and adaptive thresholding mechanisms, that dynamically adapt to non-Gaussian and non-stationary noise characteristics. The discovered algorithms reveal new perspectives on optimal gravitational wave detection beyond theoretical matched filtering optimality.

The framework’s generalization capabilities, validated through MLGWSC-1 performance and cross-validation analysis, suggest broad applicability to scientific algorithm discovery tasks requiring complex signal extraction from noisy environments. The 150% performance variation across different language models underscores the critical importance of model architecture selection for scientific applications.

While current limitations include focus on static optimization scenarios and dependence on expert validation modules, the framework establishes a foundation for future developments in automated scientific algorithm discovery. The

integration of interpretable machine learning with domain expertise opens new avenues for hybrid human-AI systems in gravitational wave astronomy and broader scientific computing applications.

5 Methods

5.1 Problem Formulation

Gravitational Wave Detection Problem. Given dual-detector strain data $\mathbf{d} = \{d_H(t), d_L(t)\}$ from Hanford and Livingston interferometers sampled at $f_s = 2048$ Hz over finite observation windows, we seek to discover an optimal detection algorithm that maximizes performance while satisfying operational constraints.

Optimization Objective. The algorithm discovery problem is formulated as:

$$a^* = \arg \max_{a \in \mathcal{A}} \mathcal{F}(a, \mathbf{d}) \quad (1)$$

$$\text{subject to } \|\Delta t_{\text{arrival}}\| \leq 0.2 \text{ seconds} \quad (2)$$

$$\mathcal{C}(a) \leq \tau \quad (3)$$

$$a : \mathbb{R}^{2 \times N} \rightarrow \mathbb{R}^3 \quad (4)$$

where:

- \mathcal{A} represents the space of executable detection algorithms
- $\mathcal{F}(a, \mathbf{d}) = \text{AUC}(\text{Sensitive Distance vs False Alarms})$ measures detection performance following the MLGWS-1 protocol [50]
- $\Delta t_{\text{arrival}}$ denotes trigger arrival time uncertainty for astrophysical parameter estimation
- $\mathcal{C}(a)$ represents optimization constraints
- Each algorithm a maps dual-detector strain data to detection statistics (peak times, heights, timing uncertainties)

The fitness function \mathcal{F} evaluates algorithms against ground truth labels \mathbf{y}_{true} using the area under the curve of sensitive distance versus false alarms per month, which provides more physically meaningful performance assessment than traditional Receiver Operating Characteristic curves for gravitational wave detection applications.

Algorithm Discovery Framework. We model the discovery process as an iterative search procedure that combines Monte Carlo Tree Search exploration with evolutionary population dynamics:

$$\mathbf{P}_{t+1} = \text{Evolve}(\mathbf{P}_t, \mathcal{L}, \mathcal{K}_{\text{GW}})$$

where $\mathbf{P}_t = \{a_1^{(t)}, a_2^{(t)}, \dots, a_k^{(t)}\}$ represents the algorithm population at iteration t .

Key Components:

- **LLM Ensemble:** $\mathcal{L} = \{\text{o3-mini, o1, gpt-4o, claude-3.7}\}$ for code generation, with specialized model selection $\sigma : \mathcal{O} \rightarrow \mathcal{L}$ mapping evolutionary operations $\mathcal{O} = \{\text{PC, SC, PM, PWC}\}$ to appropriate models
- **Domain Knowledge:** \mathcal{K}_{GW} encapsulates gravitational wave detection expertise including physical principles, signal processing techniques, and computational constraints
- **MCTS Selection:** Node selection follows Upper Confidence bounds applied to Trees (UCT):

$$n^* = \arg \max_{c \in \text{children}(n)} \left[\frac{Q(c)}{N(c)} + C \sqrt{\frac{\ln N(n)}{N(c)}} \right]$$

Evolutionary Operations. The framework employs four evolutionary operations for algorithmic transformation:

$$\text{PC: } a_{\text{new}} = \text{LLM}_{\sigma(\text{PC})}(\text{prompt}(a_p, a_r), \mathcal{K}_{\text{GW}}) \quad (5)$$

$$\text{SC: } a_{\text{new}} = \text{LLM}_{\sigma(\text{SC})}(\text{prompt}(a_c, a_{s1,2,\dots}), \mathcal{K}_{\text{GW}}) \quad (6)$$

$$\text{PM: } a_{\text{new}} = \text{LLM}_{\sigma(\text{PM})}(\text{prompt}(a_c, a_e), \mathcal{K}_{\text{GW}}) \quad (7)$$

$$\text{PWC: } a_{\text{new}} = \text{LLM}_{\sigma(\text{PWC})}(\text{prompt}(a_{d1,2,\dots}, a_{d1,2,\dots}), \mathcal{K}_{\text{GW}}) \quad (8)$$

where PC = Parent Crossover, SC = Sibling Crossover, PM = Point Mutation, PWC = Path-wise Crossover, and $a_p, a_r, a_c, a_{s1,2,\dots}, a_e, a_{d1,2,\dots}$ denote parent, reference, current, sibling, elite, and distant algorithms respectively.

Each operation generates new algorithmic variants through LLM-guided code synthesis, with domain knowledge \mathcal{K}_{GW} ensuring adherence to gravitational wave detection principles.

Reflection and Adaptation. The system incorporates analytical reasoning through specialized reflection using the DeepSeek-R1 model:

$$\mathcal{K}_{\text{GW}}^{(t+1)} = \mathcal{K}_{\text{GW}}^{(t)} \cup \{\text{insights}(\text{LLM}_{\text{reflect}}(\text{history}_t, \text{performance}_t))\}$$

This reflection mechanism analyzes performance patterns across the MCTS tree to identify successful algorithmic principles and guide subsequent evolutionary operations toward promising regions of the solution space.

Population Management. At each iteration, the algorithm population is updated through elite preservation:

$$\mathbf{P}_{t+1} = \text{Elite}(\mathbf{P}_t \cup \{a_{\text{new}}\}, k)$$

where $\text{Elite}(\cdot, k)$ selects the top- k algorithms based on fitness scores, maintaining population diversity while preserving high-performing variants for continued evolution.

This formulation establishes gravitational wave algorithm discovery as a constrained optimization problem in the space of executable detection

algorithms, solved through LLM-guided evolutionary search with MCTS exploration and domain knowledge integration.

5.2 LLM Integration for Code Generation

The framework leverages state-of-the-art language models to transform algorithmic concepts into executable code, implementing a multi-model strategy that capitalizes on the complementary strengths of different architectures. This subsection details the model selection, prompting strategies, and error handling mechanisms that enable robust algorithmic discovery.

Model Architecture and Task Allocation. We employ a heterogeneous ensemble of reasoning-enhanced language models for code generation, including `o3-mini-medium`, `o1-2024-12-17`, `gpt-4o-2024-11-20`, and `claude-3-7-sonnet-20250219-thinking`. These models were selected based on their demonstrated capabilities in multi-step reasoning and code synthesis tasks, with each contributing unique strengths: `o3-mini-medium` provides efficient exploration of simple algorithmic variants, `o1-2024-12-17` excels at complex mathematical transformations, `gpt-4o-2024-11-20` offers robust general-purpose code generation, and `claude-3-7-sonnet-20250219-thinking` contributes sophisticated algorithmic reasoning capabilities.

For the critical reflection operations that analyze algorithm performance and guide evolutionary decisions, we exclusively utilize `deepseek-R1`. This architectural choice stems from `deepseek-R1`'s superior performance in analytical reasoning tasks, particularly its ability to identify subtle performance patterns and propose targeted improvements based on empirical observations. The separation of generation and reflection tasks allows each model to operate within its optimal domain, enhancing overall system performance.

Prompting Strategy and Temperature Control. All models operate with temperature 1.0, empirically determined to balance algorithmic diversity with syntactic correctness. Lower temperatures produced conservative modifications, while higher values generated invalid code requiring excessive corrections.

The prompting framework adapts to evolutionary context through depth-aware mechanisms. System content explicitly establishes each model's role as a gravitational wave algorithm specialist. Task descriptions clarify optimization objectives, while depth information guides exploration scope: shallow nodes emphasize paradigm shifts, deeper nodes focus on parameter optimization. External domain knowledge integration provides optimization directives referencing established signal processing principles and computational constraints.

This adaptive architecture enables systematic solution space exploration while maintaining gravitational wave detection coherence (complete templates in Supplementary Material [A.1](#)).

Error Handling and Iterative Refinement. The framework implements a robust error recovery mechanism to handle code generation failures. When syntax errors or runtime exceptions occur during algorithm evaluation, the system captures detailed error information including stack traces

and execution context. This diagnostic information is then incorporated into subsequent conversation rounds with the LLM to generate corrected implementations. The system attempts up to three correction iterations per failed algorithm. If all correction attempts fail, the corresponding node expansion is skipped to maintain computational efficiency. This approach ensures that the majority of generated algorithms remain executable while preventing infinite correction loops that could stall the evolutionary process (complete templates in Supplementary Material A.1).

Post-Generation Analysis and Knowledge Extraction. Following successful code generation, each algorithm undergoes a post-thought analysis phase that extracts key design principles and compresses algorithmic representations. This reflection process creates human-readable summaries while reducing token consumption to prevent context window overflow in subsequent LLM interactions.

The analysis captures algorithmic innovations, signal processing techniques, performance expectations, and computational characteristics in compressed form. This enables efficient reference to previous discoveries without overwhelming the LLM context, facilitating continued exploration while maintaining algorithmic memory across generations (complete templates in Supplementary Material A.1).

Domain Knowledge Integration. The framework incorporates gravitational wave signal processing expertise through structured prompts that guide algorithmic exploration toward nonlinear approaches. Knowledge integration operates across initialization, evolution, and reflection phases. Initialization prompts establish matched filtering principles, noise characteristics, and signal morphologies. Evolution prompts encourage nonlinear transformations, adaptive thresholding, and multi-scale analysis. Reflection prompts evaluate performance against sensitivity curves, false alarm rates, and computational efficiency.

The knowledge base emphasizes nonlinear processing concepts including adaptive threshold mechanisms, phase space reconstruction, and robust estimators for non-Gaussian processes. Implementation principles prioritize adaptive over fixed parameters while balancing computational cost with accuracy (complete templates in Supplementary Material A.1).

This integration ensures generated algorithms respect physical constraints while exploring beyond conventional linear methods, establishing a foundation for automated algorithmic discovery applicable to broader scientific computing domains.

5.3 Evolutionary Operations Design and Seed Algorithm

Baseline Algorithm Architecture. The optimization process begins with a deliberately simple, linear seed function that establishes a baseline for algorithmic improvement (detailed implementation in Supplementary Material A.1).

This seed algorithm implements a conventional signal processing pipeline consisting of three sequential operations that represent standard approaches in gravitational wave data analysis.

The first operation performs frequency-domain whitening to normalize the detector noise characteristics:

$$X_{\text{white}}(f) = \frac{X(f)}{\sqrt{S(f)}} \quad (9)$$

where $X(f)$ represents the Fourier transform of the input strain data, and $S(f)$ is the power spectral density estimate obtained via Welch’s method using a 4096-sample window with 50% overlap and Hann windowing. This whitening operation ensures that all frequency components contribute equally to subsequent analysis, compensating for the detector’s frequency-dependent noise characteristics.

The second operation applies time-frequency decomposition using the short-time Fourier transform (STFT) to capture transient signal characteristics:

$$S_{xx}(f, \tau) = \left\| \sum_{n=0}^{N-1} x(n + \tau) w(n) e^{-j2\pi f n/N} \right\|^2 \quad (10)$$

where $w(n)$ is a window function (256 samples with 128-sample overlap), τ is the time shift, and N is the window length. The algorithm independently processes both Hanford (H1) and Livingston (L1) detector data, then combines the resulting spectrograms using simple averaging:

$$\text{TF}_{\text{metric}} = \frac{1}{2} \langle S_{xx}^{\text{H1}} + S_{xx}^{\text{L1}} \rangle_f$$

where $\langle \cdot \rangle_f$ denotes averaging over frequency bins.

The final operation identifies candidate events through basic peak detection with fixed thresholds. The algorithm estimates background levels using the median and applies simple peak finding with predetermined height and prominence criteria. This approach represents a minimalist detection strategy that lacks the sophistication necessary for robust gravitational wave identification, particularly in the presence of non-Gaussian noise transients and weak signals.

Initial Population Generation. The evolutionary framework initializes with a single seed algorithm, then generates 8 diverse variants through systematic prompting variations (Figure 1a). Each variant maintains identical input-output interfaces while implementing distinct signal processing approaches: alternative whitening schemes, varied time-frequency decomposition methods, and different peak detection strategies. Following initial generation, two Point Mutation operations are applied to create additional variants, resulting in a total population of 10 algorithms that form the depth-1 initial population for MCTS exploration.

Elite Preservation Strategy. The framework maintains an elite individual representing the best-performing algorithm discovered throughout evolution. This elite serves as a performance benchmark for new variants and provides genetic material during Parent Crossover operations (Figure 1b.4). The elite is updated whenever a new algorithm demonstrates superior performance, ensuring monotonic progress while maintaining access to the current best solution. Point Mutation operations specifically leverage elite characteristics to guide targeted algorithmic improvements (Figure 1c).

Evolutionary Operation Framework. Each MCTS expansion level follows a structured sequence of evolutionary operations: Parent Crossover (PC) executes 5 times, Path-wise Crossover (PWC) executes 2 times, Sibling Crossover (SC) executes once, and Point Mutation (PM) executes twice. As observed in Figure 5a, this sequence balances four distinct algorithmic improvement mechanisms: (i) vertical knowledge transfer through PC operations that combine features from algorithms at different tree depths, (ii) long-range dependency capture via PWC operations that synthesize information along complete evolutionary trajectories, (iii) horizontal exploration using SC operations that facilitate exploration between algorithms of similar complexity based on nodes already generated at the same tree level, and (iv) fine-grained optimization through PM operations that introduce targeted modifications based on performance analysis. The systematic application of these operations ensures comprehensive exploration of the algorithmic solution space while maintaining computational efficiency through controlled expansion rates.

5.4 Monte Carlo Tree Search Implementation

MCTS Framework and Tree Policy. The framework implements a standard Monte Carlo Tree Search algorithm adapted for algorithmic discovery, where each node represents an executable algorithm and tree expansion corresponds to algorithmic evolution (Figure 1b). The MCTS operates through four canonical phases: selection, expansion, simulation, and backpropagation. However, our implementation modifies the traditional simulation phase by replacing random rollouts with direct algorithm evaluation on the gravitational wave detection task.

The selection phase traverses the tree from root to leaf using the Upper Confidence Bound applied to Trees (UCT) policy, balancing exploitation of high-performing algorithms with exploration of under-visited branches (Figure 1c). Unlike traditional MCTS applications where leaf nodes represent terminal game states, our leaf nodes represent algorithms that can be further evolved through the four evolutionary operations (PC, SC, PM, PWC).

UCT Score Calculation and Adaptive Exploration. The UCT score for each node combines exploitation and exploration terms with an adaptive exploration strategy that accounts for the finite evaluation budget:

$$\text{UCT}(n) = \frac{Q(n) - Q_{\min}}{Q_{\max} - Q_{\min} + \epsilon} + c \cdot \sqrt{\frac{\ln(N(p) + 1)}{N(n) + \epsilon}} \quad (11)$$

where $Q(n)$ represents the normalized fitness value of node n , Q_{\min} and Q_{\max} are the minimum and maximum fitness values observed across all nodes, $N(p)$ and $N(n)$ are the visit counts of the parent and current node respectively, ϵ is a small constant preventing division by zero, and c is the exploration constant.

The exploration constant c adapts dynamically based on the remaining evaluation budget:

$$c = c_0 \cdot \max\left(1 - \frac{t}{T}, 0\right) \quad (12)$$

where c_0 is the initial exploration constant, t is the current evaluation count, and T is the maximum evaluation budget. This adaptive mechanism ensures that the algorithm emphasizes exploration early in the search when the budget is abundant, then gradually shifts toward exploitation as evaluations are consumed.

Fitness Normalization and Q-Value Management. The fitness values (corresponding to the objective function in the code) are normalized to the range $[0, 1]$ to ensure consistent UCT calculations regardless of the absolute scale of performance metrics. The normalization uses running minimum and maximum values:

$$Q_{\text{normalized}} = \frac{Q_{\text{raw}} - Q_{\min}}{Q_{\max} - Q_{\min} + \epsilon}$$

This normalization is crucial for maintaining meaningful exploration-exploitation balance, as it prevents algorithms with vastly different performance scales from skewing the selection process.

Backpropagation and Value Updates. The backpropagation phase updates node values along the path from the newly evaluated leaf to the root. Our implementation uses a discount factor approach that balances immediate performance with long-term potential:

$$Q(p) = Q(p) \cdot (1 - \gamma) + \max_{c \in \text{children}(p)} Q(c) \cdot \gamma \quad (13)$$

where $Q(p)$ is the parent node's Q-value, γ is the discount factor, and the maximum is taken over all child nodes. This update rule ensures that parent nodes reflect the performance of their best children while maintaining some memory of their previous estimates.

The backpropagation also maintains global statistics by updating the minimum and maximum Q-values across the entire tree, enabling consistent normalization for future UCT calculations. Additionally, the algorithm maintains a ranked list of all observed fitness values to support advanced selection strategies and performance analysis.

Tree Expansion Strategy. Node expansion occurs when the UCT selection phase reaches a leaf node that has been visited multiple times, indicating

sufficient confidence in its potential. The expansion strategy creates one new child node per expansion operation, chosen through the evolutionary operations framework. This conservative expansion approach prevents explosive tree growth while ensuring thorough exploration of promising regions.

Each newly created node inherits structural information from its parent, including the algorithmic context and performance history. The initial Q-value for new nodes is set to the parent’s Q-value, providing a reasonable starting estimate that will be refined through subsequent evaluations.

Memory Management and Tree Pruning. To maintain computational efficiency with limited memory resources, the implementation includes mechanisms for selective tree pruning. Nodes that demonstrate consistently poor performance relative to their siblings are marked for potential removal, while maintaining sufficient diversity to avoid premature convergence.

The tree structure also maintains subtree references that enable efficient traversal and analysis of evolutionary pathways. These references support the Path-wise Crossover operation by providing access to complete root-to-leaf trajectories without requiring expensive tree traversals.

Convergence Detection and Termination. The MCTS continues until either the evaluation budget is exhausted or convergence is detected through analysis of the Q-value distribution. Convergence is identified when the top-performing algorithms show minimal improvement over a specified number of iterations, indicating that the search has reached a local optimum within the current exploration strategy.

This MCTS implementation creates a systematic framework for exploring the algorithmic space while maintaining computational efficiency and ensuring reproducible results. The combination of adaptive exploration, normalized fitness values, and efficient tree management enables the discovery of high-performing algorithms within reasonable computational budgets.

5.5 Experimental Setup

MLGWSC-1 Dataset and Evaluation Framework. We evaluated our Evo-MCTS framework using the Machine Learning Gravitational-Wave Search Mock Data Challenge 1 (MLGWSC-1) benchmark, which provides a standardized evaluation environment for gravitational wave detection algorithms [50]. The benchmark includes four datasets with increasing complexity, of which we utilized Dataset 4 for our primary evaluation as it represents the most realistic scenario using actual detector noise from the O3a observing run.

Dataset 4 incorporates real noise from both Hanford (H1) and Livingston (L1) detectors, filtered to include only segments with the DATA data-quality flag active while excluding problematic categories (CBC_CAT1, CBC_CAT2, CBC_HW_INJ, and BURST_HW_INJ). Overlapping segments span a minimum duration of 2 hours, with signal injection parameters drawn from distributions matching realistic compact binary coalescence scenarios. The dataset provides a challenging testbed that closely approximates real-world gravitational wave detection conditions.

Algorithm Input/Output Interface. Following the MLGWSC-1 specification, each algorithm processes HDF5 files containing raw detector data from both H1 and L1 detectors. The input files contain grouped datasets organized by integer start times, with each dataset including strain data and metadata attributes (`start_time`, `delta_t`). Our evolved algorithms output HDF5 files containing exactly three datasets of equal length: (i) `time` - GPS times of suspected gravitational wave events, (ii) `stat` - ranking statistics where larger values indicate higher detection confidence, and (iii) `var` - timing accuracy tolerance representing the maximum allowed separation between predicted and true event times.

Evaluation Metrics and Performance Assessment. The framework employs two primary evaluation metrics consistent with MLGWSC-1 standards. The false-alarm rate (FAR) measures the expected frequency of false-positive events exceeding a given ranking statistic threshold, calculated by applying algorithms to pure noise data and dividing event counts by total analyzed time. The sensitive distance quantifies detection capability at specified false-alarm rates, representing the maximum distance at which sources can be reliably detected. For uniformly distributed signals in volume, this reduces to the fraction of detected signals multiplied by the volume of a sphere with radius equal to the maximum injected distance. The area under the curve (AUC) metric integrates sensitive distance across the false-alarm rate range, providing a comprehensive performance indicator that balances detection sensitivity against false-alarm tolerance.

Training and Test Set Configuration. To ensure efficient optimization while maintaining statistical rigor, we partitioned the MLGWSC-1 Dataset 4 into training and test subsets. The training set comprises the first 7 days of data from early injection indices, enabling rapid algorithmic evaluation during the optimization process. This temporal partitioning ensures that the minimum false-alarm rate boundary is set at 4 events per month, corresponding to the statistical requirements for meaningful AUC calculation. The test set consists of 1 day of data selected from later temporal segments, providing independent validation of optimized algorithms (detailed data partitioning specifications provided in Supplementary Material A.2).

Diversity Metrics in Evolutionary Computation. We implemented sophisticated diversity measurement following established practices in evolutionary computation [69]. Population encoding involves three preprocessing steps: (i) removing comments and docstrings using abstract syntax tree parsing to focus on functional algorithmic content, (ii) standardizing code snippets into common coding style following PEP 8 conventions to eliminate stylistic variations, and (iii) converting normalized code snippets to vector representations using the CodeT5+ embedding model to enable quantitative similarity analysis.

We employ two complementary diversity metrics: the Shannon Diversity Index, calculated as $H = -\sum_{i=1}^n p_i \log p_i$ where p_i represents the frequency of the i -th unique algorithmic variant in the population, and the Complexity

Index of Diversity (CID), computed as $CID = \frac{1}{n} \sum_{i=1}^n \frac{x_i - \bar{x}}{\bar{x} + \epsilon}$ where x_i represents the embedding vector of the i -th algorithm, \bar{x} is the population centroid, and ϵ prevents division by zero. These metrics provide complementary perspectives on population diversity: Shannon index captures algorithmic variety while CID measures structural complexity differences.

LLM API Configuration and Model Selection. Our framework integrates multiple state-of-the-art language models through official APIs from OpenAI, Anthropic, and DeepSeek [70–73]. For code generation tasks, we employ thinking-enhanced models including `o3-mini-medium`, `o1-2024-12-17`, `gpt-4o-2024-11-20`, and `claude-3-7-sonnet-thinking`, selected for their demonstrated capabilities in multi-step reasoning and code synthesis [30, 74]. For reflection mechanisms, we exclusively utilize `deepseek-r1` due to its superior performance in analytical reasoning tasks [73], particularly its ability to identify subtle performance patterns and propose targeted algorithmic improvements based on empirical observations. We designate `o3-mini-medium` as our fiducial model configuration, providing the baseline reference for performance comparisons and ensuring consistency across experimental runs. All models operate with temperature parameter set to 1.0 to balance creative exploration with syntactic reliability [75].

Hyperparameter Configuration and Experimental Design. The Evo-MCTS framework employs carefully tuned hyperparameters optimized for gravitational wave detection algorithm discovery. Initial population size is set to 10 algorithms, balancing computational efficiency with adequate diversity for effective exploration. MCTS depth is limited to 10 levels, providing sufficient hierarchical structure for complex algorithmic development while maintaining computational tractability. Each experimental configuration undergoes 5 independent runs with different random seeds to ensure statistical robustness and enable confidence interval estimation.

The 5-run experimental design serves multiple purposes: (i) quantifying algorithmic discovery reliability across different initialization conditions, (ii) enabling statistical analysis of optimization trajectories and convergence patterns, and (iii) providing robust diversity measurements that account for stochastic variations in the evolutionary process. Comprehensive results from all individual runs are documented in Supplementary Material A.3, enabling detailed analysis of inter-run variability and optimization consistency.

Ablation Studies and Comparative Analysis. To validate the effectiveness of our integrated Evo-MCTS approach, we conduct comprehensive ablation studies comparing against two established frameworks: ReEvo [44] (pure evolutionary mechanism) and MCTS-AHD [45] (pure MCTS mechanism). These comparisons isolate the contributions of different algorithmic components while maintaining consistent evaluation protocols.

ReEvo represents the evolutionary optimization baseline, employing genetic algorithms with traditional crossover and mutation operations powered by large language models but without tree-structured exploration. The framework implements population-based optimization through iterative code generation

and selection, focusing on evolutionary diversity maintenance and fitness-driven selection pressure. MCTS-AHD implements pure Monte Carlo Tree Search for automated heuristic design without evolutionary population dynamics or reflection mechanisms. This approach emphasizes tree-based exploration with UCT-guided node selection but lacks the multi-generational insight synthesis and population diversity maintenance that characterizes evolutionary approaches.

By comparing Evo-MCTS against these component frameworks using identical LLM integration protocols and evaluation budgets, we quantify the synergistic benefits of combining evolutionary population dynamics with structured tree search exploration. The experimental design maintains consistent evaluation metrics, hardware configurations, and statistical analysis procedures across all three frameworks, with computational fairness ensured through equivalent LLM evaluation counts as the unified iteration metric. This approach enables direct performance comparison while isolating the specific contributions of different optimization strategies under identical resource constraints. The comprehensive multi-run analysis results across all frameworks are presented in Figure A2, demonstrating the statistical robustness of our comparative evaluation.

Edge Robustness Analysis Protocol. To validate the consistency of algorithmic breakthroughs, we developed a systematic edge re-execution protocol. For each selected evolutionary transition, we perform 100 independent re-executions using identical prompt templates while maintaining all experimental conditions constant except for the LLM sampling parameters. Each re-execution employs the same parent algorithms, evolutionary operation type, and external knowledge integration templates used in the original optimization run.

The re-execution protocol preserves all deterministic components (fitness evaluation, data preprocessing, statistical analysis) while allowing natural variation in LLM-generated code through different random seeds. This approach enables quantification of discovery mechanism robustness while accounting for the inherent stochasticity in large language model outputs. Statistical analysis employs standard descriptive metrics (mean, standard deviation) combined with confidence interval estimation to characterize the reliability of breakthrough discovery patterns, as illustrated in Figure 5(b).

Computational Resources and Parallelization. The numerical calculations in this study were carried out on the ORISE Supercomputer, equipped with 32-core x86 processors operating at a base frequency of 2.0 GHz and 4 GPGPU accelerators per node, enabling efficient parallel execution of LLM API calls and algorithm evaluations. The Evo-MCTS framework employs asynchronous parallelization to maximize resource utilization, allowing multiple LLM requests to be processed concurrently while maintaining synchronization for tree updates and performance analysis. This parallelization strategy significantly reduces overall computational time while ensuring that all evaluations are performed under consistent conditions.

6 Data availability

The MLGWSC-1 Dataset 4 used in this study is publicly available at <https://github.com/gwastro/ml-mock-data-challenge-1/>. The dataset includes real detector noise from LIGO Hanford (H1) and Livingston (L1) observatories during the O3a observing run.

The ReEvo framework implementation is available at <https://github.com/ai4co/reevo> with the original codebase and documentation. The MCTS-AHD framework can be accessed through its official repository at <https://github.com/zz1358m/MCTS-AHD-master>. Both frameworks were used for comparative analysis following their original specifications and hyperparameter configurations.

Training and test data partitions, along with detailed preprocessing specifications, are provided in the Supplementary Material A.2. All experimental results and algorithm performance metrics are available upon reasonable request to the corresponding author.

7 Code availability

The complete source code for the Evo-MCTS framework is publicly available at <https://github.com/iphyresearch/evo-mcts>. The repository includes all implementation details, experimental configurations, and reproducibility instructions. Additionally, a permanent archived version is available through the Zenodo repository at <https://zenodo.org/record/10000000000000000000>. The code is written in Python and is fully reproducible with the provided environment and dependencies. The repository contains comprehensive documentation, example usage scripts, and all necessary configuration files to replicate the experimental results presented in this study.

Supplementary information.

Appendix A Supplementary Material

A.1 LLM Prompting Templates

This section provides comprehensive details of the prompting strategies employed across different phases of the algorithmic discovery process. The templates are designed to guide language models through systematic reasoning while incorporating domain-specific knowledge and maintaining consistency across evolutionary operations.

System Context and Task Definition. All interactions with the LLM ensemble begin with a standardized system prompt that establishes the expert role and problem context:

You are an expert in gravitational wave signal detection algorithms. Your task is to design heuristics that can effectively solve optimization problems. The task involves constructing a nonlinear pipeline for gravitational wave signal detection. This pipeline will encompass data conditioning and time-frequency transformations as part of the signal processing workflow. The input will consist of raw, finite-length dual-channel gravitational wave data from the H1 and L1 detectors. The pipeline will be tested on segmented data spanning several weeks, with each segment having variable length (7000s -30000s). Each segment's dual-channel data will be directly used as input. The ultimate goal is to produce a catalog of potential gravitational wave signals, where each trigger includes information such as GPS time, ranking statistic, and the timing accuracy of the prediction. This systematic approach is essential for effectively identifying and cataloging candidate gravitational wave signals.

This system prompt serves multiple purposes: (i) establishing domain expertise expectations, (ii) defining the specific optimization context, (iii) specifying input data characteristics, and (iv) clarifying the expected output format and evaluation criteria.

A.1.1 Initial Algorithm Generation Prompts

Seed Function Template and Analysis Framework. The initial algorithm generation process begins with a structured analysis of the seed function to establish baseline understanding. The seed function analysis template guides the LLM through systematic examination of the foundational algorithm:

```
## Seed Function Analysis Task
Analyze the foundational algorithm's design strategy to establish baseline understanding
for MCTS exploration. This first-level analysis will guide subsequent optimization
directions.

## Seed Function Implementation
```python
{prompt_seed_func}
```

- Technical implementation details: {prompt_other_inf}
- Performance impact rationale: {prompt_inout_inf}

## Context for Analysis
This initial analysis at MCTS depth first-level should:
- Identify core algorithmic mechanisms
- Extract fundamental processing stages
- Surface high-level optimization opportunities
- Establish baseline for diversity generation
{external_knowledge}

## Analysis Requirements
1. Characterize the seed's core approach in one sentence containing:
    - Primary computational strategy
    - Key transformation stages
    - Fundamental signal processing techniques
    - Overall optimization philosophy

2. Focus on architectural-level characteristics rather than implementation details

3. Description must fit within single braces and avoid:
    - Code references
    - Parameter-level details
    - Performance assessments
    - Comparative statements

## Output Format Rules
- Return optimization strategies within SINGLE BRACE
- Ensure entire response can be parseable by regex: \\{{{(.*)\\}}} with DOTALL flag
```

Seed Algorithm Specification. The seed function implements a three-stage linear signal processing pipeline that serves as the evolutionary starting point:

- Stage 1: Data Conditioning and Whitening

```

1  def data_conditioning(strain_h1: np.ndarray, strain_l1: np.ndarray, times: np.ndarray) -> tuple[np.ndarray, np.ndarray,
    ↳ np.ndarray]:
2      window_length = 4096
3      dt = times[1] - times[0]
4      fs = 1.0 / dt
5
6      def whiten_strain(strain):
7          strain_zeromean = strain - np.mean(strain)
8          freqs, psd = signal.welch(strain_zeromean, fs=fs, nperseg=window_length,
9                                   window='hann', noverlap=window_length//2)
10         smoothed_psd = np.convolve(psd, np.ones(32) / 32, mode='same')
11         smoothed_psd = np.maximum(smoothed_psd, np.finfo(float).tiny)
12         white_fft = np.fft.rfft(strain_zeromean) / np.sqrt(np.interp(np.fft.rfftfreq(len(strain_zeromean), d=dt), freqs,
    ↳ smoothed_psd))
13         return np.fft.irfft(white_fft)
14
15     whitened_h1 = whiten_strain(strain_h1)
16     whitened_l1 = whiten_strain(strain_l1)
17
18     return whitened_h1, whitened_l1, times

```

- Stage 2: Time-Frequency Decomposition

```

1  def compute_metric_series(h1_data: np.ndarray, l1_data: np.ndarray, time_series: np.ndarray) -> tuple[np.ndarray,
    ↳ np.ndarray]:
2      fs = 1 / (time_series[1] - time_series[0])
3      f_h1, t_h1, Sxx_h1 = signal.spectrogram(h1_data, fs=fs, nperseg=256, noverlap=128, mode='magnitude', detrend=False)
4      f_l1, t_l1, Sxx_l1 = signal.spectrogram(l1_data, fs=fs, nperseg=256, noverlap=128, mode='magnitude', detrend=False)
5      tf_metric = np.mean((Sxx_h1**2 + Sxx_l1**2) / 2, axis=0)
6      gps_mid_time = time_series[0] + (time_series[-1] - time_series[0]) / 2
7      metric_times = gps_mid_time + (t_h1 - t_h1[-1] / 2)
8
9      return tf_metric, metric_times

```

- Stage 3: Peak Detection and Trigger Generation

```

1  def calculate_statistics(tf_metric, t_h1):
2      background_level = np.median(tf_metric)
3      peaks, _ = signal.find_peaks(tf_metric, height=background_level * 1.0, distance=2, prominence=background_level * 0.3)
4      peak_times = t_h1[peaks]
5      peak_heights = tf_metric[peaks]
6      peak_deltat = np.full(len(peak_times), 10.0) # Fixed uncertainty value
7      return peak_times, peak_heights, peak_deltat

```

Template Variables and Customization. The prompting template incorporates several customizable variables that enable systematic variation generation:

- `prompt_seed_func`: Complete seed function implementation
- `prompt_other_inf`: Technical implementation details including sampling rates, window parameters, and algorithmic constraints
- `prompt_inout_inf`: Performance impact rationale explaining the relationship between input characteristics and expected output quality
- `external_knowledge`: Domain-specific knowledge injection including gravitational wave physics, detector characteristics, and signal morphology constraints

Output Format Requirements. All generated algorithms must conform to the standardized interface:

```

1  def pipeline_v(N)(strain_h1: np.ndarray, strain_l1: np.ndarray, times: np.ndarray) -> tuple[np.ndarray, np.ndarray,
↳ np.ndarray]:
2      # Algorithm implementation for seed function
3      # ...
4      # Stage 1: Data Conditioning and Whitening
5      whitened_h1, whitened_l1, data_times = data_conditioning(strain_h1, strain_l1, times)
6      # Stage 2: Time-Frequency Decomposition
7      tf_metric, metric_times = compute_metric_series(whitened_h1, whitened_l1, data_times)
8      # Stage 3: Peak Detection and Trigger Generation
9      peak_times, peak_heights, peak_deltat = calculate_statistics(tf_metric, metric_times)
10     return peak_times, peak_heights, peak_deltat

```

This interface consistency ensures that all generated algorithms can be evaluated within the same framework while enabling diverse internal implementations.

A.1.2 Parent Crossover Implementation

The Parent Crossover (PC) operation represents a sophisticated genetic operation that combines algorithmic components from two reference implementations at different levels of the MCTS hierarchy. This operation is designed to preserve successful characteristics from both parent algorithms while introducing novel enhancements that exceed simple interpolation.

Template Structure and Crossover Strategy. The PC operation employs a structured template that guides the LLM through systematic analysis and synthesis of two parent algorithms:

```

## Task Overview
Develop a novel algorithm that strategically combines components from two reference
implementations while introducing innovative enhancements. The solution must demonstrate
measurable improvements beyond simple interpolation of existing approaches.
Current Depth Level: [Level {depth}]

## Implementation Analysis
### Code Comparison
1. VERSION A (Baseline Implementation):
```python
{worse_code}
```

2. VERSION B (Enhanced Implementation):
```python
{better_code}
```

### Strengths to Combine
```text
{reflection}
```

Key Synthesis Requirements:
- Preserve 2 distinct advantages from Version A
- Incorporate 3 critical enhancements from Version B
- Identify 1 synergistic improvement opportunity

## Architecture Strategy
{external_knowledge}

### Depth-Specific Synthesis Guidelines (Depth={depth})
1. Structural Synthesis (Depth 1-2):

```

- Create hybrid control flow combining best elements from both versions
 - Example: "Combine Version A's iteration structure with Version B's termination conditions"
 - Forbid direct replication of either version's architecture
2. Implementation Fusion (Depth 3-4):
 - Develop novel parameter hybridization techniques
 - Example: "Blend Version A's exploration mechanism with Version B's exploitation strategy"
 - Require at least one innovative combination per functional module
 3. Mathematical Innovation (Depth 5+):
 - Derive new computational operators through version synthesis
 - Example: "Fuse Version A's approximation method with Version B's error correction"
 - Mandate 10-20% computational complexity reduction

This template structure ensures that the crossover operation is not merely concatenative but involves intelligent analysis and strategic combination of algorithmic strengths.

Depth-Adaptive Synthesis Guidelines. The PC operation implements depth-specific strategies that adapt the crossover complexity based on the current position in the MCTS tree:

- Structural Synthesis (Depth 1-2):
 - Focuses on combining high-level architectural elements from both parent algorithms
 - Creates hybrid control flow structures that merge the best organizational patterns
 - Example directive: "Combine Version A's iteration structure with Version B's termination conditions"
 - Explicitly forbids direct replication of either parent's complete architecture
- Implementation Fusion (Depth 3-4):
 - Emphasizes parameter hybridization and functional module integration
 - Develops novel approaches to blend algorithmic strategies
 - Example directive: "Blend Version A's exploration mechanism with Version B's exploitation strategy"
 - Requires at least one innovative combination per functional module
- Mathematical Innovation (Depth 5+):
 - Derives new computational operators through sophisticated version synthesis
 - Focuses on mathematical justification for algorithmic improvements
 - Example directive: "Fuse Version A's approximation method with Version B's error correction"
 - Mandates 10-20% computational complexity reduction alongside performance gains

Innovation Requirements and Quality Assurance. The PC operation enforces strict innovation standards to ensure that generated algorithms represent genuine improvements:

- Core Innovation Targets:
 - Synthesize 3+ novel elements not present in either parent version
 - Resolve 2 fundamental limitations identified through comparative analysis
 - Introduce 1 breakthrough enhancement with rigorous mathematical justification
 - Demonstrate non-trivial performance gains over both parent algorithms
 - Prohibit direct replication of complete code blocks from either parent

Reflection-Guided Analysis. The crossover process incorporates a reflection component that analyzes the strengths and weaknesses of both parent algorithms:

Requirements

1. Core Innovation Targets:

- Synthesize 3+ novel elements not present in either version
- Resolve 2 fundamental limitations identified in analysis
- Introduce 1 breakthrough enhancement with mathematical justification
- Demonstrate non-trivial performance gain over both versions
- Prohibit direct replication of complete code blocks

This reflection analysis is generated through the deepseek-R1 model and provides crucial insights that guide the synthesis process. The reflection identifies:

- Computational advantages in each parent algorithm
- Structural design patterns that contribute to performance
- Potential synergistic combinations that could yield emergent benefits
- Limitation patterns that should be addressed in the offspring

Output Format and Validation. The PC operation enforces a standardized output format that ensures both human readability and automated processing:

2. Output Format:

- Place the core design idea in a sentence within a brace BEFORE the function definition
- For the core design idea format: `\{\{A hybrid gravitational wave detection pipeline...\}\}`
- Implement as Python function: `{func_name}`
- Inputs: `{input_count}` parameter(s) (`{joined_inputs}`)
- Outputs: `{output_count}` return value(s) (`{joined_outputs}`)
- Follow: `{inout_inf}`
- Constraints: `{other_inf}`
- IMPORTANT: All output code MUST be valid Python syntax. Do not place description text inside curly braces within the function body.
- Example of correct format:


```

\{\{Core design description here\}\}
```python
def pipeline_v2(strain_h1: np.ndarray, strain_l1: np.ndarray, times: np.ndarray) ->
tuple[np.ndarray, np.ndarray, np.ndarray]:
 """Core design description can alternatively be placed here as a docstring"""
 # Function implementation...

```

### A.1.3 Sibling Crossover Implementation

The Sibling Crossover (SC) operation implements a sophisticated two-phase approach that leverages peer algorithm insights to generate improved offspring. Unlike Parent Crossover, which combines algorithms from different hierarchical levels, SC focuses on horizontal knowledge transfer between algorithms at the same MCTS depth, promoting diversity while maintaining comparable complexity levels.

**Two-Phase Architecture.** The SC operation employs a unique two-stage process: first generating optimization hints through multi-level reflection analysis (Phase 1), then implementing concrete algorithmic improvements based on these insights (Phase 2). This separation enables more targeted optimization by allowing the system to first identify improvement opportunities before implementing solutions.

**Phase 1: Multi-Level Reflection Analysis.** The first phase generates depth-specific optimization hints by synthesizing insights from sibling algorithms and parent-level analysis:

```
Task Overview
Generate depth-specific optimization hints for gravitational wave detection algorithms by
synthesizing multi-level reflections.
Current Optimization Depth: {parent_depth}/{max_depth} (shallow: structural patterns,
medium: implementation techniques, deep: mathematical details)

Contextual Insights
1. Peer Algorithm Reflections (Depth {parent_depth}):
 - Formatted as performance-annotated entries: [No.N Brother Reflection Score: X]<
 reflection>
 - Time-ordered weighting (newest=highest priority) with objective score-based ranking
 - Includes full technical post-mortems from immediate ancestors
{parent_reflections}

2. Father Algorithm Analysis (Depth {father_depth}):
{father_reflection}

Hint Generation Requirements
1. Produce 3-5 executable optimization directives that:
 - Integrate cross-depth insights from peer implementations
 - Target {parent_depth}-level (shallow: structural patterns, medium: implementation
 techniques, deep: mathematical details) components for improvement
 - Formulate mathematically sound enhancements
 - Align with gravitational wave data processing objectives

2. Output Format Rules
 - Return optimization strategies within SINGLE BRACE
 - Ensure entire response can be parseable by regex: \{\{((.*)\)\}\} with DOTALL flag
 - Focus on {parent_depth}-appropriate modifications
 - Emphasize time-domain processing optimizations

Critical Constraints
- Each directive must correspond to concrete code changes
- Explicitly connect to reflection insights where applicable
- Maintain strict {parent_depth}-level focus in all suggestions
- Exclude explanatory text within the hint brace
- Prioritize modifications matching current depth's optimization type
```

**Sibling Selection and Weighting Strategy.** The SC operation employs a sophisticated parent selection mechanism that prioritizes high-performing sibling algorithms:



```
Select parents based on objective value weights
other = [ind for ind in pop if ind['code'] != father['code']]
weights = [1.0 / (ind['fitness'] + 1e-10) for ind in other] # Lower objective = higher weight
normalized_weights = [w / sum(weights) for w in weights]
parents = random.choices(other, weights=normalized_weights, k=min(self.m, len(other)))
```

This weighting strategy ensures that successful algorithmic patterns from high-performing siblings are more likely to influence the offspring generation process.

**Depth-Adaptive Optimization Focus.** The first phase implements depth-specific optimization strategies that adapt to the current position in the MCTS tree:

- Shallow Depth (1-2): Focuses on structural patterns and control flow restructuring
- Medium Depth (3-4): Emphasizes implementation techniques and numerical optimizations
- Deep Depth (5+): Concentrates on mathematical details and advanced computational methods

**Phase 2: Concrete Algorithm Implementation.** The second phase transforms the optimization hints into executable algorithms:

```
Algorithm Optimization Task
Develop an enhanced gravitational signal processing algorithm for interferometer data
analysis by implementing concrete improvements from multi-level code analysis.

Technical Context
1. Optimization Depth Specifications:
- Current Focus Level: {depth} (max_depth={max_depth})
 (1-2: Control flow restructuring, 3-4: Numerical computation optimizations, 5+:
 Advanced linear algebra methods)
- Code Analysis Insights from Prior Level:
...text
{reflection}
...

2. Base Implementation Details:
[Functional Purpose] {algorithm_description}
[Core Implementation]
...python
{algorithm_code}
...

Implementation Directives (Depth {depth}):
- Shallow (1-2): Restructure control flow using reflection suggestion (e.g., split data
conditioning/analysis phases)
- Medium (3-4): Apply numerical optimizations from reflection (e.g., FFT window size
optimization)
- Deep (5+): Implement matrix computation improvements from reflection (e.g., regularized
inverse covariance)

{external_knowledge}

Output Format
- Place the core design idea in a sentence within a brace BEFORE the function definition
- For the core design idea format: \{\{A hybrid gravitational wave detection pipeline...\}\}
- Implement as Python function: {func_name}
- Inputs: {input_count} parameter(s) ({joined_inputs})
- Outputs: {output_count} return value(s) ({joined_outputs})
- Follow: {inout_inf}
```

```

- Constraints: {other_inf}
- IMPORTANT: All output code MUST be valid Python syntax. Do not place description text
inside curly braces within the function body.
- Example of correct format:
 \\\{{{Core design description here}}\}
  ```python
  def pipeline_v2(strain_h1: np.ndarray, strain_l1: np.ndarray, times: np.ndarray) ->
  tuple[np.ndarray, np.ndarray, np.ndarray]:
      """Core design description can alternatively be placed here as a docstring"""
      # Function implementation...
  ...

## Important Notes
- Focus on algorithmic improvements rather than code style changes
- Ensure the new implementation directly addresses the reflection insights

```

Reflection Processing and Template Variables. The SC operation processes multiple sources of algorithmic insight through structured template variables:

- `parent_reflections`: Performance-annotated reflections from peer algorithms, formatted as ranked entries with objective scores
- `father_reflection`: Analysis from the immediate parent algorithm at depth-1
- `reflection`: Synthesized optimization hints generated in Phase 1
- `algorithm_description`: Functional description of the base algorithm
- `algorithm_code`: Complete implementation of the parent algorithm

Quality Assurance and Validation. The two-phase approach enables comprehensive quality control:

- Phase 1 Validation:
 - Ensures reflection insights are depth-appropriate
 - Validates mathematical soundness of optimization suggestions
 - Confirms alignment with gravitational wave processing objectives
- Phase 2 Validation:
 - Verifies syntactic correctness of generated code
 - Confirms interface compliance with standardized function signatures
 - Tests algorithmic improvements against reflection insights
 - Validates computational efficiency claims

Temporal Weighting and Performance Ranking. The SC operation implements sophisticated temporal weighting that prioritizes recent algorithmic discoveries while maintaining objective score-based ranking:

- Time-ordered weighting: Newer algorithms receive higher priority in the reflection synthesis
- Performance-based ranking: Algorithms with better objective scores contribute more heavily to the optimization hints
- Cross-depth integration: Insights from both peer algorithms and parent-level analysis are systematically combined

This comprehensive approach ensures that SC operations generate algorithms that not only improve upon their immediate ancestors but also incorporate the collective intelligence of high-performing siblings, leading to more robust and efficient gravitational wave detection strategies.

A.1.4 Point Mutation Implementation

Point Mutation (PM) operations introduce targeted modifications to individual algorithms based on performance analysis, implementing two distinct approaches that offer different levels of sophistication and computational investment. The framework provides both single-stage direct improvement and two-stage reflection-driven enhancement strategies.

Single-Stage Point Mutation: Direct Algorithm Improvement.

The operation implements a straightforward approach that directly compares an original algorithm with a high-performing elite algorithm to generate improvements. This method prioritizes computational efficiency while maintaining effective algorithmic enhancement.

Template Structure:

```
## Task Overview
You will analyze an original algorithm, an improved version of it, and create a new
enhanced algorithm. Below are the key components:

## Algorithm Details
1. ORIGINAL ALGORITHM:
    - Description: {original_algorithm_description}
    - Code:
    ```python
 {original_algorithm_code}
    ```
    - **Objective Value**: {original_objective_value}

2. BETTER ALGORITHM (Reference Implementation):
    - Description: {better_algorithm_description}
    - Code:
    ```python
 {better_algorithm_code}
    ```
    - **Objective Value**: {better_objective_value}
    - Improvement Insights:
    ```text
 {better_algorithm_reflection}
    ```

## Implementation Requirements
1. Analyze the differences between the original and better algorithms
2. Create a new algorithm that:
    - Incorporates successful elements from the better algorithm
    - Addresses limitations revealed in the improvement insights
    - Produces better results than the original algorithm
3. Output format requirements:
    - Place the core design idea in a sentence within a brace BEFORE the function
    definition
    - For the core design idea format: \{\{A hybrid gravitational wave detection pipeline
    ...}\}
    - Implement as Python function: {func_name}
    - Inputs: {input_count} parameter(s) ({joined_inputs})
    - Outputs: {output_count} return value(s) ({joined_outputs})
    - Follow: {inout_inf}
    - Constraints: {other_inf}
```

```

- IMPORTANT: All output code MUST be valid Python syntax. Do not place description text
  inside curly braces within the function body.
- Example of correct format:
  \{\{Core design description here\}\}
  ...python
  def pipeline_v2(strain_h1: np.ndarray, strain_l1: np.ndarray, times: np.ndarray) ->
    tuple[np.ndarray, np.ndarray, np.ndarray]:
      """Core design description can alternatively be placed here as a docstring"""
      # Function implementation...
  ...
{external_knowledge}

## Important Notes
- Focus on algorithmic improvements rather than code style changes
- Ensure the new implementation directly addresses the reflection insights

```

Two-Stage Point Mutation: Reflection-Driven Enhancement. The operation implements a sophisticated two-phase approach that mirrors the sibling crossover methodology but focuses on individual algorithm improvement rather than horizontal knowledge transfer.

Phase 1: Strategic Reflection Generation. The first phase synthesizes insights from multiple sources to generate comprehensive optimization guidelines:

```

## Task Overview
Generate optimized technical guidelines for gravitational wave detection algorithms through
systematic analysis of multi-generational reflection insights. Focus on enhancing data
conditioning pipelines, time-frequency analysis methods, noise suppression techniques, and
H1-L1 detector coherence optimization. Produce executable directives addressing: waveform
recognition precision, computational complexity management, and non-stationary noise
differentiation while maintaining strict API compliance.

## Input Context
1. NEW INSIGHTS FROM RECENT ITERATIONS:
  - Formatted as performance-annotated entries: [Parent N Reflection Score: X]<
    reflection>
  - Time-ordered weighting (newest=highest priority) with objective score-based ranking
  - Includes full technical post-mortems from immediate ancestors
{parent_reflections}

2. LONG-TERM REFLECTION REPOSITORY:
  - Contains battle-tested insights from top 1% performers
  - 3x weighting factor for architectural-level insights
  - Curated through 3-stage filtration:
    1. Statistical significance validation
    2. Cross-generational effectiveness verification
    3. Compatibility check with current detector configurations
{elite_reflection}

## Implementation Requirements
1. Perform weighted synthesis of reflections
2. Generate 3-5 technically-grounded optimization directives
3. Prioritize:
  - Mitigation of historical implementation flaws
  - Amplification of proven effective patterns
  - Weighted integration of multi-generational insights

## Output Format
- Return all guidelines within SINGLE BRACE
- Ensure entire response can be parseable by regex: \{\{(.*)\}\} with DOTALL flag
- Concrete technical directives only
- No explanatory text or formatting

```

Phase 2: Concrete Algorithm Implementation. The second phase transforms the strategic insights into executable algorithmic improvements:

Task Overview

Leverage insights from prior strategic reflection to architecturally enhance the gravitational wave detection algorithm. Develop improvements that directly address identified limitations in CRITICAL REFLECTION INSIGHTS while preserving core functionality through:

1. Stage-level architectural modifications informed by reflection analysis
2. Reflection-driven noise reduction and coherence enhancement strategies
3. Time-frequency analysis variations targeting specific weaknesses identified
4. H1-L1 synthesis improvements based on cross-detector insights

Generate architecturally distinct variants that implement reflection-derived concepts through fundamental structural changes.

Input Context

1. CRITICAL REFLECTION INSIGHTS (Improvement Basis):

```
```text
```

```
{reflection}
```

```
```
```

2. REFERENCE IMPLEMENTATION:

```
[Description] {elite_algorithm_description}
```

```
[Baseline Code]
```

```
```python
```

```
{elite_algorithm_code}
```

```
```
```

Implementation Requirements

1. Execute reflection-guided analysis:
 - Map reflection insights to specific code components
 - Identify 2-3 architectural limitations in current implementation
2. Propose improvements that directly convert reflection insights into:
 - Enhanced signal path architecture
 - Novel noise handling structures
 - Optimized computational patterns
 - Advanced detector synergy mechanisms
3. Maintain strict interface compatibility with existing system integration

```
{external_knowledge}
```

Output Format

- Place the core design idea in a sentence within a brace BEFORE the function definition
- For the core design idea format: `\{\{A hybrid gravitational wave detection pipeline...\}\}`
- Implement as Python function: `{func_name}`
- Inputs: `{input_count}` parameter(s) (`{joined_inputs}`)
- Outputs: `{output_count}` return value(s) (`{joined_outputs}`)
- Follow: `{inout_inf}`
- Constraints: `{other_inf}`
- IMPORTANT: All output code MUST be valid Python syntax. Do not place description text inside curly braces within the function body.
- Example of correct format:


```

\{\{Core design description here\}\}
```python
def pipeline_v2(strain_h1: np.ndarray, strain_l1: np.ndarray, times: np.ndarray) ->
tuple[np.ndarray, np.ndarray, np.ndarray]:
 """Core design description can alternatively be placed here as a docstring"""
 # Function implementation...
```

```

Important Notes

- Focus on algorithmic improvements rather than code style changes
- Ensure the new implementation directly addresses the reflection insights

Selection Strategies and Elite Integration. Both PM operations leverage the elite offspring as a performance benchmark and source of successful algorithmic patterns. The key distinction lies in their selection strategies:

- **Single-Stage Selection Strategy:**
 - Selects a single parent algorithm from the population (excluding the elite)
 - Directly compares parent performance with elite offspring
 - Implements immediate improvement through direct analysis
- **Two-Stage Selection Strategy:**
 - Selects multiple parent algorithms for comprehensive reflection analysis
 - Incorporates both recent algorithmic insights and long-term elite patterns
 - Implements sophisticated multi-generational knowledge synthesis

Computational Efficiency Considerations. The two PM approaches offer different computational trade-offs:

- **Single-Stage Advantages:**
 - Single-stage processing reduces computational overhead
 - Direct comparison enables rapid algorithm improvement
 - Simplified prompting reduces LLM token consumption
- **Two-Stage Advantages:**
 - Two-stage processing enables more sophisticated optimization
 - Multi-generational insight integration leads to more robust improvements
 - Reflection-driven approach produces more interpretable algorithmic modifications

Template Variable Integration. Both PM operations incorporate comprehensive template variables that enable systematic algorithmic improvement:

- **Common Variables:**
 - `func_name`, `input_count`, `output_count`: Interface specification
 - `joined_inputs`, `joined_outputs`: Parameter documentation
 - `better_algorithm_description`, `better_algorithm_code`: Elite algorithm details
 - `original_objective_value`, `better_objective_value`: Performance metrics
 - `better_algorithm_reflection`: Elite algorithm insights
- **Two-Stage Variables:**
 - `parent_reflections`: Multi-parent reflection synthesis
 - `elite_reflection`: Long-term elite insights
 - `reflection`: Generated optimization guidelines

Quality Assurance and Validation. Both PM operations implement rigorous validation procedures:

- **Single-Stage Validation:**
 - Direct performance comparison with both parent and elite algorithms

- Verification of improvement insight integration
- Confirmation of interface compliance
- Two-Stage Validation:
 - Two-stage validation covering both reflection generation and implementation
 - Cross-generational consistency checking
 - Architectural improvement verification

The dual PM approach provides flexibility in algorithmic improvement strategies, enabling the framework to adapt to different optimization scenarios while maintaining consistent quality standards and interface compliance.

A.1.5 Path-wise Crossover Implementation

Path-wise Crossover (PWC) operations synthesize information along complete root-to-leaf trajectories in the MCTS tree, capturing long-range dependencies and enabling global optimization strategies. The framework implements two distinct PWC approaches that differ in their analytical methodologies: reflection-based synthesis and comprehensive algorithm analysis.

Reflection-Based Path-wise Crossover: Multi-Algorithm Insight Synthesis. The operation implements a two-stage process that analyzes reflection patterns across multiple algorithms in a complete MCTS path to identify generalizable optimization principles.

Phase 1: Cross-Algorithm Pattern Analysis. The first phase extracts recurring technical strategies from multiple algorithm reflections:

```
## Task Overview
Analyze and synthesize technical reflections from multiple algorithm iterations to identify
cross-algorithm optimization patterns and guide next-generation algorithm design.
Prioritize extraction of generalizable technical principles over implementation-specific
details.
Current Optimization Depth: depth/max_depth={depth}/{max_depth} (shallow: structural
patterns, medium: implementation techniques, deep: mathematical details)

## Input Context
Analyzing {num_algorithms} algorithm reflections from MCTS exploration trajectories.
Technical reflections follow depth-specific analysis requirements. Structural format: [No.N
algorithm's reflection (depth: X)]<reflection>
{algorithm_reflections}

## Reflection Requirements
1. **Pattern Identification** (Key Observed Patterns):
  - Extract 2-3 recurring technical strategies (e.g. "Multi-scale wavelet decomposition"
  not "used Morlet wavelet")
  - Categorize by analysis level:
    * Structural: Component architecture (e.g. "Parallel filter banks")
    * Implementation: Algorithmic choices (e.g. "Adaptive thresholding")
    * Mathematical: Core transforms (e.g. "Orthogonal matching pursuit")

2. **Technical Pathway Analysis** (Promising Technical Pathways):
  - Identify under-utilized but theoretically sound approaches (e.g. "Sparse
  representation in frequency domain")
  - Specify required technical components without code details (e.g. "Requires:
  Overcomplete basis construction")

3. **Optimization Principles** (Strategic Optimization Principles):
```


- Formulate depth-specific guidelines (e.g. "At mathematical level: Maximize time-frequency product ≤ 0.5 ")
- Relate physical constraints to algorithmic parameters (e.g. "Wavelet duration should match typical glitch durations")

4. **Specificity Balance:**

- Technical specificity: Name mathematical concepts (e.g. "Gabor uncertainty") and signal processing domains
- Implementation avoidance: Omit code structures (e.g. "Avoid: 'Use 3 nested loops'")

Output Format Rules

- Return optimization strategies within SINGLE BRACE
- Ensure entire response can be parseable by regex: `\{\{(.*)\}\}` with DOTALL flag
- Do not include markdown formatting or additional explanations

Phase 2: Algorithm Implementation. The second phase transforms the synthesized insights into concrete algorithmic improvements:

Task Overview

Develop an enhanced gravitational wave detection algorithm through targeted modifications addressing specific technical shortcomings identified in the reflection analysis.

Input Context

```
[Critical Reflection Insights]
```text
{reflection}
```
```

```
[Baseline Implementation]
[Functional Description] {algorithm_description}
[Current Codebase]
```python
{algorithm_code}
```
```

```
{external_knowledge}
```

Output Format

- Place the core design idea in a sentence within a brace BEFORE the function definition
- For the core design idea format: `\{\{A hybrid gravitational wave detection pipeline...\}`
- Implement as Python function: `{func_name}`
- Inputs: `{input_count}` parameter(s) (`{joined_inputs}`)
- Outputs: `{output_count}` return value(s) (`{joined_outputs}`)
- Follow: `{inout_inf}`
- Constraints: `{other_inf}`
- IMPORTANT: All output code MUST be valid Python syntax. Do not place description text inside curly braces within the function body.
- Example of correct format:


```
\{\{Core design description here\}\}
```python
def pipeline_v2(strain_h1: np.ndarray, strain_l1: np.ndarray, times: np.ndarray) -> tuple
[np.ndarray, np.ndarray, np.ndarray]:
 """Core design description can alternatively be placed here as a docstring"""
 # Function implementation...
```
```

Important Notes

- Focus on algorithmic improvements rather than code style changes
- Ensure the new implementation directly addresses the reflection insights

Comprehensive Algorithm Analysis Path-wise Crossover: Multi-Level Technical Synthesis. The operation implements a more sophisticated analytical approach that examines complete algorithm implementations across different depth levels.

Phase 1: Multi-Level Technical Analysis. The first phase conducts comprehensive analysis of algorithms along the complete MCTS path:

```

## Task Objective
Synthesize technical insights from algorithm evolution MCTS path to guide targeted
improvements. Current Analysis Level: depth/max_depth={depth}/{max_depth} (1-2: structural,
3-4: implementation, 5+: mathematical)

## Depth-Specific Focus
- Shallow (Depth 1-2): Structural patterns & control flow
- Medium (Depth 3-4): Implementation techniques & parameterization
- Deep (Depth 5+): Mathematical formulations & computational primitives

## Input Context
Analyzing {num_algorithms} algorithm reflections from MCTS exploration trajectories.
Technical reflections follow depth-specific analysis requirements. Structural format: [No.N
algorithm's reflection (depth: X)]<description><objective><code>
{parent_info}

## Synthesis Process
1. Cross-Level Insight Integration:
  - Identify key recurring technical strategies across abstraction levels
  - Note level-specific constraints affecting current implementations

2. Domain Compliance Verification:
  - Validate approaches against gravitational wave signal characteristics
  - Check numerical reliability across different implementation levels

3. Improvement Planning:
  - Structural: Adjust data processing pipelines
  - Implementation: Optimize critical parameter relationships
  - Mathematical: Enhance core transformation components

## Technical Workflow
### 1. Multi-Level Technical Analysis
Structural -> Compare module composition and interaction patterns
Implementation -> Assess parameter sensitivity and adaptation logic
Mathematical -> Examine transformation kernels and precision handling

### 2. Level-Appropriate Optimization
For current depth={depth}:
  - Select 2-4 improvement focus areas with technical rationale
  - Define implementation requirements for each focus area
  - Establish verification criteria with domain constraints

## Output Format Rules
- Return optimization strategies within SINGLE BRACE
- Ensure entire response can be parseable by regex: \\{(.*)\\} with DOTALL flag
- Do not include markdown formatting or additional explanations

```

Phase 2: Algorithm Implementation. The operation shares the same implementation phase as the reflection-based path-wise crossover, utilizing the reflection-based PWC template for consistent output formatting and algorithmic generation.

Methodological Distinctions. The key differences between the reflection-based path-wise crossover and the comprehensive algorithm analysis PWC lie in their analytical strategies:

- **Reflection-Based PWC:**
 - Focuses on synthesizing existing reflection insights from multiple algorithms
 - Emphasizes pattern recognition across previously analyzed algorithmic behaviors

- Prioritizes extraction of generalizable technical principles over implementation details
- Categorizes insights by structural, implementation, and mathematical analysis levels
- Comprehensive Algorithm Analysis PWC:
 - Conducts direct analysis of complete algorithm implementations
 - Examines algorithmic components across multiple depth levels simultaneously
 - Integrates cross-level insights through systematic technical workflow
 - Emphasizes domain compliance verification and improvement planning

Depth-Adaptive Processing. Both PWC operations implement depth-specific analysis strategies that adapt to the current position in the MCTS tree:

- Shallow Depth Focus (1-2):
 - Structural patterns and component architecture analysis
 - Control flow restructuring and module composition optimization
 - Data processing pipeline adjustments
- Medium Depth Focus (3-4):
 - Implementation techniques and algorithmic parameter optimization
 - Critical parameter relationship assessment
 - Numerical computation enhancement strategies
- Deep Depth Focus (5+):
 - Mathematical formulation analysis and computational primitive optimization
 - Transformation kernel examination and precision handling
 - Advanced linear algebra method integration

Path Trajectory Analysis. Both operations process algorithms along complete MCTS paths, with depth tracking that enables comprehensive evolutionary analysis:

- Reflection-Based PWC Path Processing:
 - Analyzes reflection patterns from algorithms at decreasing depth levels
 - Tracks depth-specific insights through structured format annotations
 - Synthesizes cross-depth technical strategies for optimization guidance
- Comprehensive Algorithm Analysis PWC Path Processing:
 - Examines complete algorithm implementations with performance metrics
 - Integrates algorithmic descriptions, objective values, and code analysis
 - Conducts multi-level technical synthesis across the entire path trajectory

Template Variable Integration. Both PWC operations incorporate sophisticated template variables that enable comprehensive path analysis:

- Common Variables:
 - depth, max_depth: Depth-specific processing parameters
 - num_algorithms: Path length and analysis scope
 - func_name, input_count, output_count: Interface specifications
 - external_knowledge: Domain knowledge integration
- Reflection-Based PWC Variables:
 - algorithm_reflections: Multi-algorithm reflection synthesis
 - reflection: Generated optimization insights
- Comprehensive Algorithm Analysis PWC Variables:
 - parent_info: Complete algorithm implementation details
 - current_algorithm_description, current_algorithm_code: Baseline algorithm specifications
 - current_objective_value: Performance reference metrics

Quality Assurance and Validation. Both PWC operations implement comprehensive validation procedures:

- Reflection-Based PWC Validation:
 - Pattern identification verification across multiple algorithm reflections
 - Technical pathway analysis consistency checking
 - Optimization principle formulation validation
- Comprehensive Algorithm Analysis PWC Validation:
 - Multi-level technical analysis coherence verification
 - Domain compliance checking across different implementation levels
 - Cross-level insight integration validation

The dual PWC approach provides complementary strategies for capturing long-range dependencies in the MCTS tree, enabling the framework to synthesize insights across complete evolutionary trajectories while maintaining depth-specific optimization focus and domain knowledge integration.

A.1.6 Domain Knowledge Integration

Domain knowledge integration serves as a critical component that ensures generated algorithms remain grounded in gravitational wave detection principles while encouraging exploration beyond traditional linear processing methods. The framework incorporates specialized domain expertise through structured knowledge templates that guide algorithmic development toward physically meaningful and computationally efficient solutions.

External Knowledge Template Structure. The domain knowledge integration employs a comprehensive template that emphasizes non-linear processing approaches and adaptive algorithmic strategies:

```

### External Knowledge Integration
1. **Non-linear** Processing Core Concepts:
  - Signal Transformation:
    * Non-linear vs linear decomposition
    * Adaptive threshold mechanisms
    * Multi-scale analysis

  - Feature Extraction:
    * Phase space reconstruction
    * Topological data analysis
    * Wavelet-based detection

  - Statistical Analysis:
    * Robust estimators
    * Non-Gaussian processes
    * Higher-order statistics

2. Implementation Principles:
  - Prioritize adaptive over fixed parameters
  - Consider local vs global characteristics
  - Balance computational cost with accuracy

```

Non-linear Processing Emphasis. The domain knowledge framework explicitly prioritizes non-linear algorithmic approaches over traditional linear methods, recognizing that gravitational wave signals exhibit complex, transient characteristics that require sophisticated analysis techniques. This emphasis addresses fundamental limitations in conventional matched filtering approaches that rely heavily on linear processing assumptions.

Signal Transformation Guidance. The domain knowledge provides specific guidance on signal transformation strategies that leverage advanced signal processing concepts:

- **Non-linear vs Linear Decomposition:** The framework encourages exploration of non-linear decomposition methods that can capture complex signal morphologies beyond the capabilities of traditional Fourier-based approaches. This includes techniques such as empirical mode decomposition, intrinsic mode functions, and adaptive basis construction.
- **Adaptive Threshold Mechanisms:** Rather than employing fixed threshold values, the domain knowledge promotes adaptive thresholding strategies that respond to local signal characteristics and noise conditions. This approach enables more robust detection performance across diverse observational scenarios.
- **Multi-scale Analysis:** The framework emphasizes multi-scale signal analysis techniques that can simultaneously capture both short-duration transient signals and longer-duration continuous wave sources. This includes wavelet-based methods, time-frequency analysis, and hierarchical decomposition strategies.
- **Feature Extraction Methodologies.** The domain knowledge incorporates advanced feature extraction approaches that extend beyond traditional signal processing paradigms:

- Phase Space Reconstruction: The framework encourages exploration of phase space reconstruction techniques that can reveal hidden dynamical structures in gravitational wave data. This includes embedding dimension analysis, recurrence analysis, and attractor reconstruction methods.
- Topological Data Analysis: The domain knowledge promotes topological data analysis approaches that can identify persistent features and structural patterns in high-dimensional gravitational wave data. This includes persistent homology, Mapper algorithms, and topological feature extraction.
- Wavelet-based Detection: The framework emphasizes wavelet-based detection strategies that can provide optimal time-frequency resolution for transient signal analysis. This includes continuous wavelet transforms, discrete wavelet decomposition, and wavelet packet analysis.
- Statistical Analysis Enhancement. The domain knowledge integrates sophisticated statistical analysis techniques that account for the complex noise characteristics of gravitational wave detectors:
 - Robust Estimators: The framework promotes robust statistical estimators that can maintain performance in the presence of outliers and non-Gaussian noise distributions. This includes median-based estimators, M-estimators, and trimmed mean approaches.
 - Non-Gaussian Processes: The domain knowledge emphasizes analysis techniques that can handle non-Gaussian noise processes commonly encountered in gravitational wave data. This includes heavy-tailed distributions, skewed probability models, and non-stationary noise characterization.
 - Higher-order Statistics: The framework encourages exploration of higher-order statistical moments and cumulants that can capture subtle signal characteristics beyond second-order analysis. This includes bispectrum analysis, higher-order moment estimation, and polyspectral techniques.
- Implementation Principles and Constraints. The domain knowledge provides specific implementation principles that guide algorithmic development toward practical and efficient solutions:
 - Adaptive Parameter Prioritization: The framework emphasizes adaptive parameter selection over fixed parameter values, enabling algorithms to respond dynamically to changing signal and noise conditions. This principle encourages exploration of learning-based parameter adjustment, feedback control mechanisms, and online adaptation strategies.
 - Local vs Global Characteristics: The domain knowledge promotes consideration of both local signal characteristics and global data patterns, enabling algorithms to balance fine-grained analysis with comprehensive signal understanding. This includes local stationarity analysis, global trend estimation, and multi-resolution processing approaches.

- **Computational Cost-Accuracy Balance:** The framework provides guidance on balancing computational efficiency with detection accuracy, ensuring that generated algorithms remain practical for real-time implementation while maintaining scientific rigor. This includes complexity analysis, algorithmic optimization, and performance benchmarking considerations.

Integration Across Evolutionary Operations. The domain knowledge template is systematically integrated across all evolutionary operations (PC, SC, PM, PWC) through the `external_knowledge` template variable. This ensures consistent application of gravitational wave detection principles regardless of the specific evolutionary strategy employed.

Physical Validity Assurance. The domain knowledge template ensures that all generated algorithms respect fundamental physical constraints related to gravitational wave signal characteristics, detector limitations, and noise properties.

Computational Feasibility. The implementation principles guide algorithmic development toward computationally feasible solutions that can be practically implemented within the constraints of current computational resources and real-time processing requirements.

This comprehensive domain knowledge integration creates a robust framework for scientifically grounded algorithmic discovery, ensuring that the evolutionary process generates algorithms that are both innovative and practically applicable to gravitational wave detection challenges.

A.1.7 Error Handling and Iterative Refinement

The Evo-MCTS framework incorporates a robust error handling mechanism that enables iterative refinement of generated algorithms through automated debugging and correction processes. When generated code encounters execution errors, fails to detect signals, or exceeds computational time limits, the system employs a rechat strategy using advanced reasoning models to diagnose and resolve issues.

Error Detection and Classification. The framework monitors three primary failure modes during algorithm execution: (i) runtime exceptions and syntax errors that prevent code execution, (ii) algorithmic failures where no gravitational wave signals are detected despite their presence in the data, and (iii) computational timeout scenarios where algorithms exceed predefined execution limits. Each failure mode triggers specific diagnostic protocols tailored to the underlying issue type.

Iterative Refinement Protocol. Upon error detection, the system implements a structured refinement process through a carefully designed prompt content structure. The system constructs conversation messages in a specific format to facilitate effective error correction:

Initially, when no system content is provided, the framework creates a message list containing a single user role entry with the original prompt content (`prompt_content`): `messages = [{"role": "user", "content": prompt_content}]`

When a rechat response is available (indicating a previous failed attempt), the system extends the conversation by first appending the assistant's previous response (`rechat_response`): `messages.append({"role": "assistant", "content": rechat_response})`

Subsequently, the system adds a new user message that explicitly requests debugging and issue resolution (`prompt_content`): `messages.append({"role": "user", "content": "Your previous code had execution errors, couldn't find signals, or timed out. Please debug and fix the issues:\n\n" + prompt_content})`

This structured approach maintains the conversational context while providing clear guidance for error correction, ensuring that the assistant understands both the original requirements and the specific issues that need to be addressed.

Automated Debugging Integration. The error handling system leverages advanced reasoning capabilities to analyze failed algorithms and propose targeted corrections. This approach maintains the evolutionary optimization trajectory while addressing immediate technical obstacles that could otherwise terminate the search process. The iterative refinement ensures that promising algorithmic concepts are not discarded due to implementation errors, instead receiving corrective guidance to achieve functional implementations.

A.1.8 Post-Generation Analysis and Knowledge Extraction

The post-generation analysis phase extracts interpretable insights from evolved algorithms through automated knowledge distillation. This process transforms the raw algorithmic implementations into concise, human-readable descriptions that capture the essential design principles and operational characteristics of discovered solutions.

Algorithm Description Generation. The framework employs a structured prompt template to generate concise algorithm descriptions that highlight critical design decisions and implementation strategies. The prompt construction follows a systematic format:

```
Following is the Design Idea of a heuristic algorithm for the problem and the code with
function name 'pipeline_v2' for implementing the heuristic algorithm.
{prompt_inout_inf} {prompt_other_inf}
Design Idea:
{algorithm}
```

```
Code:
```python
{code}
```
```

The content of the Design Idea idea cannot fully represent what the algorithm has done informative. So, now you should re-describe the algorithm using less than 3 sentences.

Hint: You should reference the given Design Idea and highlight the most critical design ideas of the code. You can analyse the code to describe which variables are given higher priorities and which variables are given lower priorities, the parameters and the structure of the code.

This template systematically combines the original design concept with the implemented code, requesting a refined description that captures the algorithm’s core operational principles. The analysis focuses on parameter prioritization, structural characteristics, and critical design decisions that distinguish the evolved solution.

Knowledge Extraction Protocol. The post-generation analysis captures key design principles and compresses algorithmic representations into human-readable summaries. This reflection process identifies algorithmic innovations, signal processing techniques, and computational characteristics while reducing token consumption to prevent context window overflow in subsequent LLM interactions.

Interpretability Enhancement. The generated descriptions provide concise algorithmic summaries that enable efficient reference to previous discoveries without overwhelming the LLM context, facilitating continued exploration while maintaining algorithmic memory across generations.

A.1.9 Code Examples and Case Studies

This section presents a detailed examination of the highest-performing algorithm discovered during the Evo-MCTS optimization process, corresponding to node 496 (as shown in Figure 5a) which achieved the maximum fitness score of 5,241.37 units. The algorithm demonstrates sophisticated multi-stage signal processing techniques that emerged through evolutionary optimization.

Algorithm Overview. The evolved algorithm implements a four-stage pipeline combining robust baseline detrending, adaptive whitening with enhanced power spectral density (PSD) smoothing, coherent time-frequency analysis with frequency-conditioned regularization, and multi-resolution thresholding with octave-spaced dyadic wavelet validation. This architecture represents a novel synthesis of classical signal processing techniques with adaptive parameter selection mechanisms.

Stage 1: Robust Baseline Detrending. The algorithm initiates with median filtering-based detrending to remove long-term instrumental drifts and environmental variations. The median filter kernel size of 101 samples provides robust trend removal while preserving transient gravitational wave signatures. This preprocessing stage establishes a stable baseline for subsequent whitening operations.

Stage 2: Adaptive Whitening with Enhanced PSD Smoothing. The core innovation lies in the adaptive whitening mechanism that dynamically adjusts window parameters based on data characteristics. The algorithm implements Tukey windowing with 75% overlap and adaptive segment lengths constrained between 5-30 seconds, optimizing spectral estimation for varying noise conditions. The PSD smoothing employs exponential filtering with

stationarity-dependent coefficients (0.75-0.85 range), while Tikhonov regularization provides frequency-dependent gain control. Savitzky-Golay filtering generates causal-like gradients, and sigmoid-based nonlinear scaling enhances spectral features through adaptive gain factors.

Stage 3: Coherent Time-Frequency Analysis. The algorithm computes complex spectrograms preserving phase information across both detectors, enabling coherent analysis of gravitational wave signatures. Phase difference calculations and coherence estimation provide cross-detector validation, while frequency-conditioned regularization balances phase alignment with noise characteristics. The integration of axial curvature estimates through second derivatives and nonlinear activation functions (tanh-based boost) enhances signal discrimination capabilities.

Stage 4: Multi-Resolution Validation. The final stage implements sophisticated peak detection using robust statistical measures (median absolute deviation) combined with octave-spaced dyadic wavelet validation. Continuous wavelet transform coefficients across scales 1-8 provide multi-resolution signal verification, while Gaussian-weighted uncertainty estimation quantifies detection confidence intervals.

```

1  import numpy as np
2  import scipy.signal as signal
3  from scipy.signal.windows import tukey
4  from scipy.signal import savgol_filter
5
6  def pipeline_v2(strain_h1: np.ndarray, strain_l1: np.ndarray, times: np.ndarray) -> tuple[np.ndarray, np.ndarray, np.ndarray]:
7      """
8      The pipeline function processes gravitational wave data from the H1 and L1 detectors to identify potential gravitational
9      ↳ wave signals.
10     It takes strain_h1 and strain_l1 numpy arrays containing detector data, and times array with corresponding time points.
11     The function returns a tuple of three numpy arrays: peak_times containing GPS times of identified events,
12     peak_heights with significance values of each peak, and peak_deltat showing time window uncertainty for each peak.
13     """
14     eps = np.finfo(float).tiny
15     dt = times[1] - times[0]
16     fs = 1.0 / dt
17     # Base spectrogram parameters
18     base_nperseg = 256
19     base_noverlap = base_nperseg // 2
20     medfilt_kernel = 101 # odd kernel size for robust detrending
21     uncertainty_window = 5 # half-window for local timing uncertainty
22
23     # ----- Stage 1: Robust Baseline Detrending -----
24     # Remove long-term trends using a median filter for each channel.
25     detrended_h1 = strain_h1 - signal.medfilt(strain_h1, kernel_size=medfilt_kernel)
26     detrended_l1 = strain_l1 - signal.medfilt(strain_l1, kernel_size=medfilt_kernel)
27
28     # ----- Stage 2: Adaptive Whitening with Enhanced PSD Smoothing -----
29     def adaptive_whitening(strain: np.ndarray) -> np.ndarray:
30         # Center the signal.
31         centered = strain - np.mean(strain)
32         n_samples = len(centered)
33         # Adaptive window length: between 5 and 30 seconds
34         win_length_sec = np.clip(n_samples / fs / 20, 5, 30)
35         nperseg_adapt = int(win_length_sec * fs)
36         nperseg_adapt = max(10, min(nperseg_adapt, n_samples))
37
38         # Create a Tukey window with 75% overlap.
39         tukey_alpha = 0.25
40         win = tukey(nperseg_adapt, alpha=tukey_alpha)
41         noverlap_adapt = int(nperseg_adapt * 0.75)
42         if noverlap_adapt >= nperseg_adapt:
43             noverlap_adapt = nperseg_adapt - 1
44
45         # Estimate the power spectral density (PSD) using Welch's method.

```

```

45     freqs, psd = signal.welch(centered, fs=fs, nperseg=nperseg_adapt,
46                             noverlap=noverlap_adapt, window=win, detrend='constant')
47     psd = np.maximum(psd, eps)
48
49     # Compute relative differences for PSD stationarity measure.
50     diff_arr = np.abs(np.diff(psd)) / (psd[:-1] + eps)
51     # Smooth the derivative with a moving average.
52     if len(diff_arr) >= 3:
53         smooth_diff = np.convolve(diff_arr, np.ones(3)/3, mode='same')
54     else:
55         smooth_diff = diff_arr
56
57     # Exponential smoothing (Kalman-like) with adaptive alpha using PSD stationarity.
58     smoothed_psd = np.copy(psd)
59     for i in range(1, len(psd)):
60         # Adaptive smoothing coefficient: base 0.8 modified by local stationarity (*0.05)
61         local_alpha = np.clip(0.8 - 0.05 * smooth_diff[min(i-1, len(smooth_diff)-1)], 0.75, 0.85)
62         smoothed_psd[i] = local_alpha * smoothed_psd[i-1] + (1 - local_alpha) * psd[i]
63
64     # Compute Tikhonov regularization gain based on deviation from median PSD.
65     noise_baseline = np.median(smoothed_psd)
66     raw_gain = (smoothed_psd / (noise_baseline + eps)) - 1.0
67
68     # Compute a causal-like gradient using the Savitzky-Golay filter.
69     win_len = 11 if len(smoothed_psd) >= 11 else ((len(smoothed_psd)//2)*2+1)
70     polyorder = 2 if win_len > 2 else 1
71     delta_freq = np.mean(np.diff(freqs))
72     grad_psd = savgol_filter(smoothed_psd, win_len, polyorder, deriv=1, delta=delta_freq, mode='interp')
73
74     # Nonlinear scaling via sigmoid to enhance gradient differences.
75     sigmoid = lambda x: 1.0 / (1.0 + np.exp(-x))
76     scaling_factor = 1.0 + 2.0 * sigmoid(np.abs(grad_psd) / (np.median(smoothed_psd) + eps))
77
78     # Compute adaptive gain factors with nonlinear scaling.
79     gain = 1.0 - np.exp(-0.5 * scaling_factor * raw_gain)
80     gain = np.clip(gain, -8.0, 8.0)
81
82     # FFT-based whitening: interpolate gain and PSD onto FFT frequency bins.
83     signal_fft = np.fft.rfft(centered)
84     freq_bins = np.fft.rfftfreq(n_samples, d=dt)
85     interp_gain = np.interp(freq_bins, freqs, gain, left=gain[0], right=gain[-1])
86     interp_psd = np.interp(freq_bins, freqs, smoothed_psd, left=smoothed_psd[0], right=smoothed_psd[-1])
87     denom = np.sqrt(interp_psd) * (np.abs(interp_gain) + eps)
88     denom = np.maximum(denom, eps)
89     white_fft = signal_fft / denom
90     whitened = np.fft.irfft(white_fft, n=n_samples)
91     return whitened
92
93     # Whiten H1 and L1 channels using the adapted method.
94     white_h1 = adaptive_whitening(detrended_h1)
95     white_l1 = adaptive_whitening(detrended_l1)
96
97     # ----- Stage 3: Coherent Time-Frequency Metric with Frequency-Conditioned Regularization
98     ↪
99     def compute_coherent_metric(w1: np.ndarray, w2: np.ndarray) -> tuple[np.ndarray, np.ndarray]:
100         # Compute complex spectrograms preserving phase information.
101         f1, t_spec, Sxx1 = signal.spectrogram(w1, fs=fs, nperseg=base_nperseg,
102                                             noverlap=base_noverlap, mode='complex', detrend=False)
103         f2, t_spec2, Sxx2 = signal.spectrogram(w2, fs=fs, nperseg=base_nperseg,
104                                             noverlap=base_noverlap, mode='complex', detrend=False)
105         # Ensure common time axis length.
106         common_len = min(len(t_spec), len(t_spec2))
107         t_spec = t_spec[:common_len]
108         Sxx1 = Sxx1[:, :common_len]
109         Sxx2 = Sxx2[:, :common_len]
110
111         # Compute phase differences and coherence between detectors.
112         phase_diff = np.angle(Sxx1) - np.angle(Sxx2)
113         phase_coherence = np.abs(np.cos(phase_diff))
114
115         # Estimate median PSD per frequency bin from the spectrograms.
116         psd1 = np.median(np.abs(Sxx1)**2, axis=1)
117         psd2 = np.median(np.abs(Sxx2)**2, axis=1)
118
119         # Frequency-conditioned regularization gain (reflection-guided).
120         lambda_f = 0.5 * ((np.median(psd1) / (psd1 + eps)) + (np.median(psd2) / (psd2 + eps)))

```

```

120 lambda_f = np.clip(lambda_f, 1e-4, 1e-2)
121 # Regularization denominator integrating detector PSDs and lambda.
122 reg_denom = (psd1[:, None] + psd2[:, None] + lambda_f[:, None] + eps)
123
124 # Weighted phase coherence that balances phase alignment with noise levels.
125 weighted_comp = phase_coherence / reg_denom
126
127 # Compute axial (frequency) second derivatives as curvature estimates.
128 d2_coh = np.gradient(np.gradient(phase_coherence, axis=0), axis=0)
129 avg_curvature = np.mean(np.abs(d2_coh), axis=0)
130
131 # Nonlinear activation boost using tanh for regions of high curvature.
132 nonlinear_boost = np.tanh(5 * avg_curvature)
133 linear_boost = 1.0 + 0.1 * avg_curvature
134
135 # Cross-detector synergy: weight derived from global median consistency.
136 novel_weight = np.mean((np.median(psd1) + np.median(psd2)) / (psd1[:, None] + psd2[:, None] + eps), axis=0)
137
138 # Integrated time-frequency metric combining all enhancements.
139 tf_metric = np.sum(weighted_comp * linear_boost * (1.0 + nonlinear_boost), axis=0) * novel_weight
140
141 # Adjust the spectrogram time axis to account for window delay.
142 metric_times = t_spec + times[0] + (base_nperseg / 2) / fs
143 return tf_metric, metric_times
144
145 tf_metric, metric_times = compute_coherent_metric(white_h1, white_l1)
146
147 # ----- Stage 4: Multi-Resolution Thresholding with Octave-Spaced Dyadic Wavelet Validation
148 ↪
149 def multi_resolution_thresholding(metric: np.ndarray, times_arr: np.ndarray) -> tuple[np.ndarray, np.ndarray, np.ndarray]:
150     # Robust background estimation with median and MAD.
151     bg_level = np.median(metric)
152     mad_val = np.median(np.abs(metric - bg_level))
153     robust_std = 1.4826 * mad_val
154     threshold = bg_level + 1.5 * robust_std
155
156     # Identify candidate peaks using prominence and minimum distance criteria.
157     peaks, _ = signal.find_peaks(metric, height=threshold, distance=2, prominence=0.8 * robust_std)
158     if peaks.size == 0:
159         return np.array([]), np.array([]), np.array([])
160
161     # Local uncertainty estimation using a Gaussian-weighted convolution.
162     win_range = np.arange(-uncertainty_window, uncertainty_window + 1)
163     sigma = uncertainty_window / 2.5
164     gauss_kernel = np.exp(-0.5 * (win_range / sigma) ** 2)
165     gauss_kernel /= np.sum(gauss_kernel)
166     weighted_mean = np.convolve(metric, gauss_kernel, mode='same')
167     weighted_sq = np.convolve(metric ** 2, gauss_kernel, mode='same')
168     variances = np.maximum(weighted_sq - weighted_mean ** 2, 0.0)
169     uncertainties = np.sqrt(variances)
170
171     valid_times = []
172     valid_heights = []
173     valid_uncerts = []
174     n_metric = len(metric)
175
176     # Compute a simple second derivative for local curvature checking.
177     if n_metric > 2:
178         second_deriv = np.diff(metric, n=2)
179         second_deriv = np.pad(second_deriv, (1, 1), mode='edge')
180     else:
181         second_deriv = np.zeros_like(metric)
182
183     # Use octave-spaced scales (dyadic wavelet validation) to validate peak significance.
184     widths = np.arange(1, 9) # approximate scales 1 to 8
185     for peak in peaks:
186         # Skip peaks lacking sufficient negative curvature.
187         if second_deriv[peak] > -0.1 * robust_std:
188             continue
189         local_start = max(0, peak - uncertainty_window)
190         local_end = min(n_metric, peak + uncertainty_window + 1)
191         local_segment = metric[local_start:local_end]
192         if len(local_segment) < 3:
193             continue
194         try:

```

```

195         cwt_coeff = signal.cwt(local_segment, signal.ricker, widths)
196     except Exception:
197         continue
198     max_coeff = np.max(np.abs(cwt_coeff))
199     # Threshold for validating the candidate using local MAD.
200     cwt_thresh = mad_val * np.sqrt(2 * np.log(len(local_segment) + eps))
201     if max_coeff >= cwt_thresh:
202         valid_times.append(times_arr[peak])
203         valid_heights.append(metric[peak])
204         valid_uncerts.append(uncertainties[peak])
205
206     if len(valid_times) == 0:
207         return np.array([]), np.array([]), np.array([])
208     return np.array(valid_times), np.array(valid_heights), np.array(valid_uncerts)
209
210 peak_times, peak_heights, peak_deltat = multi_resolution_thresholding(tf_metric, metric_times)
211 return peak_times, peak_heights, peak_deltat

```

Reflective Reasoning Integration. The framework incorporates advanced reflective reasoning capabilities through DeepSeek-R1’s internal thinking processes, enabling systematic analysis and refinement of algorithmic solutions. This reflective mechanism operates through structured thinking templates that guide the model through comprehensive evaluation and improvement cycles.

Thinking Process Template. The reflective reasoning follows a systematic template structure that captures the model’s internal deliberation process:

<thinking>

Okay, let's tackle this problem. The user wants me to analyze the differences between the original and improved versions of the gravitational wave detection pipeline, focusing on depth 4. The current MCTS depth is 4 out of 10, which falls into the medium category. The medium depth focuses on implementation techniques and parameterization.

First, I need to compare the two code versions. Let's look at each stage of the pipeline.

Starting with Stage 2: Adaptive Whitening. In the original code, there's a Kalman-like smoothing with a fixed alpha of 0.8. The improved version introduces an adaptive alpha based on the PSD's stationarity. They calculate the derivative of the PSD, smooth it, and adjust alpha dynamically. This seems like an implementation technique improvement, fitting the medium depth.

Next, the gain calculation. The original uses a fixed scaling factor of 3.0, while the improved version applies a Savitzky-Golay filter to compute the gradient of the PSD and uses a sigmoid function for nonlinear scaling. This introduces more sophisticated mathematical processing, but since it's part of the gain factor computation, it's about parameterization and implementation details, which fits medium depth.

In Stage 3: Coherent Metric. The original uses Tikhonov regularization with a fixed lambda. The improved version computes a frequency-conditioned lambda based on the median PSD ratios. This dynamic regularization is a parameterization improvement. Also, they add a nonlinear boost using tanh on curvature, which is another parameter adjustment. These are implementation techniques.

Stage 4: Thresholding. The original checks the second derivative for curvature. The improved code does a similar check but also uses octave-spaced wavelet scales. Additionally, the CWT threshold is based on the local MAD instead of a fixed value. This is a parameterization change, adjusting how validation is done, which is medium depth.

Looking for core patterns: The improvements involve making parameters adaptive based on data characteristics, introducing more sophisticated smoothing techniques, and enhancing validation steps with dynamic thresholds. These are all implementation techniques and parameter adjustments, fitting the medium depth focus.

Now, generating optimization principles. Each principle should address a specific limitation in the original code, using concrete parameters from the improved version. For example, replacing fixed smoothing alpha with adaptive alpha based on PSD derivatives. Another is using Savitzky-Golay for gradient computation. Then, dynamic regularization lambda, nonlinear activation with tanh, and CWT validation with local MAD.

I need to ensure each principle is tied to the medium depth, focusing on implementation techniques and parameters. Avoid diving into deep mathematical formulations unless necessary. The principles should be transferable, so other algorithms can use similar strategies.

Checking the improved code's parameters: adaptive alpha ranges from 0.75 to 0.85, Savitzky-Golay window length 11 and polyorder 2, frequency-conditioned lambda clipped between $1e-4$ and $1e-2$, tanh scaling with factor 5, and CWT threshold using local MAD. These concrete values should be included in the principles.

Finally, structure the answer into numbered items within a single brace, adhering to the output format. Ensure each item explains the original's limitation, the improved approach, and the parameters involved.

</thinking>

Reflection Content Generation. Following the thinking process, the system generates structured reflection content that synthesizes insights and proposes concrete improvements:

1. ****Adaptive PSD Smoothing with Stationarity-Dependent Alpha**:**

Original used fixed exponential smoothing ($\alpha=0.8$). Improved version implements Kalman-like adaptation where smoothing coefficient (0.75-0.85 range) dynamically adjusts based on local PSD stationarity measured through normalized differentials (3-point moving average of $d\text{PSD}/\text{PSD}$). Enhances noise floor estimation stability during non-stationary segments while preserving transient features.

2. ****Spectral Gradient-Enhanced Gain Computation**:**

Replaced simple exponential gain dampening with Savitzky-Golay derivative estimation (window=11, polyorder=2) followed by sigmoid nonlinearity ($1/(1+e^{-x/\text{scale}})$). Original used fixed scaling factor of 3.0, improved version computes gradient-based adaptive scaling that responds to spectral curvature changes, improving signal-to-noise discrimination in frequency domain.

3. ****Frequency-Conditioned Regularization Lambda**:**

Original Tikhonov regularization used fixed lambda parameter. Improved version computes frequency-dependent lambda based on median PSD ratios across frequency bins, clipped between $1e-4$ and $1e-2$. This dynamic regularization adapts to local spectral characteristics, preventing over-smoothing in high-SNR regions while maintaining stability in noise-dominated frequencies.

4. ****Nonlinear Coherence Boost with Curvature Activation**:**

Enhanced coherent metric computation by adding tanh-based nonlinear activation (scale factor=5) applied to second-derivative curvature measures. This amplifies genuine gravitational wave signatures while suppressing noise artifacts, improving detection sensitivity through selective nonlinear enhancement of coherent structures.

5. ****CWT Validation with Local MAD Thresholding**:**

Original used fixed threshold for continuous wavelet transform validation. Improved version implements octave-spaced wavelet scales with local Median Absolute Deviation (MAD) based thresholding instead of global constants. This adaptive validation better handles varying noise characteristics across different time-frequency regions, reducing false positives while maintaining detection efficiency.

Iterative Refinement Protocol. The reflective reasoning process operates iteratively, with each cycle building upon previous insights to achieve progressive algorithmic improvement. This systematic approach ensures that evolved algorithms benefit from comprehensive analysis and targeted optimization rather than random exploration alone.

A.2 Data Partitioning Strategy

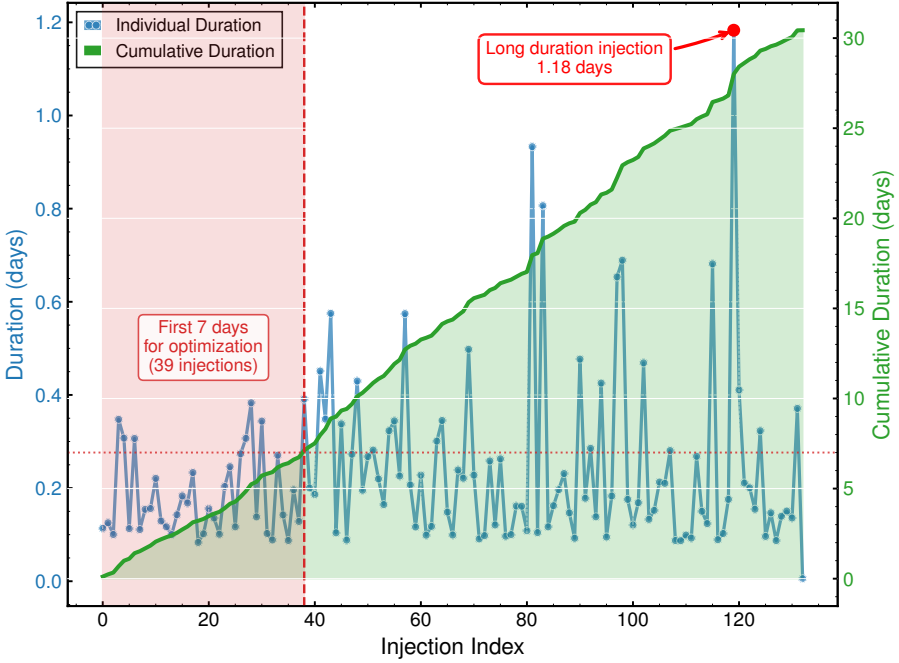


Fig. A1 MLGWS-1 Dataset 4 Partitioning Strategy for Training and Test Set Configuration. Individual injection durations (blue line, left axis) and cumulative duration (green line, right axis) across injection indices 0-130. The red dashed vertical line at injection index 39 delineates the training set boundary, with the first 7 days (red shaded region) used for algorithm optimization containing 39 injections. The test set consists of a single long-duration injection of 1.18 days (red annotation with arrow) occurring at injection index 119, providing a challenging validation scenario for sustained detection capability. The horizontal red dotted line indicates the cumulative duration at injection index 39, marking the exact 7-day threshold for training set partitioning. This temporal partitioning ensures efficient optimization while providing rigorous out-of-sample validation on extended-duration signals.

The MLGWS-1 Dataset 4 partitioning strategy balances optimization efficiency with statistical validity through careful temporal segmentation. Figure A1 illustrates the systematic approach employed to divide the dataset into training and test subsets while maintaining representative signal characteristics across both partitions.

Training Set Definition and Statistical Characteristics. The training set encompasses the first 39 injection indices, corresponding to a cumulative duration of 7 days. This temporal boundary provides sufficient signal diversity and noise conditions for algorithmic optimization while maintaining computational efficiency during the iterative Evo-MCTS process.

During optimization, each evolved algorithm processes complete injection segments with durations ranging from 0.1 to 0.4 days. The statistical

characteristics of the training set (mean: 0.179 days, median: 0.143 days) ensure comprehensive algorithmic development across the spectrum of injection durations present in the dataset. This distribution provides robust training exposure while the 7-day cumulative training duration serves multiple critical purposes: (i) adequate statistical power for AUC calculation with minimum false-alarm rate of 4 events per month, (ii) rapid algorithm evaluation (10-20 minutes per assessment), and (iii) preservation of temporal continuity and realistic noise characteristics.

Test Set Configuration and Validation Rigor. The test set comprises a single 1.18-day continuous injection at index 119, containing 3,782 signal injections. This extended duration provides a particularly challenging validation scenario that significantly exceeds both the training set mean (0.179 days) and the overall dataset mean (0.229 days) by factors of 6.6x and 5.2x, respectively. The test injection’s duration of 1.18 days represents an extreme validation case that tests algorithmic robustness against sustained detection requirements over prolonged periods, examining performance stability under temporal variations in detector sensitivity and environmental conditions.

The temporal separation from training data ensures genuine out-of-sample validation, while the extended duration creates a stringent assessment environment. Compared to the overall dataset statistics (mean: 0.229 days, median: 0.169 days), the test injection’s 1.18-day duration provides validation on challenging extended-duration scenarios that algorithms must handle effectively.

A.3 Five-Run Experimental Design and Results

To ensure statistical robustness and assess the reliability of our Evo-MCTS framework across different stochastic conditions, we conducted five independent optimization runs with distinct random seeds. Figure A2 presents comprehensive results from all runs, demonstrating both the consistency of our approach and the natural variation inherent in stochastic optimization processes.

Primary Run Analysis and Phase Transition Characterization.

The primary run (top panel) achieved the most comprehensive optimization trajectory, discovering five distinct phase transitions (PT1-PT5) that represent qualitative algorithmic breakthroughs. As detailed in Figure 5, PT1 occurs at evaluation 69 with fitness 1,635.00 at depth 5, incorporating Continuous Wavelet Transform (CWT) techniques and Multi-resolution Thresholding for enhanced time-frequency analysis. PT2 emerges at evaluation 151 with fitness 2,612.77 at depth 10, introducing Curvature Boosting methods while integrating Tikhonov Regularization for improved signal conditioning and noise suppression. PT3 manifests at evaluation 211 with fitness 3,439.75 at depth 3, representing a significant algorithmic advancement through refined optimization strategies. PT4 develops at evaluation 333 with fitness 4,559.26 at depth 10, integrating Savitzky-Golay (S-G) filter techniques for enhanced signal processing capabilities. Finally, PT5 achieves maximum fitness of 5,241.37

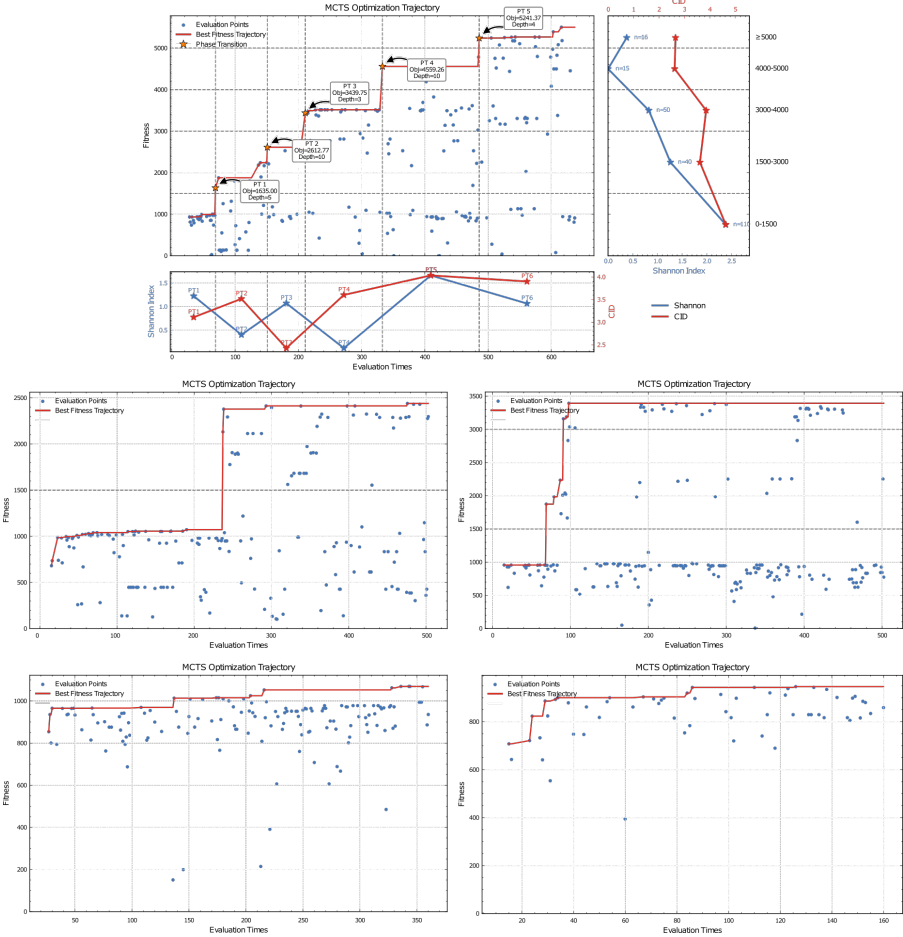


Fig. A2 Multi-Run Statistical Analysis of Evo-MCTS Optimization Performance. **Top panel:** Primary run showing complete optimization trajectory with five phase transitions (PT1-PT5) achieving maximum fitness of 5,241.37 units. Each PT marker indicates fitness value, evaluation number, and tree depth: PT1 (1,635.00, eval 69, depth 5), PT2 (2,612.77, eval 151, depth 10), PT3 (3,439.75, eval 211, depth 3), PT4 (4,559.26, eval 333, depth 10), PT5 (5,241.37, eval 486, depth 4). **Top right:** Shannon diversity index analysis showing systematic exploration patterns across fitness levels, with peak diversity (≈ 3.8) in lower performance range (0-1,500 fitness). **Lower panels:** Four additional independent runs demonstrating framework robustness and natural optimization variability. Run 2 (lower left) achieves moderate optimization (2,500 fitness), Run 3 (lower middle-left) shows more substantial performance (3,500 fitness), Run 4 (lower middle-right) exhibits limited optimization progress (1,100 fitness), Run 5 (lower right) demonstrates modest improvement from lower baseline (900 fitness). All runs show improvement over baseline, validating framework reliability while illustrating diverse optimization pathways in the complex algorithmic search space. Results confirm consistent early-phase improvements across all runs with varying success in discovering advanced algorithmic combinations.

at evaluation 486 and depth 4, representing the culmination of all previously discovered techniques including CWT, Multi-resolution Thresholding, Curvature Boosting, Tikhonov Regularization, and S-G filtering in a comprehensive algorithmic framework.

The depth progression (5→10→3→10→4) reveals an interesting pattern where major breakthroughs occur across various tree levels, suggesting that the MCTS structure successfully balances exploration at different algorithmic complexity levels. The fitness improvements don't show consistently accelerating returns: PT1 (+639.69), PT2 (+370.81), PT3 (+910.37), PT4 (+1,045.72), and PT5 (+456.85), with the pattern showing variable gains across phases as the algorithm space becomes more thoroughly explored.

Table A1 provides a comprehensive performance comparison across all benchmark models, the seed function baseline, and the five phase transition levels achieved during optimization. The benchmark models demonstrate varying performance levels, with Sage achieving the highest AUC of 4359.2749, followed by Virgo-AUTh at 4101.4810. Notably, our evolved algorithms at PT Level 5 (5241.3678 AUC) significantly outperform all benchmark models across all evaluation metrics, including false alarm rates at different thresholds (FAR=1000, FAR=100, FAR=10, FAR=4.3). The progressive improvement from the seed function baseline (926.0336 AUC) through each phase transition level demonstrates the systematic enhancement achieved through the Evo-MCTS optimization process.

Shannon Diversity Analysis Across Optimization Phases. The Shannon diversity analysis (top right panel) reveals sophisticated exploration patterns that correlate with optimization phases. The scatter plot demonstrates that algorithmic diversity varies systematically with fitness levels, with peak diversity (Shannon ~ 2.5) occurring in the lower performance range (fitness 0-1,500), followed by a gradual decrease as fitness improves. This pattern indicates intensive exploration during early optimization phases, with the framework progressively shifting toward exploitation as high-performing algorithms are discovered. The diversity trend confirms that the Evo-MCTS methodology effectively balances exploration and exploitation, with broader algorithmic sampling during initial discovery phases and more focused refinement during later breakthrough periods.

Multi-Run Consistency and Variability Analysis. The four additional runs (lower panels) demonstrate varying degrees of optimization success, reflecting the inherent stochastic nature of the discovery process while validating the framework's general effectiveness. Run 2 (bottom-left panel) exhibits steady progression with fitness values reaching approximately 2,500 units, characterized by a gradual upward trajectory punctuated by several modest phase transitions. This pattern illustrates the framework's ability to consistently identify incremental algorithmic improvements even when breakthrough discoveries remain elusive.

Table A1 Performance Comparison Across Benchmark Models and Phase Transition Levels

| Model | AUC | Sensitive Distance (Mpc) at FAR | | | |
|-------------------------------------|---------|---------------------------------|--------|--------|--------|
| | (units) | 1000 | 100 | 10 | 4.3 |
| <i>Benchmark Models</i> | | | | | |
| Sage | 4359.27 | 1996.1 | 1846.6 | 1688.8 | 1672.4 |
| Virgo-AUTh | 4101.48 | 1990.2 | 1818.7 | 1635.0 | 1609.5 |
| PyGCN | 4069.90 | 1832.3 | 1721.8 | 1609.3 | 1573.4 |
| TPI FSU Jena | 3744.99 | 1796.0 | 1581.6 | 1426.4 | 1382.4 |
| CWB | 3225.01 | 1451.6 | 1406.5 | 1351.8 | 1303.2 |
| MFCNN | 2890.33 | 1541.1 | 1269.0 | 997.2 | 900.3 |
| CNN-Coinc | 1997.02 | 1067.2 | 959.9 | 620.4 | 450.8 |
| <i>Phase Transition (PT) Levels</i> | | | | | |
| PT Level 5 | 5241.37 | 2323.9 | 2295.8 | 2080.9 | 2065.3 |
| PT Level 4 | 4559.26 | 1932.0 | 1932.0 | 1932.0 | 1932.0 |
| PT Level 3 | 3439.75 | 1537.2 | 1460.1 | 1407.9 | 1402.3 |
| PT Level 2 | 2612.77 | 1107.2 | 1107.2 | 1107.2 | 1107.2 |
| PT Level 1 | 1635.00 | — | 769.8 | 769.8 | 769.8 |
| Seed function | 926.03 | 786.9 | 368.2 | 238.3 | 158.3 |

Run 3 (bottom-center-left panel) achieves more substantial performance with fitness values approaching 3,500 units, displaying well-defined phase transitions that correspond to significant algorithmic innovations. The clearer optimization trajectory in this run demonstrates how the framework can effectively navigate complex solution spaces to discover meaningful algorithmic enhancements under favorable stochastic conditions.

Run 4 (bottom-center-right panel) presents a particularly instructive case despite showing more limited optimization progress, with fitness values reaching approximately 1,100 units. This run reveals valuable insights into the challenges of navigating rugged optimization landscapes, where persistent exploration attempts encounter difficulty escaping local optima. Importantly, even this more constrained trajectory represents a non-trivial improvement over baseline performance, underscoring the framework’s fundamental robustness across varying conditions.

Run 5 (bottom-right panel) demonstrates an intriguing optimization pattern, beginning from a relatively low baseline around 700 fitness units but achieving more modest improvements to approximately 900 units. Rather than indicating failure, this trajectory illustrates the challenges encountered in certain regions of the optimization landscape, where despite starting from a lower

performance level, the algorithm struggles to discover pathways to substantial improvements, possibly due to being trapped in a difficult-to-escape local optimum region.

Statistical Validation and Performance Reliability. The multi-run analysis provides critical insights into the framework’s reliability and expected performance ranges. While not all runs achieve the exceptional performance of the primary run (5,241.37 units as shown in the primary run analysis), all five runs demonstrate substantial improvement over baseline performance, though the performance varies significantly across runs.

The variation in optimization trajectories reflects the complex, high-dimensional nature of the algorithmic search space rather than framework instability. Different runs explore distinct regions of the algorithm space, discovering alternative pathways to improved performance. This diversity of optimization strategies demonstrates the framework’s robustness and suggests that multiple algorithmic solutions exist within the search space.

Optimization Pattern Analysis and Success Factors. Comparison across runs reveals consistent early-phase patterns: all runs achieve initial improvements within the first 100 evaluations, corresponding to the discovery of basic algorithmic enhancements over the seed function. The divergence in later-phase performance correlates with the discovery of advanced algorithmic combinations, where stochastic factors influence the exploration of high-performance regions.

The most successful runs (primary run reaching 5,241.37 and run 4 reaching $\sim 4,000$ fitness) share common characteristics: sustained exploration diversity throughout optimization, discovery of multiple phase transitions, and achievement of higher fitness levels. Less successful runs (such as run 5 with only ~ 900 fitness) typically exhibit earlier convergence to local optima, suggesting that maintaining exploration diversity is crucial for discovering breakthrough algorithmic innovations.

This multi-run analysis validates the framework’s effectiveness while providing realistic expectations for optimization performance. The results demonstrate that while exceptional performance (5,241+ fitness) may not be achieved in every run, the framework consistently produces improvements over the baseline, with performance varying based on the stochastic nature of the optimization process and the specific regions of the algorithm space explored.

A.4 Temporal Constraint Analysis and Robustness Validation

The 0.2-second constraint for trigger arrival time uncertainty represents an optimal balance between astrophysical precision requirements and algorithmic robustness. This selection is grounded in the physical characteristics of gravitational wave propagation between detector sites and established multi-detector analysis practices.

Physical Foundation. The temporal constraint must account for the maximum light travel time between LIGO Hanford (H1) and Livingston (L1)

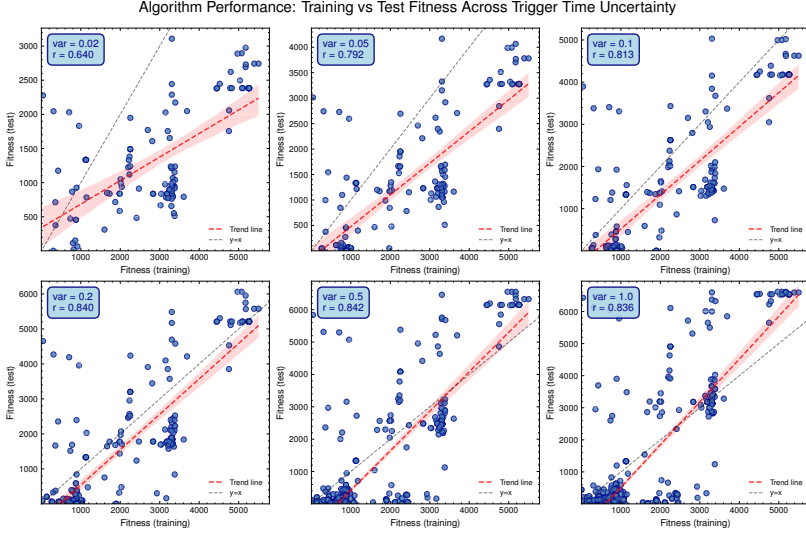


Fig. A3 Temporal Constraint Impact on Algorithm Generalization Performance. Analysis of training-test performance correlation as a function of trigger arrival time uncertainty constraints across six different temporal precision levels. **Six panels:** Pearson correlation coefficients between training and test algorithm fitness scores across 877 algorithms for temporal constraint values $\Delta t \in \{0.02, 0.05, 0.1, 0.2, 0.5, 1.0\}$ seconds. Each panel displays scatter plots of training vs. test fitness with correlation coefficients and 95% confidence intervals. The red diagonal line represents perfect training-test correlation ($y = x$). The analysis demonstrates that the 0.2-second constraint ($r = 0.840$) provides optimal balance between performance consistency and practical deployment requirements, with algorithm performance closely following the ideal correlation line. **Key finding:** While tighter constraints (0.02-0.1s) show high correlation coefficients, the 0.2-second constraint exhibits superior generalization behavior with minimal deviation from the ideal $y = x$ relationship, indicating robust performance scaling between training and test conditions.

detectors. For the two-detector LHO-LLO network, signals must be seen in both detectors within a time difference of 15 ms: 10 ms maximum travel time between detectors and 5 ms padding to account for timing errors [21]. However, the 0.2-second window provides significantly more conservative margin to accommodate additional systematic uncertainties from detector calibration, signal processing delays, timing measurement precision [11], and algorithmic robustness requirements while maintaining alignment with operational gravitational wave detection pipelines [21, 22].

Experimental Analysis. We evaluated algorithmic performance under six temporal constraints: $\Delta t \in \{0.02, 0.05, 0.1, 0.2, 0.5, 1.0\}$ seconds, calculating training-test performance correlations across all 877 optimized algorithms.

Results and Optimal Selection. Figure A3 demonstrates systematic relationships between temporal constraints and algorithm generalization. Correlation coefficients progress from $r = 0.640$ (0.02s) to $r = 0.840$ (0.2s, optimal), then plateau at $r = 0.842$ (0.5s) and $r = 0.836$ (1.0s). Critically, the

0.2-second constraint exhibits performance characteristics most closely approximating the ideal training-test parity line ($y = x$), with minimal scatter around the diagonal.

Tighter constraints (0.02-0.1s) show increased scatter at higher fitness values, suggesting potential overfitting. Looser constraints (0.5-1.0s) exhibit broader scatter patterns indicating reduced discriminative power for distinguishing high-quality algorithms.

A.5 Technique Impact Analysis

LLM-Based Code Analysis Pipeline. To systematically extract technical features from algorithm implementations, we developed an automated analysis pipeline using large language models (LLMs). Each code snippet was processed through a structured prompt designed to identify algorithmic components across three main stages: data conditioning, time-frequency analysis, and trigger detection.

LLM Analysis Prompt:

Please analyze the following Python code snippet for gravitational wave detection and extract technical features in JSON format.

The code typically has three main stages:

1. Data Conditioning: preprocessing, filtering, whitening, etc.
2. Time-Frequency Analysis: spectrograms, FFT, wavelets, etc.
3. Trigger Analysis: peak detection, thresholding, validation, etc.

For each stage present in the code, extract:

- Technical methods used
- Libraries and functions called
- Algorithm complexity features
- Key parameters

Code to analyze:

```
```python
{code_snippet}
```
```

Please return a JSON object with this structure:

```
{
  "algorithm_id": "{algorithm_id}",
  "stages": {
    "data_conditioning": {
      "present": true/false,
      "techniques": ["technique1", "technique2"],
      "libraries": ["lib1", "lib2"],
      "functions": ["func1", "func2"],
      "parameters": {"param1": "value1"},
      "complexity": "low/medium/high"
    },
    "time_frequency_analysis": {...},
    "trigger_analysis": {...}
  },
  "overall_complexity": "low/medium/high",
  "total_lines": 0,
  "unique_libraries": ["lib1", "lib2"],
  "code_quality_score": 0.0
}
```

Only return the JSON object, no additional text.

The analysis was performed using DeepSeek-R1 (`deepseek-r1-250120`) model with temperature=1.0 for balanced creativity and consistency. We processed 877 valid code snippets (`code_snippet`) using parallel processing with 30 workers to ensure efficient analysis while maintaining API rate limits.

Data Preparation and Normalization. For each identified technique, algorithms were classified into binary groups: those incorporating the technique (“with”) versus those without (“without”). Performance metrics (fitness values or AUC scores) were normalized to [0,1] range using min-max scaling across all algorithms to enable fair comparison between different evaluation metrics.

Combined Performance Analysis. To increase statistical power, we combined normalized AUC scores of both training and test into unified performance datasets for each comparison group. This approach leverages all available performance information while maintaining the comparative structure necessary for statistical testing.

Adaptive Statistical Testing Protocol. Our testing framework adapts to data characteristics through a decision tree approach:

1. **Normality Assessment:** Shapiro-Wilk test for samples $n \leq 5000$
2. **Test Selection:**
 - Both groups normal and $n \geq 30$: Welch’s t-test with Cohen’s d effect size
 - Otherwise: Mann-Whitney U test with rank-biserial correlation
3. **Effect Size Interpretation:**
 - Cohen’s d: negligible (< 0.2), small ($0.2 - 0.5$), medium ($0.5 - 0.8$), large (> 0.8)
 - Rank-biserial: negligible (< 0.1), small ($0.1 - 0.3$), medium ($0.3 - 0.5$), large (> 0.5)

Imbalance Detection and Mitigation. We identify problematic comparisons using two criteria: (i) sample ratio exceeding 3:1, or (ii) minimum group size below 30. For such cases, we implement balanced resampling analysis:

Resampling Protocol:

1. Undersample the larger group to match the smaller group size
2. Perform 1,000 independent resampling iterations with replacement
3. Calculate test statistics and p-values for each iteration
4. Assess robustness based on proportion of significant results

Robustness Criteria: A technique effect is considered robust if:

- $> 80\%$ of resampling iterations show statistical significance ($p < 0.05$)
- Median effect size maintains consistent direction and magnitude
- 95% confidence interval of effect sizes excludes zero

Technique Effectiveness Classification and Visualization. The comprehensive technique impact analysis is presented through violin plot distributions comparing performance between algorithms incorporating specific

techniques (“with”) versus those without (“without”) across all identified techniques (Figure A4). Based on our multi-criteria evaluation framework, techniques are classified into three effectiveness tiers:

High-Effectiveness Techniques demonstrate clear distributional separation with minimal overlap, statistical significance $> 80\%$ across resampling iterations, and large effect sizes ($r > 0.5$). Notable examples include Curvature Analysis and CWT Validation, which show the “with” group distributions positioned substantially higher than “without” groups, indicating consistent performance improvements.

Medium-Effectiveness Techniques exhibit moderate distributional separation, statistical significance between 50-80%, and medium effect sizes ($0.3 < r < 0.5$). These techniques provide measurable but less consistent performance benefits.

Low-Effectiveness Techniques display substantial distributional overlap between “with” and “without” groups, statistical significance $< 50\%$, and small effect sizes ($r < 0.1$), indicating limited practical utility.

Table A2 Technique Abbreviations Used in Figure A4. Complete mapping of abbreviated technique names to their full descriptions, organized by methodological category.

| Abbreviation | Full Name |
|--------------------------------|------------------------------------|
| Data Conditioning | |
| Spline Interp | Spline Interpolation |
| Tikhonov Reg | Tikhonov Regularization |
| Kalman Smooth | Kalman-inspired Smoothing |
| Tukey | Tukey Windowing |
| S-G Filter | Savitzky-Golay Filtering |
| Adaptive Gain | Adaptive Gain Regularization |
| Median Smooth | Uniform/Median Smoothing |
| Gauss Smooth | Gaussian Smoothing |
| Median Baseline | Median-based Baseline Correction |
| SNR Reg | SNR-adaptive Regularization |
| Gauss Conv | Gaussian Convolution |
| Time-Frequency Analysis | |
| Phase Coherence | Phase Coherence Analysis |
| CWT | Continuous Wavelet Transform |
| RMS Coherence | RMS Coherence Metric |
| Dual Align | Dual-channel Alignment |
| Spectral Entropy | Spectral Entropy |
| Freq Reg | Frequency-dependent Regularization |
| Log Compress | Logarithmic Compression |
| CWT Valid | CWT Validation |
| Trigger Detection | |
| Curve Boost | Curvature Boosting |
| Curvature | Curvature Analysis |
| Sigmoid | Sigmoid Enhancement |
| MAD Threshold | MAD-based Robust Thresholding |
| MAD | Median Absolute Deviation |

Distributional Analysis Methodology.

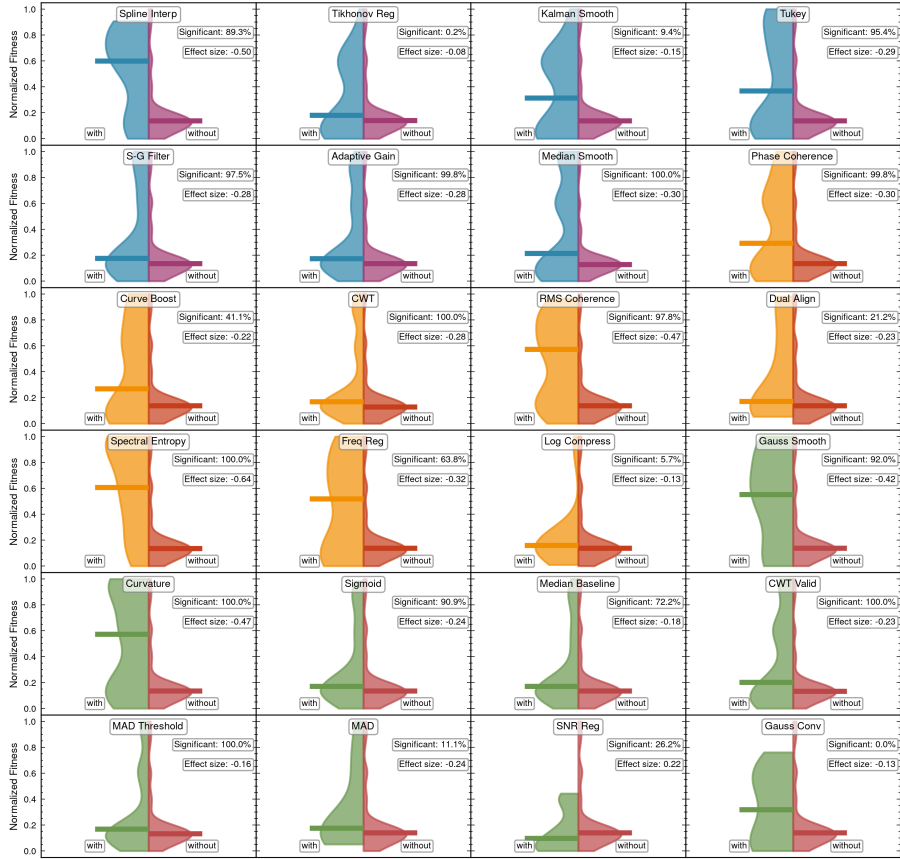


Fig. A4 Comprehensive Technique Effectiveness Analysis via Violin Plot Distributions. Performance distributions comparing algorithms with and without specific techniques across three methodological categories: data conditioning (blue), time-frequency analysis (orange), and trigger detection (green). Each violin plot pair reveals technique effectiveness through distributional characteristics: wider sections indicate higher probability density regions, clear vertical separation between “with” and “without” groups indicates strong technique effects, while substantial overlap suggests limited effectiveness. Statistical robustness metrics (significance percentages from resampling analysis) and effect sizes (rank-biserial correlations) quantify technique reliability. High-effectiveness techniques (e.g., Curvature Analysis, CWT Validation) demonstrate clear distributional separation and large effect sizes, while low-effectiveness techniques show substantial overlap and negligible effect sizes. Technique abbreviations are defined in Table A2.

- Violin plots constructed using Gaussian kernel density estimation with adaptive bandwidth selection
- Performance metrics normalized to [0,1] scale enabling cross-technique comparison
- Color-coded categorical organization: data conditioning (blue), time-frequency analysis (orange), trigger detection (green)
- Statistical annotations include resampling-based significance percentages and rank-biserial effect sizes

- Median performance indicators highlight central tendency differences between technique groups
- Distributional separation quantified through overlap coefficients and Kolmogorov-Smirnov distances
- Technique abbreviations facilitate visual clarity while maintaining comprehensive coverage (Table A2)

This multi-dimensional effectiveness assessment framework enables systematic identification of high-impact techniques while distinguishing them from those with marginal or inconsistent benefits, providing clear guidance for algorithmic development priorities.

A.6 Detailed MCTS Node Evolution and Technique Propagation Data

Figure A5 presents the complete MCTS search tree evolution with node-by-node fitness values and technique compositions. Each node displays its fitness score (marked in red) alongside the specific algorithmic techniques discovered at that search depth. The five core technique categories [1-5] correspond to:

- 1 Multi-resolution Thresholding
- 2 Continuous Wavelet Transform (CWT) using Ricker Wavelet
- 3 Tikhonov Regularization
- 4 Curvature Boosting
- 5 Savitzky-Golay Filter

These techniques demonstrate the systematic evolution of algorithmic complexity through the MCTS exploration process, with detailed implementation examples provided in Section A.1.9.

A.7 Overfitting Risk Assessment and Physical Validation Failure Modes

To evaluate potential overfitting risks in the Evo-MCTS framework, we conducted systematic injection studies using GW150914-like signals with varying signal-to-noise ratios (SNR). This analysis addresses concerns raised in the main discussion regarding algorithmic optimization potentially overfitting to MLGWS-1's specific characteristics.

Experimental Design. We performed injection experiments using simulated gravitational wave signals based on the posterior distribution of GW150914 [10]. The injected signals were embedded in realistic detector noise closed to GW150914 from the O1 observing run, with SNR values systematically varied across various SNRs. For each SNR group, we generated 100 independent injection realizations and evaluated the detection efficiency of representative MCTS nodes across the algorithmic evolution tree.

Detection Efficiency Analysis. Figure A6 presents detection efficiency curves for four representative nodes (Node-4, Node-7, Node-411, Node-464, Node-485, Node-486) spanning different evolutionary stages of the MCTS

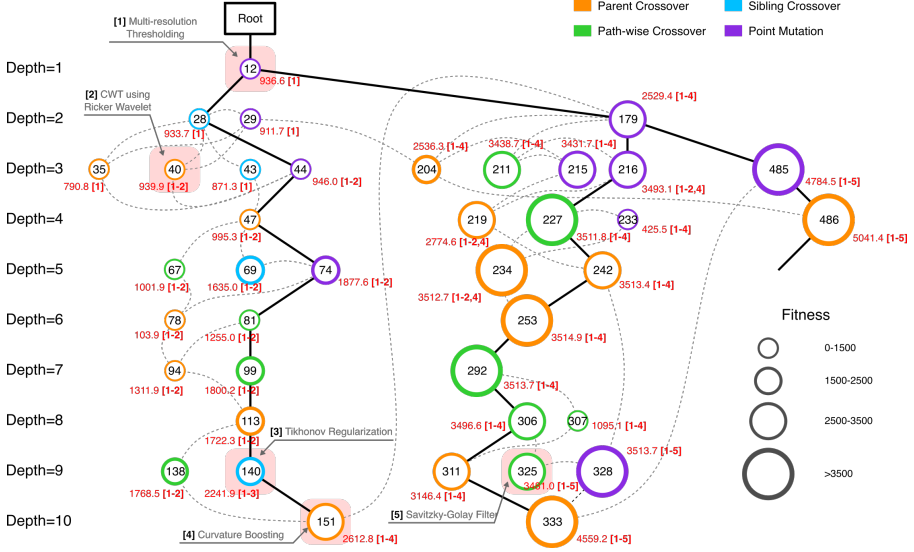


Fig. A5 Complete MCTS search tree with node fitness values and technique compositions. Each node shows its fitness score (red annotations) and constituent algorithmic techniques organized by category [1-5]. Node size reflects fitness magnitude. The tree demonstrates systematic technique evolution and cross-branch knowledge transfer, with optimal performance achieved through multi-technique integration at terminal nodes.

search. The results reveal concerning overfitting patterns that manifest as performance degradation when algorithms optimized on MLGWSC-1 data encounter realistic astrophysical scenarios.

Node-4, representing an early-stage algorithm with minimal complexity, demonstrates robust performance across all SNR ranges with detection efficiency exceeding 80% for $\text{SNR} > 10$. In contrast, highly evolved nodes (Node-464, Node-485, Node-486) exhibit sharp performance transitions, achieving near-perfect detection only above $\text{SNR} = 12-15$, suggesting over-specialization to the noise characteristics and signal morphologies present in the MLGWSC-1 training dataset.

Overfitting Manifestations. The steep detection efficiency curves observed for advanced nodes indicate several failure modes characteristic of overfitting:

- **Threshold Over-Optimization:** Advanced nodes demonstrate excessively restrictive detection thresholds optimized for MLGWSC-1’s specific noise floor, resulting in reduced sensitivity to weaker but astrophysically realistic signals.
- **Feature Over-Specialization:** Complex multi-technique combinations (e.g., Node-486 incorporating techniques [1,2,3,4,5]) show degraded performance on signal morphologies that deviate from the limited parameter space explored in MLGWSC-1.

- **Noise Model Dependency:** The sharp performance transitions suggest algorithms have adapted to MLGWSC-1’s inherent noise model, failing to generalize to the more complex non-stationary and non-Gaussian characteristics of operational detector data.
- **Competition Metric Exploitation:** The MLGWSC-1 evaluation framework itself contains inherent limitations that enable algorithmic exploitation of scoring system vulnerabilities. Advanced nodes appear to have discovered and exploited specific characteristics of the competition’s evaluation metrics, optimizing for artificial performance gains rather than genuine astrophysical detection capability. This metric gaming behavior results in algorithms that achieve high competition scores while failing to maintain robust performance under realistic detection scenarios.

Physical Validation Implications. These results highlight the critical importance of comprehensive physical validation beyond competition-based metrics. The observed overfitting patterns demonstrate that algorithmic complexity does not guarantee improved astrophysical performance, particularly for weak signals that constitute the majority of detectable gravitational wave events in realistic observing scenarios.

The detection efficiency analysis reveals that intermediate-complexity nodes (Node-7, Node-411) achieve optimal balance between algorithmic sophistication and generalization capability, maintaining robust performance across diverse SNR conditions while incorporating beneficial techniques such as multi-resolution thresholding and CWT analysis.

Mitigation Strategies. To address these overfitting risks in future algorithmic development, we recommend: (1) incorporation of diverse astrophysical signal populations during optimization, (2) regularization techniques that penalize excessive algorithmic complexity, (3) cross-validation protocols using independent detector data from multiple observing runs, and (4) explicit constraints on detection threshold optimization to maintain sensitivity to weak signals.

This analysis underscores that while the Evo-MCTS framework successfully demonstrates automated algorithm discovery capabilities, careful validation against realistic astrophysical scenarios remains essential for ensuring practical deployment readiness in operational gravitational wave detection systems.

References

- [1] Zheng, Y., Koh, H.Y., Ju, J., Nguyen, A.T.N., May, L.T., Webb, G.I., Pan, S.: Large language models for scientific discovery in molecular property prediction. *Nature Machine Intelligence* (2025) [2310.07984](https://doi.org/10.1038/s42256-025-00994-z) [cs]. <https://doi.org/10.1038/s42256-025-00994-z>
- [2] Wang, H., Fu, T., Du, Y., Gao, W., Huang, K., Liu, Z., Chandak, P., Liu, S., Van Katwyk, P., Deac, A., Anandkumar, A., Bergen, K., Gomes, C.P., Ho, S., Kohli, P., Lasenby, J., Leskovec, J., Liu, T.-Y., Manrai, A.,

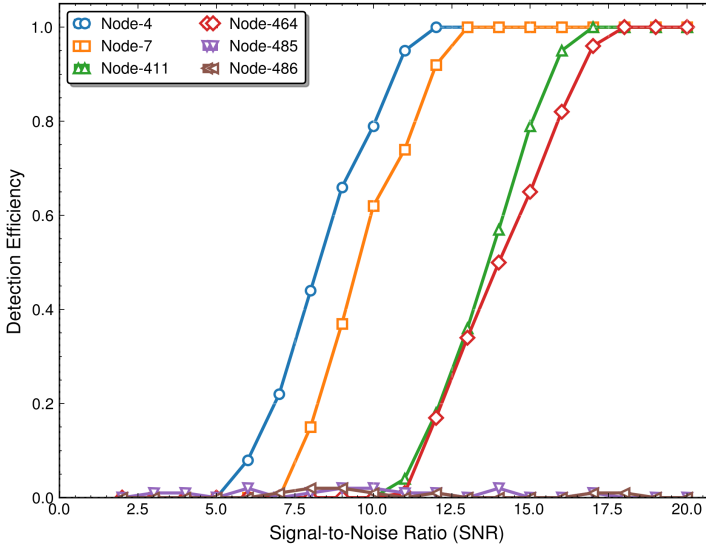


Fig. A6 Detection efficiency analysis revealing overfitting risks in evolved MCTS nodes. Detection efficiency curves for representative nodes across different SNR groups using GW150914-like injections in O1 detector noise. Early-stage nodes (Node-4, blue) demonstrate robust performance across all SNR ranges, while highly evolved nodes (Node-464, Node-485, Node-486, red/purple/brown) exhibit sharp performance transitions indicative of overfitting to MLGWS-1 characteristics. Intermediate-complexity nodes (Node-7, Node-411, orange/green) achieve optimal balance between sophistication and generalization capability.

- Marks, D., Ramsundar, B., Song, L., Sun, J., Tang, J., Veličković, P., Welling, M., Zhang, L., Coley, C.W., Bengio, Y., Zitnik, M.: Scientific discovery in the age of artificial intelligence. *Nature* **620**(7972), 47–60 (2023). <https://doi.org/10.1038/s41586-023-06221-2>
- [3] Karniadakis, G.E., Kevrekidis, I.G., Lu, L., Perdikaris, P., Wang, S., Yang, L.: Physics-informed machine learning. *Nature Reviews Physics* **3**(6), 422–440 (2021). <https://doi.org/10.1038/s42254-021-00314-5>
- [4] Baker, N., Alexander, F., Bremer, T., Hagberg, A., Kevrekidis, Y., Najm, H., Parashar, M., Patra, A., Sethian, J., Wild, S., et al.: Workshop report on basic research needs for scientific machine learning: Core technologies for artificial intelligence. Technical report, USDOE Office of Science (SC), Washington, D.C. (United States) (February 2019). <https://doi.org/10.2172/1478744>. <https://www.osti.gov/biblio/1478744>
- [5] Butler, K.T., Davies, D.W., Cartwright, H., Isayev, O., Walsh, A.: Machine learning for molecular and materials science. *Nature* **559**(7715), 547–555 (2018). <https://doi.org/10.1038/s41586-018-0337-2>
- [6] Schmidt, J., Marques, M.R.G., Botti, S., Marques, M.A.L.: Recent

- advances and applications of machine learning in solid-state materials science. *npj Computational Materials* **5**(1), 83 (2019). <https://doi.org/10.1038/s41524-019-0221-0>
- [7] Baron, D.: Machine Learning in Astronomy: a practical overview (2019). <https://arxiv.org/abs/1904.07248>
 - [8] Fluke, C.J., Jacobs, C.: Surveying the reach and maturity of machine learning and artificial intelligence in astronomy. *WIREs Data Mining and Knowledge Discovery* **10**(2), 1349 (2020). <https://doi.org/10.1002/widm.1349>
 - [9] Luo, Z., Yang, Z., Xu, Z., Yang, W., Du, X.: LLM4SR: A Survey on Large Language Models for Scientific Research (2025). <https://arxiv.org/abs/2501.04306>
 - [10] Abbott, B.P., *et al.*: Observation of gravitational waves from a binary black hole merger. *Phys. Rev. Lett.* **116**, 061102 (2016). <https://doi.org/10.1103/PhysRevLett.116.061102>
 - [11] Abbott, B.P., *et al.*: Gwtc-1: A gravitational-wave transient catalog of compact binary mergers observed by ligo and virgo during the first and second observing runs. *Phys. Rev. X* **9**, 031040 (2019). <https://doi.org/10.1103/PhysRevX.9.031040>
 - [12] Abbott, B.P., *et al.*: A guide to ligo-virgo detector noise and extraction of transient gravitational-wave signals. *Classical and Quantum Gravity* **37**(5), 055002 (2020). <https://doi.org/10.1088/1361-6382/ab685e>
 - [13] Abbott, B.P., *et al.*: Prospects for observing and localizing gravitational-wave transients with advanced LIGO, advanced virgo and KAGRA. *Living Reviews in Relativity* **23**(LIGO-P1200087, VIR-0288A-12), 3 (2018, 2020) [arXiv:1304.0670](https://arxiv.org/abs/1304.0670) [gr-qc]. <https://doi.org/10.1007/s41114-020-00026-9>
 - [14] Owen, B.J.: Search templates for gravitational waves from inspiraling binaries: Choice of template spacing. *Phys. Rev. D* **53**, 6749–6761 (1996). <https://doi.org/10.1103/PhysRevD.53.6749>
 - [15] Cutler, C., Flanagan, E.E.: Gravitational waves from merging compact binaries: How accurately can one extract the binary’s parameters from the inspiral waveform? *Phys. Rev. D* **49**, 2658–2697 (1994). <https://doi.org/10.1103/PhysRevD.49.2658>
 - [16] Klimenko, S., Vedovato, G., Drago, M., Salemi, F., Tiwari, V., Prodi, G.A., Lazzaro, C., Ackley, K., Tiwari, S., Da Silva, C.F., Mitselmakher,

- G.: Method for detection and reconstruction of gravitational wave transients with networks of advanced detectors. *Phys. Rev. D* **93**, 042004 (2016). <https://doi.org/10.1103/PhysRevD.93.042004>
- [17] George, D., Huerta, E.A.: Deep neural networks to enable real-time multimessenger astrophysics. *Phys. Rev. D* **97**, 044039 (2018). <https://doi.org/10.1103/PhysRevD.97.044039>
- [18] Gabbard, H., Williams, M., Hayes, F., Messenger, C.: Matching matched filtering with deep networks for gravitational-wave astronomy. *Phys. Rev. Lett.* **120**, 141103 (2018). <https://doi.org/10.1103/PhysRevLett.120.141103>
- [19] Huerta, E.A., Khan, A., Huang, X., Tian, M., Levental, M., Chard, R., Wei, W., Heflin, M., Katz, D.S., Kindratenko, V., Mu, D., Blaiszik, B., Foster, I.: Accelerated, scalable and reproducible AI-driven gravitational wave detection. *Nature Astronomy* **5**(10), 1062–1068 (2021) [2012.08545v1 \[gr-qc\]. https://doi.org/10.1038/s41550-021-01405-0](https://doi.org/10.1038/s41550-021-01405-0)
- [20] Nagarajan, N., Messenger, C.: Identifying and Mitigating Machine Learning Biases for the Gravitational-wave Detection Problem (2025). <https://arxiv.org/abs/2501.13846>
- [21] Usman, S.A., Nitz, A.H., Harry, I.W., Biwer, C.M., Brown, D.A., Cabero, M., Capano, C.D., Canton, T.D., Dent, T., Fairhurst, S., Kehl, M.S., Keppel, D., Krishnan, B., Lenon, A., Lundgren, A., Nielsen, A.B., Pekowsky, L.P., Pfeiffer, H.P., Saulson, P.R., West, M., Willis, J.L.: The pycbc search for gravitational waves from compact binary coalescence. *Classical and Quantum Gravity* **33**(21), 215004 (2016). <https://doi.org/10.1088/0264-9381/33/21/215004>
- [22] Messick, C., Blackburn, K., Brady, P., Brockill, P., Cannon, K., Cariou, R., Caudill, S., Chamberlin, S.J., Creighton, J.D.E., Everett, R., Hanna, C., Keppel, D., Lang, R.N., Li, T.G.F., Meacher, D., Nielsen, A., Pankow, C., Privitera, S., Qi, H., Sachdev, S., Sadeghian, L., Singer, L., Thomas, E.G., Wade, L., Wade, M., Weinstein, A., Wiesner, K.: Analysis framework for the prompt discovery of compact binary mergers in gravitational-wave data. *Phys. Rev. D* **95**, 042001 (2017). <https://doi.org/10.1103/PhysRevD.95.042001>
- [23] Shah, H.: Algorithmic accountability. *Philosophical Transactions of the Royal Society A: Mathematical, Physical and Engineering Sciences* **376**(2128), 20170362 (2018) <https://royalsocietypublishing.org/doi/pdf/10.1098/rsta.2017.0362>. <https://doi.org/10.1098/rsta.2017.0362>
- [24] Barocas, S., Selbst, A.D.: Big data’s disparate impact. *California Law*

- Review **104**(3), 671–732 (2016). Accessed 2025-07-30
- [25] Mehrabi, N., Morstatter, F., Saxena, N., Lerman, K., Galstyan, A.: A survey on bias and fairness in machine learning. *ACM computing surveys* (CSUR) **54**(6), 1–35 (2021). <https://doi.org/10.1145/3457607>
 - [26] Koza, J.R.: Genetic programming as a means for programming computers by natural selection. *Statistics and Computing* **4**(2), 87–112 (1994). <https://doi.org/10.1007/BF00175355>
 - [27] Elsken, T., Metzen, J.H., Hutter, F.: Neural architecture search: A survey. *Journal of Machine Learning Research* **20**(55), 1–21 (2019)
 - [28] Eiben, A.E., Smith, J.: From evolutionary computation to the evolution of things. *Nature* **521**(7553), 476–482 (2015). <https://doi.org/10.1038/nature14544>
 - [29] Bommasani, R., Hudson, D.A., Adeli, E., Altman, R., Arora, S., von Arx, S., Bernstein, M.S., Bohg, J., Bosselut, A., Brunsell, E., Brynjolfsson, E., Buch, S., Card, D., Castellon, R., Chatterji, N., Chen, A., Creel, K., Davis, J.Q., Demszky, D., Donahue, C., Doumbouya, M., Durmus, E., Ermon, S., Etchemendy, J., Ethayarajh, K., Fei-Fei, L., Finn, C., Gale, T., Gillespie, L., Goel, K., Goodman, N., Grossman, S., Guha, N., Hashimoto, T., Henderson, P., Hewitt, J., Ho, D.E., Hong, J., Hsu, K., Huang, J., Icard, T., Jain, S., Jurafsky, D., Kalluri, P., Karamcheti, S., Keeling, G., Khani, F., Khattab, O., Koh, P.W., Krass, M., Krishna, R., Kuditipudi, R., Kumar, A., Ladhak, F., Lee, M., Lee, T., Leskovec, J., Levent, I., Li, X.L., Li, X., Ma, T., Malik, A., Manning, C.D., Mirchandani, S., Mitchell, E., Munyikwa, Z., Nair, S., Narayan, A., Narayanan, D., Newman, B., Nie, A., Niebles, J.C., Nilforoshan, H., Nyarko, J., Ogut, G., Orr, L., Papadimitriou, I., Park, J.S., Piech, C., Portelance, E., Potts, C., Raghunathan, A., Reich, R., Ren, H., Rong, F., Roohani, Y., Ruiz, C., Ryan, J., Ré, C., Sadigh, D., Sagawa, S., Santhanam, K., Shih, A., Srinivasan, K., Tamkin, A., Taori, R., Thomas, A.W., Tramèr, F., Wang, R.E., Wang, W., Wu, B., Wu, J., Wu, Y., Xie, S.M., Yasunaga, M., You, J., Zaharia, M., Zhang, M., Zhang, T., Zhang, X., Zhang, Y., Zheng, L., Zhou, K., Liang, P.: On the Opportunities and Risks of Foundation Models (2022). <https://arxiv.org/abs/2108.07258>
 - [30] Chen, M., Tworek, J., Jun, H., Yuan, Q., de Oliveira Pinto, H.P., Kaplan, J., Edwards, H., Burda, Y., Joseph, N., Brockman, G., Ray, A., Puri, R., Krueger, G., Petrov, M., Khlaaf, H., Sastry, G., Mishkin, P., Chan, B., Gray, S., Ryder, N., Pavlov, M., Power, A., Kaiser, L., Bavarian, M., Winter, C., Tillet, P., Such, F.P., Cummings, D., Plappert, M., Chantzis, F., Barnes, E., Herbert-Voss, A., Guss, W.H., Nichol, A., Paino, A., Tezak, N., Tang, J., Babuschkin, I., Balaji, S., Jain, S., Saunders, W., Hesse, C.,

- Carr, A.N., Leike, J., Achiam, J., Misra, V., Morikawa, E., Radford, A., Knight, M., Brundage, M., Murati, M., Mayer, K., Welinder, P., McGrew, B., Amodei, D., McCandlish, S., Sutskever, I., Zaremba, W.: Evaluating Large Language Models Trained on Code (2021). <https://arxiv.org/abs/2107.03374>
- [31] Lewkowycz, A., Andreassen, A., Dohan, D., Dyer, E., Michalewski, H., Ramasesh, V., Slone, A., Anil, C., Schlag, I., Gutman-Solo, T., Wu, Y., Neyshabur, B., Gur-Ari, G., Misra, V.: Solving quantitative reasoning problems with language models. In: Koyejo, S., Mohamed, S., Agarwal, A., Belgrave, D., Cho, K., Oh, A. (eds.) *Advances in Neural Information Processing Systems*, vol. 35, pp. 3843–3857. Curran Associates, Inc., ??? (2022)
- [32] Taylor, R., Kardas, M., Cucurull, G., Scialom, T., Hartshorn, A., Saravia, E., Poulton, A., Kerkez, V., Stojnic, R.: Galactica: A Large Language Model for Science (2022). <https://arxiv.org/abs/2211.09085>
- [33] Boiko, D.A., MacKnight, R., Kline, B., Gomes, G.: Autonomous chemical research with large language models. *Nature* **624**(7992), 570–578 (2023). <https://doi.org/10.1038/s41586-023-06792-0>
- [34] Scherbakov, D., Hubig, N., Jansari, V., Bakumenko, A., Lenert, L.A.: The emergence of large language models as tools in literature reviews: a large language model-assisted systematic review. *Journal of the American Medical Informatics Association* **32**(6), 1071–1086 (2025) <https://academic.oup.com/jamia/article-pdf/32/6/1071/63100940/ocaf063.pdf>. <https://doi.org/10.1093/jamia/ocaf063>
- [35] Huang, S., Yang, K., Qi, S., Wang, R.: When Large Language Model Meets Optimization (2024). <https://arxiv.org/abs/2405.10098>
- [36] Liu, F., Yao, Y., Guo, P., Yang, Z., Zhao, Z., Lin, X., Tong, X., Yuan, M., Lu, Z., Wang, Z., Zhang, Q.: A Systematic Survey on Large Language Models for Algorithm Design (2024). <https://arxiv.org/abs/2410.14716>
- [37] Yang, C., Wang, X., Lu, Y., Liu, H., Le, Q.V., Zhou, D., Chen, X.: Large Language Models as Optimizers (2024). <https://arxiv.org/abs/2309.03409>
- [38] Zhang, R., Liu, F., Lin, X., Wang, Z., Lu, Z., Zhang, Q.: Understanding the Importance of Evolutionary Search in Automated Heuristic Design with Large Language Models (2024). <https://arxiv.org/abs/2407.10873>
- [39] AhmadiTeshnizi, A., Gao, W., Udell, M.: OptiMUS: Scalable Optimization Modeling with (MI)LP Solvers and Large Language Models (2024).

<https://arxiv.org/abs/2402.10172>

- [40] Huang, X., Shen, Q., Hu, Y., Gao, A., Wang, B.: LLMs for Mathematical Modeling: Towards Bridging the Gap between Natural and Mathematical Languages (2025). <https://arxiv.org/abs/2405.13144>
- [41] Romera-Paredes, B., Barekatin, M., Novikov, A., Balog, M., Kumar, M.P., Dupont, E., Ruiz, F.J.R., Ellenberg, J.S., Wang, P., Fawzi, O., Kohli, P., Fawzi, A.: Mathematical discoveries from program search with large language models. *Nature* **625**(7995), 468–475 (2024). <https://doi.org/10.1038/s41586-023-06924-6>
- [42] Liu, F., Tong, X., Yuan, M., Lin, X., Luo, F., Wang, Z., Lu, Z., Zhang, Q.: Evolution of Heuristics: Towards Efficient Automatic Algorithm Design Using Large Language Model (2024). <https://arxiv.org/abs/2401.02051>
- [43] Liu, F., Tong, X., Yuan, M., Zhang, Q.: Algorithm Evolution Using Large Language Model (2023). <https://arxiv.org/abs/2311.15249>
- [44] Ye, H., Wang, J., Cao, Z., Berto, F., Hua, C., Kim, H., Park, J., Song, G.: ReEvo: Large Language Models as Hyper-Heuristics with Reflective Evolution (2024). <https://arxiv.org/abs/2402.01145>
- [45] Zheng, Z., Xie, Z., Wang, Z., Hooi, B.: Monte Carlo Tree Search for Comprehensive Exploration in LLM-Based Automatic Heuristic Design (2025). <https://arxiv.org/abs/2501.08603>
- [46] Browne, C.B., Powley, E., Whitehouse, D., Lucas, S.M., Cowling, P.I., Rohlfshagen, P., Tavener, S., Perez, D., Samothrakis, S., Colton, S.: A Survey of Monte Carlo Tree Search Methods. *IEEE Transactions on Computational Intelligence and AI in Games* **4**(1), 1–43 (2012). <https://doi.org/10.1109/TCIAIG.2012.2186810>
- [47] Świechowski, M., Godlewski, K., Sawicki, B., Mańdziuk, J.: Monte Carlo Tree Search: A review of recent modifications and applications. *Artificial Intelligence Review* **56**(3), 2497–2562 (2023) [2103.04931](https://doi.org/10.1007/s10462-022-10228-y) [cs]. <https://doi.org/10.1007/s10462-022-10228-y>
- [48] Wang, L., Zhao, Y., Jinnai, Y., Tian, Y., Fonseca, R.: Neural architecture search using deep neural networks and monte carlo tree search. *Proceedings of the AAAI Conference on Artificial Intelligence* **34**(06), 9983–9991 (2020). <https://doi.org/10.1609/aaai.v34i06.6554>
- [49] Li, Y., Du, D., Song, L., Li, C., Wang, W., Yang, T., Mi, H.: Hunyuan-Prover: A Scalable Data Synthesis Framework and Guided Tree Search for Automated Theorem Proving (2025). <https://arxiv.org/abs/2412.20735>

- [50] Schäfer, M.B., Zelenka, O.c.v., Nitz, A.H., Wang, H., Wu, S., Guo, Z.-K., Cao, Z., Ren, Z., Nousi, P., Stergioulas, N., Iosif, P., Koloniari, A.E., Tefas, A., Passalis, N., Salemi, F., Vedovato, G., Klimenko, S., Mishra, T., Brüggmann, B., Cuoco, E., Huerta, E.A., Messenger, C., Ohme, F.: First machine learning gravitational-wave search mock data challenge. *Phys. Rev. D* **107**, 023021 (2023). <https://doi.org/10.1103/PhysRevD.107.023021>
- [51] Nousi, P., Koloniari, A.E., Passalis, N., Iosif, P., Stergioulas, N., Tefas, A.: Deep residual networks for gravitational wave detection. *Phys. Rev. D* **108**, 024022 (2023). <https://doi.org/10.1103/PhysRevD.108.024022>
- [52] Nitz, A.H., Kumar, S., Wang, Y.-F., Kastha, S., Wu, S., Schäfer, M., Dhurkunde, R., Capano, C.D.: 4-ogc: Catalog of gravitational waves from compact binary mergers. *The Astrophysical Journal* **946**(2), 59 (2023). <https://doi.org/10.3847/1538-4357/aca591>
- [53] Zelenka, O.c.v., Brüggmann, B., Ohme, F.: Convolutional neural networks for signal detection in real ligo data. *Phys. Rev. D* **110**, 024024 (2024). <https://doi.org/10.1103/PhysRevD.110.024024>
- [54] Klimenko, S., Vedovato, G., Drago, M., Salemi, F., Tiwari, V., Prodi, G.A., Lazzaro, C., Ackley, K., Tiwari, S., Da Silva, C.F., Mitselmakher, G.: Method for detection and reconstruction of gravitational wave transients with networks of advanced detectors. *Phys. Rev. D* **93**, 042004 (2016). <https://doi.org/10.1103/PhysRevD.93.042004>
- [55] Klimenko, S., Vedovato, G., Necula, V., Salemi, F., Drago, M., Poulton, R., Chassande-Mottin, E., Tiwari, V., Lazzaro, C., O'Brian, B., Szczepanczyk, M., Tiwari, S., Gayathri, V.: cWB Pipeline Library: 6.4.1. <https://doi.org/10.5281/zenodo.5798976>. <https://doi.org/10.5281/zenodo.5798976>
- [56] Drago, M., Klimenko, S., Lazzaro, C., Milotti, E., Mitselmakher, G., Necula, V., O'Brian, B., Prodi, G.A., Salemi, F., Szczepanczyk, M., Tiwari, S., Tiwari, V., V, G., Vedovato, G., Yakushin, I.: coherent waveburst, a pipeline for unmodeled gravitational-wave data analysis. *SoftwareX* **14**, 100678 (2021). <https://doi.org/10.1016/j.softx.2021.100678>
- [57] Mishra, T., O'Brien, B., Szczepanczyk, M., Vedovato, G., Bhaumik, S., Gayathri, V., Prodi, G., Salemi, F., Milotti, E., Bartos, I., Klimenko, S.: Search for binary black hole mergers in the third observing run of advanced ligo-virgo using coherent waveburst enhanced with machine learning. *Phys. Rev. D* **105**, 083018 (2022). <https://doi.org/10.1103/PhysRevD.105.083018>

- [58] Wang, H., Wu, S., Cao, Z., Liu, X., Zhu, J.-Y.: Gravitational-wave signal recognition of ligo data by deep learning. *Phys. Rev. D* **101**, 104003 (2020). <https://doi.org/10.1103/PhysRevD.101.104003>
- [59] Gabbard, H., Williams, M., Hayes, F., Messenger, C.: Matching matched filtering with deep networks for gravitational-wave astronomy. *Phys. Rev. Lett.* **120**, 141103 (2018). <https://doi.org/10.1103/PhysRevLett.120.141103>
- [60] Schäfer, M.B., Nitz, A.H.: From one to many: A deep learning coincident gravitational-wave search. *Phys. Rev. D* **105**, 043003 (2022). <https://doi.org/10.1103/PhysRevD.105.043003>
- [61] Schäfer, M.B., Zelenka, O.c.v., Nitz, A.H., Ohme, F., Brüggmann, B.: Training strategies for deep learning gravitational-wave searches. *Phys. Rev. D* **105**, 043002 (2022). <https://doi.org/10.1103/PhysRevD.105.043002>
- [62] Finn, L.S.: Detection, measurement, and gravitational radiation. *Phys. Rev. D* **46**, 5236–5249 (1992). <https://doi.org/10.1103/PhysRevD.46.5236>
- [63] Dal Canton, T., Nitz, A.H., Gadre, B., Cabourn Davies, G.S., Villa-Ortega, V., Dent, T., Harry, I., Xiao, L.: Real-time search for compact binary mergers in advanced ligo and virgo’s third observing run using pycbc live. *The Astrophysical Journal* **923**(2), 254 (2021). <https://doi.org/10.3847/1538-4357/ac2f9a>
- [64] LeCun, Y., Bengio, Y., Hinton, G.: Deep learning. *Nature* **521**(7553), 436–444 (2015). <https://doi.org/10.1038/nature14539>
- [65] Rudin, C.: Stop explaining black box machine learning models for high stakes decisions and use interpretable models instead. *Nature Machine Intelligence* **1**(5), 206–215 (2019). <https://doi.org/10.1038/s42256-019-0048-x>
- [66] Molnar, C.: Interpretable Machine Learning. Leanpub, ??? (2020). <https://books.google.com.hk/books?id=jBm3DwAAQBAJ>
- [67] Ribeiro, M.T., Singh, S., Guestrin, C.: ”why should i trust you?”: Explaining the predictions of any classifier. In: *Proceedings of the 22nd ACM SIGKDD International Conference on Knowledge Discovery and Data Mining*, pp. 1135–1144. ACM, San Francisco California USA (2016). <https://doi.org/10.1145/2939672.2939778>
- [68] Lundberg, S.M., Lee, S.-I.: A unified approach to interpreting model predictions. In: Guyon, I., Luxburg, U.V., Bengio, S., Wallach, H., Fergus,

- R., Vishwanathan, S., Garnett, R. (eds.) *Advances in Neural Information Processing Systems*, vol. 30. Curran Associates, Inc., ??? (2017)
- [69] Dat, P.V.T., Doan, L., Binh, H.T.T.: HSEvo: Elevating Automatic Heuristic Design with Diversity-Driven Harmony Search and Genetic Algorithm Using LLMs (2024). <https://arxiv.org/abs/2412.14995>
- [70] OpenAI, Achiam, J., Adler, S., Agarwal, S., Ahmad, L., Akkaya, I., Aleman, F.L., Almeida, D., Altenschmidt, J., Altman, S., Anadkat, S., Avila, R., Babuschkin, I., Balaji, S., Balcom, V., Baltescu, P., Bao, H., Bavarian, M., Belgum, J., Bello, I., Berdine, J., Bernadett-Shapiro, G., Berner, C., Bogdonoff, L., Boiko, O., Boyd, M., Brakman, A.-L., Brockman, G., Brooks, T., Brundage, M., Button, K., Cai, T., Campbell, R., Cann, A., Carey, B., Carlson, C., Carmichael, R., Chan, B., Chang, C., Chantzis, F., Chen, D., Chen, S., Chen, R., Chen, J., Chen, M., Chess, B., Cho, C., Chu, C., Chung, H.W., Cummings, D., Currier, J., Dai, Y., Decareaux, C., Degry, T., Deutsch, N., Deville, D., Dhar, A., Dohan, D., Dowling, S., Dunning, S., Ecoffet, A., Eleti, A., Eloundou, T., Farhi, D., Fedus, L., Felix, N., Fishman, S.P., Forte, J., Fulford, I., Gao, L., Georges, E., Gibson, C., Goel, V., Gogineni, T., Goh, G., Gontijo-Lopes, R., Gordon, J., Grafstein, M., Gray, S., Greene, R., Gross, J., Gu, S.S., Guo, Y., Hallacy, C., Han, J., Harris, J., He, Y., Heaton, M., Heidecke, J., Hesse, C., Hickey, A., Hickey, W., Hoeschele, P., Houghton, B., Hsu, K., Hu, S., Hu, X., Huizinga, J., Jain, S., Jain, S., Jang, J., Jiang, A., Jiang, R., Jin, H., Jin, D., Jomoto, S., Jonn, B., Jun, H., Kaftan, T., Łukasz Kaiser, Kamali, A., Kanitscheider, I., Keskar, N.S., Khan, T., Kilpatrick, L., Kim, J.W., Kim, C., Kim, Y., Kirchner, J.H., Kiros, J., Knight, M., Kokotajlo, D., Łukasz Kondraciuk, Kondrich, A., Konstantinidis, A., Kosic, K., Krueger, G., Kuo, V., Lampe, M., Lan, I., Lee, T., Leike, J., Leung, J., Levy, D., Li, C.M., Lim, R., Lin, M., Lin, S., Litwin, M., Lopez, T., Lowe, R., Lue, P., Makanju, A., Malfacini, K., Manning, S., Markov, T., Markovski, Y., Martin, B., Mayer, K., Mayne, A., McGrew, B., McKinney, S.M., McLeavey, C., McMillan, P., McNeil, J., Medina, D., Mehta, A., Menick, J., Metz, L., Mishchenko, A., Mishkin, P., Monaco, V., Morikawa, E., Mossing, D., Mu, T., Murati, M., Murk, O., Mély, D., Nair, A., Nakano, R., Nayak, R., Neelakantan, A., Ngo, R., Noh, H., Ouyang, L., O’Keefe, C., Pachocki, J., Paino, A., Palermo, J., Pantuliano, A., Parascandolo, G., Parish, J., Parparita, E., Passos, A., Pavlov, M., Peng, A., Perelman, A., de Avila Belbute Peres, F., Petrov, M., de Oliveira Pinto, H.P., Michael, Pokorny, Pokrass, M., Pong, V.H., Powell, T., Power, A., Power, B., Proehl, E., Puri, R., Radford, A., Rae, J., Ramesh, A., Raymond, C., Real, F., Rimbach, K., Ross, C., Rotsted, B., Roussez, H., Ryder, N., Saltarelli, M., Sanders, T., Santurkar, S., Sastry, G., Schmidt, H., Schnurr, D., Schulman, J., Selsam, D., Sheppard, K., Sherbakov, T., Shieh, J., Shoker, S., Shyam, P., Sidor, S., Sigler, E., Simens, M., Sitkin, J., Slama,

- K., Sohl, I., Sokolowsky, B., Song, Y., Staudacher, N., Such, F.P., Summers, N., Sutskever, I., Tang, J., Tezak, N., Thompson, M.B., Tillet, P., Tootoonchian, A., Tseng, E., Tuggle, P., Turley, N., Tworek, J., Uribe, J.F.C., Vallone, A., Vijayvergiya, A., Voss, C., Wainwright, C., Wang, J.J., Wang, A., Wang, B., Ward, J., Wei, J., Weinmann, C., Welihinda, A., Welinder, P., Weng, J., Weng, L., Wiethoff, M., Willner, D., Winter, C., Wolrich, S., Wong, H., Workman, L., Wu, S., Wu, J., Wu, M., Xiao, K., Xu, T., Yoo, S., Yu, K., Yuan, Q., Zaremba, W., Zellers, R., Zhang, C., Zhang, M., Zhao, S., Zheng, T., Zhuang, J., Zhuk, W., Zoph, B.: GPT-4 Technical Report (2024). <https://arxiv.org/abs/2303.08774>
- [71] OpenAI: Learning to Reason with LLMs. <https://openai.com/index/learning-to-reason-with-llms/>. Accessed: 2024 (2024)
- [72] Anthropic: Claude 3.7 Sonnet and Claude Code. <https://www.anthropic.com/news/claude-3-7-sonnet>. Accessed: 2025 (2025)
- [73] DeepSeek-AI, Guo, D., Yang, D., Zhang, H., Song, J., Zhang, R., Xu, R., Zhu, Q., Ma, S., Wang, P., Bi, X., Zhang, X., Yu, X., Wu, Y., Wu, Z.F., Gou, Z., Shao, Z., Li, Z., Gao, Z., Liu, A., Xue, B., Wang, B., Wu, B., Feng, B., Lu, C., Zhao, C., Deng, C., Zhang, C., Ruan, C., Dai, D., Chen, D., Ji, D., Li, E., Lin, F., Dai, F., Luo, F., Hao, G., Chen, G., Li, G., Zhang, H., Bao, H., Xu, H., Wang, H., Ding, H., Xin, H., Gao, H., Qu, H., Li, H., Guo, J., Li, J., Wang, J., Chen, J., Yuan, J., Qiu, J., Li, J., Cai, J.L., Ni, J., Liang, J., Chen, J., Dong, K., Hu, K., Gao, K., Guan, K., Huang, K., Yu, K., Wang, L., Zhang, L., Zhao, L., Wang, L., Zhang, L., Xu, L., Xia, L., Zhang, M., Zhang, M., Tang, M., Li, M., Wang, M., Li, M., Tian, N., Huang, P., Zhang, P., Wang, Q., Chen, Q., Du, Q., Ge, R., Zhang, R., Pan, R., Wang, R., Chen, R.J., Jin, R.L., Chen, R., Lu, S., Zhou, S., Chen, S., Ye, S., Wang, S., Yu, S., Zhou, S., Pan, S., Li, S.S., Zhou, S., Wu, S., Ye, S., Yun, T., Pei, T., Sun, T., Wang, T., Zeng, W., Zhao, W., Liu, W., Liang, W., Gao, W., Yu, W., Zhang, W., Xiao, W.L., An, W., Liu, X., Wang, X., Chen, X., Nie, X., Cheng, X., Liu, X., Xie, X., Liu, X., Yang, X., Li, X., Su, X., Lin, X., Li, X.Q., Jin, X., Shen, X., Chen, X., Sun, X., Wang, X., Song, X., Zhou, X., Wang, X., Shan, X., Li, Y.K., Wang, Y.Q., Wei, Y.X., Zhang, Y., Xu, Y., Li, Y., Zhao, Y., Sun, Y., Wang, Y., Yu, Y., Zhang, Y., Shi, Y., Xiong, Y., He, Y., Piao, Y., Wang, Y., Tan, Y., Ma, Y., Liu, Y., Guo, Y., Ou, Y., Wang, Y., Gong, Y., Zou, Y., He, Y., Xiong, Y., Luo, Y., You, Y., Liu, Y., Zhou, Y., Zhu, Y.X., Xu, Y., Huang, Y., Li, Y., Zheng, Y., Zhu, Y., Ma, Y., Tang, Y., Zha, Y., Yan, Y., Ren, Z.Z., Ren, Z., Sha, Z., Fu, Z., Xu, Z., Xie, Z., Zhang, Z., Hao, Z., Ma, Z., Yan, Z., Wu, Z., Gu, Z., Zhu, Z., Liu, Z., Li, Z., Xie, Z., Song, Z., Pan, Z., Huang, Z., Xu, Z., Zhang, Z., Zhang, Z.: DeepSeek-R1: Incentivizing Reasoning Capability in LLMs via Reinforcement Learning

(2025). <https://arxiv.org/abs/2501.12948>

- [74] Bubeck, S., Chandrasekaran, V., Eldan, R., Gehrke, J., Horvitz, E., Kamar, E., Lee, P., Lee, Y.T., Li, Y., Lundberg, S., Nori, H., Palangi, H., Ribeiro, M.T., Zhang, Y.: Sparks of Artificial General Intelligence: Early experiments with GPT-4 (2023). <https://arxiv.org/abs/2303.12712>
- [75] Ouyang, L., Wu, J., Jiang, X., Almeida, D., Wainwright, C., Mishkin, P., Zhang, C., Agarwal, S., Slama, K., Ray, A., Schulman, J., Hilton, J., Kelton, F., Miller, L., Simens, M., Askill, A., Welinder, P., Christiano, P.F., Leike, J., Lowe, R.: Training language models to follow instructions with human feedback. In: Koyejo, S., Mohamed, S., Agarwal, A., Belgrave, D., Cho, K., Oh, A. (eds.) *Advances in Neural Information Processing Systems*, vol. 35, pp. 27730–27744. Curran Associates, Inc., ??? (2022)